UNIVERSITY OF SOUTHAMPTON

ANALYTICAL APPROACHES TO PREDICT FLEXURAL BEHAVIOUR OF CURVED COMPOSITE BEAMS

By

Wei-bo WANG

Thesis for the degree of Ph.D.

School of Engineering Sciences

Faculty of Engineering and Applied Science

February 2002

UNIVERSITY OF SOUTHAMPTON

ABSTRACT

FACULTY OF ENGINEERING AND APPLIED SCIENCE
SCHOOL OF ENGINEERING SCIENCES, SHIP SCIENCE

Doctor of Philosophy

ANALYTICAL APPROACHES TO PREDICT FLEXURAL BEHAVIOUR OF CURVED COMPOSITE BEAMS

By Wei-bo WANG

This thesis is concerned with the analysis of curved laminates and sandwich beams with a focus on delamination and instability.

An elasticity-theory-based approach is developed for delamination and flexural strength of curved layered composite laminates and sandwich beams. The governing equations in this case are derived from the results of curved orthotropic beam on an elastic foundation under flexural loading. The approach ensures an accurate description of the through-thickness and in-plane stresses in curved laminate beams. The solutions for various geometrical configurations are provided. The effects of key parameters, such as stacking sequence of the laminate, thickness of the skin, the curvature radius etc. are studied.

The critical load for instability of a curved beam on an elastic foundation, which is correspondent to the skin of sandwich beam under pure bending, is derived by beam theory and virtual displacement principle. The flexural strength of curved sandwich beam is studied with a view to identify delamination and local instability characteristics.

The delamination buckling in curved composite beam is also investigated in this document. Based on linear and non-linear curved beam theory coupled with fracture mechanics concepts, two theoretical approaches are developed respectively for linear and nonlinear problems of delamination buckling which are concerned in the cases of normal delamination buckling and snap buckling of the inner layer.

KEY WORDS: Layered structures, geometry curvature, elastic foundation, through-thickness stress, delamination, instability, delamination buckling

Acknowledgements

Firstly the author wishes to express his sincere gratitude to his supervisor, Professor R. A. Shenoi for the great help and support in accomplishing every aspect of this work.

Secondly the author would like to thank: Professor J. T. Xing and Dr. S. Clark for their enthusiastic help in his Ph.D. studying period; Dr. M. Y. Tan and Professor P. Wilson for their coping with the computer problems; Mr. Z. H. Wang and Mr. J. Xing for their help in drawing figures; Dr. H. K. Jeong and Dr. X. P. Zheng for discussing mechanical questions, as well as all the other colleagues involved in way or another with this research work.

Most importantly, the author would also like to state his eternal appreciation of his parents and his wife for their never ending support in his life.

List of Contents

List of Figures and Tables

Nomenclature

Letters

a,b,c	coefficients in the expression for stresses in isotropic material
a_i	coefficients in Fourier series
b	width of the sample
d	thickness of the delaminated layer (outer layer)
k	elastic stiffness of foundation
l	length of the beam
m	cross-ply stacking ratio which signifying the ratio of the thickness sum of odd number plies to that of even number plies.
n	the number of layers in laminate
n	the number of buckling half-waves
p	reaction force of elastic foundation; the modulus in elliptic integrals
p_0	known constant reaction force of an elastic foundation
q	distributed pressure
q_0	known constant distributed pressure
t	thickness of beam
t_s	thickness of the skin of sandwich beam
t_c	thickness of the core of sandwich beam
u	displacement component in x direction (or cylinder axis)
v	displacement component in y direction (or θ direction)
w	displacement component in z direction (or r direction)
A	tension stiffness matrix
B	coupling stiffness matrix
D	flexible stiffness matrix
C_0	constant radial displacement
C_i	coefficients in the expression for stresses in anisotropic material

D	the flexural rigidity
E	Young's modulus of elasticity
$E(p,\phi)$	Legendre's standard form of second kind elliptic integral
$E(p)$	complete elliptic integral of the second kind
F, F_h, F_v	Load and load components in horizontal and vertical direction respectively
$F(p,\phi)$	Legendre's standard form of first kind elliptic integral
$K(p)$	complete elliptic integral of the first kind
M	general expression for bending moment
N	general expression for axial force
N_{cr}	critical value of the load for buckling
Q	general expression for shear force
M_0, N_0	known constant bending moment and axial force
$\overline{M}_0, \overline{N}_0$	the bending moment and axial force for global layered beam
$Q_{ij}^{(k)}$	stiffness matrix component of the kth layer
R, R_o, R_i	radius of midplane of the curved beam
R_o	outer radius of the curved beam
R_i	inner radius of the curved beam
R^*	curvature radius of delamination crack
V	potential energy
V_f	volume fraction of fibre in fibre reinforced composites
α	arc angle of curved beam
β	arc angle of delamination crack in curved beam
α, β, η $\alpha^*, \beta^*, \eta^*$	coefficients in the expressions of reaction forces
μ	shear modulus of elasticity
ν	Poisson's ratio of material
λ	anisotropy ratio
δ	ratio of inner radius to outer radius of the beam ($=R_i/R_o$)
σ, τ	normal stress and shear stress
ε, γ	normal strain and shear strain

ϕ	parameter in elliptic integrals
ρ	density
$\{\kappa\}$	the curvature change of mid-plane of laminate or mid-surface of shell
κ	curvature change of the curved beam
ξ^*	location of the maximum through-thickness stress σ_r, measured from the midplane of the beam
Φ	Airy stress function
Γ	surface energy
K_i, Λ_i	coefficients in the expressions of v and p

Subscripts

1	in relation to in-plane direction
2	in relation to through-thickness direction
1,2,3	in relation to undelaminated and two delaminated parts of global curved beam
c	in relation to core of the sandwich beam
r	in relation to radial or through-thickness direction
s	in relation to tangential direction of curve
	in relation to skin of the sandwich beam
x	in relation to x direction (or longitudinal direction of cylindrical shell)
L	in relation to longitudinal direction of fibre reinforced laminae
T	in relation to transverse direction of fibre reinforced laminae
θ	in relation to circumferential direction

Superscripts

0	in relation to mid-plane or mid-surface of the laminated shell
(1), (2)	in relation to the states of a beam respectively before and after its delamination buckling
(I),(II),...	in relation to every part in a curved beam whose buckled shape has an inflection
(i)	in relation to ith layer in layered composite beam

Chapter 1 Introduction

1.1 Background of the work

Fibre reinforced plastic (FRP) composite materials are finding increased usage in a wide variety of structural applications in the aerospace, civil construction, marine and offshore industries. A key feature of most such structures is the presence of bonded joints connecting two plate panels either butted together in-plane or placed in a tee fashion for out-of plane load transfer. In either case straps of laminated plates (or overlaminates) are bonded together to the base place to effect the load transfer. The good performance of the joints then is decided by correct selection of the adhesive and proper design of the overlaminate. There is a large body of literature dealing with specific aspects of adhesion and adhesively bonded joints, for example, Kinloch (1997), Thomas et al (1998) and Charalambidi et al (1998). One of the objectives of this thesis is the mechanical characterisation of such curved composite structure elements as the overlaminate.

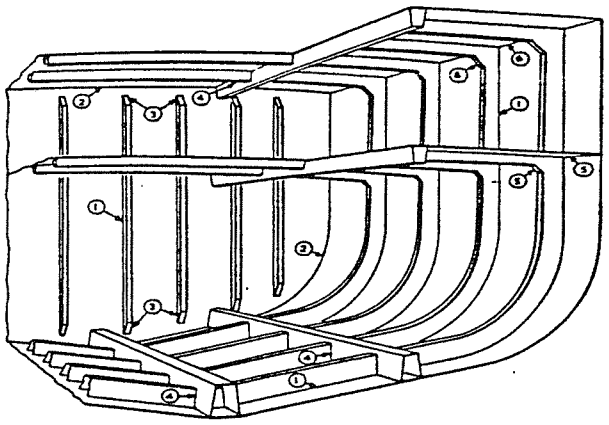

(1) Frame/shell
(2) Bulkhead/shell
(3) Stiffener ending
(4) Stiffener intersection
(5) Deck-edge (tee)
(6) Deck-edge (knee)

Figure 1.1 Ship Hull Compartment Showing Typical Tee Connections

Tee joints, curved sandwich beams and top-hat stiffeners as well as curved layered beams are widely used in many applications, for example, ship hulls. A typical tee-joint and curved sandwich beam configuration is shown in Figure 1.2. The behaviour of such curved structural elements has been studied to a certain extent (Pei & Shenoi, 1996). It has been known that the strength of tee joint is a great deal dependent on the nature of boundary angles, especially the geometry curvature and thickness as well as its material (Shenoi et al, 1992, 1993 and 1998). It is found that increasing the thickness of the overlamination, traditionally the criterion used for the design of joints, has a detrimental effect on the properties of the joint; on the other hand, the radius of the fillet, which traditionally is given little or no consideration by current design methods, is critical to the performance of the joint (Hawkins et al, 1993). The effect of geometry curvature on the strength of the beam is also always neglected in the traditional design of curved composite beam or sandwich beam. Designers with composites generally estimate the mechanical behaviour of these curved structure elements with the conventional treatment of laminates and the strength criteria for flat beam or laminates.

However, up to now, most work in this area has focused on experimental and numerical analyses, for example, Shenoi & Hawkins (1994 and 1995) besides those which have been mentioned in the above. There are few theoretical analyses relating to the strength and other mechanical characteristics such as local instability and delamination buckling of these curved composite structural elements.

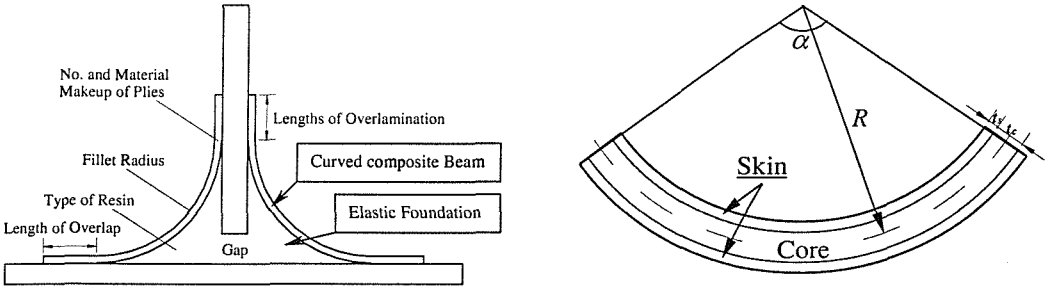

Figure 1.2 A typical tee-joint and curved sandwich beam configuration

1.2 The aims and objectives

The aims of thesis are therefore to investigate the flexural behaviour of curved laminates and sandwich beams, and predict their strengths by theoretical approaches.

The key objectives of this thesis are four-fold:

- To develop a model for characterising flexural behaviour of a curved beam on an elastic foundation;
- To obtain accurate elasticity solutions for stresses, especially through-thickness tensile stress in curved laminates and sandwich beams, and investigate the effects of some key parameters such as radius of curvature, stacking sequence, and foundation modulus (if the beam resting on an elastic foundation) etc.;
- To find a theoretical solution for buckling/wrinkling of curved composite beams on an elastic foundation and, then based on the results, to estimate the bending strength of global curved sandwich beam in terms of local instability of the skin;
- To investigate delamination buckling of a curved layered beam by analytical approaches under conditions of opening and closing bending moments respectively.

1.3 Scope of the work and literature review

1.3.1 Flexural response of curved beam on an elastic foundation

In the first stage of our analytical research work, a model for this kind of curved structure element such as tee-joint and curved sandwich beam is developed. Overlaminate in a tee joint or the skin of curved sandwich beam are considered as curved composite beam, meanwhile the fillet in tee joint or core in sandwich beam are considered as elastic

foundation. Thus the first problem under consideration becomes evaluating the flexural response of curved composite beam on an elastic foundation.

There is a wide body of literature on the analysis of beams and plates resting on elastic foundations. Sinha (1963) has examined the flexural behaviour of uniformly loaded, isotropic plates resting on a Winkler elastic foundation by using Berger's approach (1955). Yang (1970) has derived load-deflection curves for uniformly loaded, isotropic plates on a Winkler foundation using the finite element method. Ghosh (1977) has obtained load versus bending moment and shear force curves for isotropic plate on elastic foundation of the Pasternak-type. Chia (1980) gives analytical formulations for the large deflection behaviour of uniformly loaded orthotropic plates on a Winkler foundation. In all these cases, the plates considered were flat.

The analysis of curved beam made from isotropic material has also been well documented, for example, Hetenyi (1946). The circular isotropic bar resting on elastic foundation with different boundary conditions and under different kinds of load is studied in detail. However, there are not many publications focusing on curved composite beam on an elastic foundation. Therefore, the first part of this thesis document is to extend current approaches of elastic foundation analysis and laminate theory to include the effects of curvature on structural response.

1.3.2 Through-thickness stresses in curved laminates and sandwich beams

One of the key features of a curved (as distinct from a straight) laminated beam is the presence of not so insignificant through-thickness tensile stresses. These can significantly affect the performance of curved composite beams due to the low values of through-thickness tensile strength. For example, the delamination is more likely to occur in such curved structural elements. Therefore, it is imperative to obtain the stress distribution through the thickness more accurately when analysing the behaviour of curved composite

beam. However, the problem of delamination in curved composite beams has mostly been investigated experimentally and numerically (Shenoi & Hawkins, 1994 and 1995; Smidt, 1993 and 1996) due to the difficulty of taking into account geometry curvature. Researchers and designers with composites are familiar with the conventional treatment of laminates such as the classical laminated plate theory (CPT) and thin shell theory (Reissner, 1961). In these classic treatments of curved shells, the assumption of a state of plane stress in the constitutive relations eliminates the possibility of rigorous calculation of interlaminar stresses. Moreover, although many high order, refined laminated plate theories and some approximate methods are available (Whitney, 1969; Reddy, 1984; Bhate, 1995), their application to curved beams is limited (Chang, 1986). Most of these theories or methods retain parts of the assumptions of classical plate and thin shell theory, and only incorporate the influence of shear deformation etc. on plate deflection in composite laminates. So while they can compute transverse shear stresses and give more accurate results for the in-plane stresses and displacements, they are unable to deal with through-thickness stresses.

Pagano (1967 and 1969) studied the multi-ply composite laminates using linear elastic theory, and provided an exact solution for composite laminates in cylindrical bending. However, the composite laminates he considered were all flat and subjected to only transverse load condition. Lekhnitskii (1981) gave a general solution to the problem "Bending of a Plane Curved Rod by Moments". He studied the curved orthotropic beam but did not consider the response of a rod on an elastic foundation. The response of a curved beam without a foundation is quite different from that with a foundation. It can only sustain load condition such as pure bending or a pair tension/compression forces at the ends, and cannot sustain the circumferential force without radial restraints. But it is obvious that the interaction generally exists between every two adjacent plies of laminate especially in a curved laminate, so the solution of Lekhnitskii cannot be directly transformed to analyse the curved layered composite beam.

Most recent reported work about the curved beams deals with plane strain applications of classical laminated plate theories (Wu, 1993; Gibson, 1994 and Chandler, 1993). The

extension of classical theories to curved beams is based on tight assumptions. For example, Wu (1993), Gibson and Chandler (1994 and 1993) adopt the same model which keeps the assumption that the stress normal to the cross-section of beam distributes linearly. This is acceptable when the longitudinal elastic modulus of composite beam does not change through thickness, such as a laminated beam composed of many layers oriented in the same direction (or unidirectional composite beam). This assumption is not valid, however, for a general layered composite beam, in which the stiffness properties vary drastically from layer to layer. Stress components are thus likely to be discontinuous in their variation. Therefore the method and results obtained by Wu et al cannot be used to analyse a general curved laminated beam. Tolf (1983) analysed homogeneous transverse isotropy condition in detail, but in his discrete model, he took the laminate as one ply fibre material by one ply matrix material, consequently each ply in laminate is considered as homogeneous and isotropic. Lu (1994) provided a solution of homogeneous anisotropy, but as with Tolf (1983), his model and solution cannot be used to study layered composite curved beam and curved sandwich beam. In the recent past, Wisnom (1995, 1996 and 1996) and Kaczmarek et al (1998) has contributed much research work on experimental analyses and numerical approaches for interlaminar failure and flexural strength of composite laminate. The focus of this work has been towards understanding delamination failure in curved laminated beams.

Interlaminar normal and shear stresses, acting either singly or interactively can lead to delamination as reported by Wisnom (1995 and 1996), thus affecting structural integrity. It is important to know through-thickness stresses even well below the delamination limit value, because these could have an interactive effect on failure under in-plane stress to some extent (Wu, 1993). Especially in curved composite structure, the distribution and effect of through-thickness stresses should be paid more attention to, because there originally exists tension-bending coupling in the mechanical behaviour of composite laminate meanwhile the through-thickness tensile stresses is not so insignificant as in flat one. Therefore, it is imperative to obtain the stress distribution through the thickness more accurately when analysing the behaviour of curved composite beam.

1.3.3 Buckling/wrinkling of curved composite beam on an elastic foundation

One other feature of the curvature of an overlaminate in a tee joint or the skin of curved sandwich beam is the effect it has on the buckling/wrinkling characterisation of the face in compression.

If the compression in the face of such structures exceeds a critical load, this compressed face is then subject to a particular kind of instability, which is either column/global buckling or local wrinkling (or rippling in which the wavelength of the buckled form is of the same order as the thickness of the core). The local instability problem of straight sandwich beam can be studied by considering a long strut supported by a continuous elastic isotropic medium (Allen, 1969; Hoff and Mautner, 1945). Ordinary buckling theory indicates that the lowest critical load is that which corresponds to a buckled form in which the half-wavelength is equal to the length of flat beam with both ends simply supported. Nevertheless in some suitable circumstances of the bar resting on an elastic foundation, short-wavelength instablity may occur at a still lower load. And the problem of the buckling of straight bar on an elastic foundation has also been considered in some literature, for example, Timoshenko (1936) and Hetenyi (1946).

However, as far as the curved sandwich beam is concerned, this problem becomes a little more complicated. The curved structure has different characteristic of instability from the straight one. For example, even under the condition that there is no foundation and both ends are pinned, the lowest critical load for curved beam subjected to uniformly distributed pressure is that which corresponds to the buckled form with two, not one, half-waves (Timoshenko, 1936). This difference just results from the geometry curvature. In our research work, the fillet or core material is still considered as elastic foundation and the Winkler Hypothesis (Selvadurai, 1979) is assumed. In this thesis document, a critical load for buckling/wrinkling of the skin is derived by virtual displacement principle under the condition that the global curved sandwich is subject to pure bending.

1.3.4 Delamination buckling of curved layered composite beam

Apart from the delamination arising from large through-thickness stress which exceeds the interlaminar strength of layered composite beam, another way in which early structural failure can be caused is by delamination buckling. Local delamination can be considered as a crack in the interlaminar bond. Under buckling of the delaminated layer there appears a high interlaminar stress level at crack tip which leads to crack growth. On the other hand, delamination growth can also adversely affect the structural instability and even lead to catastrophic collapse of overall structure. They are coupled with each other.

In recent years the problem of delamination buckling of composite beam has been studied by several researchers, both experimentally and theoretically. Chai et al (1981) used the energy release rate criterion based on a fracture mechanics approach to model the process using a post-buckling solution for a delaminated beam-column. Wang et al (1985) studied the compressive stability of delaminated random short-fibre composites by Rayleigh-Ritz method as well as by a finite element analysis. Moshaiov (1991) gave a characteristic equation for the buckling involving the length of delamination and its location the beam. Chattopadhyay (1996) and Gu (1998) give an exact elasticity solution for buckling of a simply supported orthotropic plate and then composite laminates whose behaviour is referred to as cylindrical bending. However, most of the work concerns straight laminated beams.

Kachanov (1988) studied two types of delamination buckling in delamination damage of fibre/glass tube. And in his research work, he considered the problem of delamination of a fibre-glass tube due to residual stresses and the problem of snap delamination buckling of a ring under external pressure, which are respectively corresponding to linear and non-linear problem of delamination buckling. Before this, Bugakov's (1977) experimental research work on fibre/glass rings subjected to uniform external pressure also revealed some characteristics in the snap buckling of its inner surface layer.

As mentioned in the beginning, delamination and delamination buckling are more likely to occur in curved composite beam due to the geometry curvature. Meanwhile, compared to the flat beam, the curved geometry also makes it more difficult to achieve the solution to the problem. Up to now, there have still been few analytical research works reported considering the delamination buckling in curved composite laminates, although many investigations on the problem of delamination buckling in flat composite beam have been received to some extent.

Toward this objective, two problems are considered in the last part of thesis – curved composite layered beam subjected to opening and closing bending moments respectively (snap buckling occurring in the latter case) – which are corresponding to the linear and non-linear problems of delamination buckling of curved composite beam.

1.4 Layout of thesis

The through-thickness stress in curved composite laminate or sandwich beam is studied in this thesis by an elasticity-theory-based approach. Chapter 2 develops a model for characterising linear-static flexural behaviour of a curved beam on an elastic foundation by classical beam theory. The supporting reaction force of elastic foundation, bending moment and shear force within the beam are obtained from the governing equations. These results are then used in Chapter 3 as boundary conditions for an elasticity solution for an orthotropic beam on an elastic foundation. Then a general solution for curved layered composite beam is achieved in Chapter 4. Chapter 5 studies the instability of curved composite beam on an elastic foundation. The critical values of compressed load for different kinds of instability--wrinkling/buckling--are obtained by beam theory and principle of virtual displacement. The effects of key variables on stress distribution within a curved beam are investigated in Chapter 6, and Chapter 7 shows the effects of stacking sequence and curvature radius of curved composite laminate on the through-thickness stress. Estimation of delamination and local instability damage in curved sandwich beams is achieved in Chapter 8 based on the approaches developed in previous chapters. The

application of the approach is also made to analyse the failure of some tee joint samples under a 45° pull-off condition in Chapter 9. Chapter 10 investigates the delamination buckling in curved composite layered beam. Both the problem of delamination coupled with buckling when curved beam is subjected to opening bending moment and the problem of snap buckling of inner layer when curved beam is subjected to closing bending moment are considered. The concluding Chapter 11 summaries the achievements of the whole research work. Further work aimed at improving the accuracy of the approaches and scope of their applications are listed and commented upon.

Chapter 2 Flexural Response of a Curved Beam on an Elastic Foundation

2.1 Background and aim

The background of the problem provided in this chapter is the strength of tee joint, curved sandwich beam etc. As mentioned in the chapter of introduction, in our research work, we adopt a model for these kinds of curved structure element which considers the overlaminate or skin as curved beam meanwhile the fillet or core as elastic foundation, as shown in Figure 2.1.

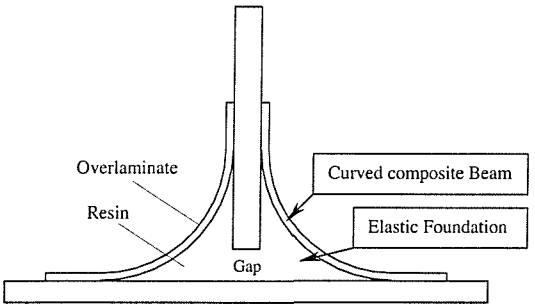

Figure 2.1a Tee joint

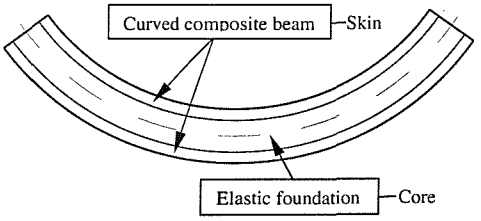

Figure 2.1b Curved sandwich beam

Figure 2.1 Model sketch for the problem statement

The aim of this chapter is to develop a model for characterising and investigating the mechanical behaviour of a curved composite beam on an elastic foundation under flexural loading. The governing differential equation for general curved composite beam on an elastic foundation is derived from force-moment equilibrium considerations and classical laminate theory. And the flexural behaviour of a circular composite beam on an elastic foundation is studied in detail.

2.2 Equilibrium equation and corresponding constitutive relation

Consider a curved beam resting on an elastic foundation. Assuming the intrinsic equation of its free shape is $\theta = \Theta(s)$, where s is measured along the length of the arc and θ is the slope at s , as shown in Figure 2.2a.

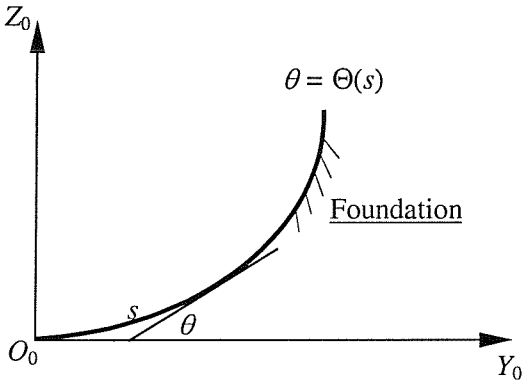

Figure 2.2a Beam geometry

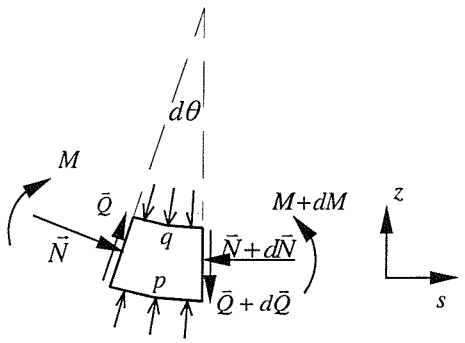

Figure 2.2b Forces on a small element

Figure 2.2 Curved beam on an elastic foundation

Consider next the conditions of equilibrium of the forces on an element of the beam, as shown in Figure 2.2b, the following can be obtained:

In radial direction: $$p \cdot ds - N \cdot d\theta - q \cdot ds = dQ \tag{2-1}$$

In tangential direction: $$Q \cdot d\theta = dN \tag{2-2}$$

Moment equilibrium: $$dM = Q \cdot ds \tag{2-3}$$

Then there has: $$p - q - N\frac{d\theta}{ds} = \frac{dQ}{ds} = \frac{d^2M}{ds^2} \tag{2-4}$$

Assuming the modulus of elastic foundation is k, and Winkler Hypothesis is taken for the elastic foundation here. Hence the reaction forces in the foundation are then normal to the axis of the beam and proportional at every point to the radial deflection of the beam w at the point, that is to say:

$$p = k \cdot w \tag{2-5}$$

By substituting equation (2-5) into (2-4) the equilibrium equation of curved beam on an elastic foundation can be obtained:

$$kw - q - N\frac{d\theta}{ds} = \frac{d^2 M}{ds^2} \tag{2-6}$$

In order to obtain the solution to the above differential equation, it is necessary to obtain a relation between the moment M and normal displacement w. In the case of laminated composite beam, the relationship is obtained from the classical plate constitutive equation (see Appendix A):

$$\begin{bmatrix} \mathbf{N} \\ --- \\ \mathbf{M} \end{bmatrix} = \begin{bmatrix} \mathbf{A} & | & \mathbf{B} \\ -- & | & -- \\ \mathbf{B} & | & \mathbf{D} \end{bmatrix} \cdot \begin{bmatrix} \varepsilon^0 \\ --- \\ \kappa \end{bmatrix} \tag{2-7}$$

where

$$[\mathbf{N}] = \begin{Bmatrix} N_x \\ N_s \\ N_{xs} \end{Bmatrix}, \quad [\mathbf{M}] = \begin{Bmatrix} M_x \\ M_s \\ M_{xs} \end{Bmatrix}, \quad [\varepsilon^0] = \begin{Bmatrix} \varepsilon_x^0 \\ \varepsilon_s^0 \\ \gamma_{xs}^0 \end{Bmatrix}, \quad [\kappa] = \begin{Bmatrix} \kappa_x \\ \kappa_s \\ \kappa_{xs} \end{Bmatrix}$$

$$(A_{ij}, B_{ij}, D_{ij}) = \int_{-h/2}^{h/2} Q_{ij}^{(k)}(1, z, z^2)dz \tag{2-8}$$

Apparently, as far as a general composite laminate is concerned, because of the tension-bending coupling and bending-torsion coupling, a simple expression of M and κ, needed for solving the differential equation (2-6), cannot be obtained easily. In the following, some pertinent cases will be considered. In the derivations, q is assumed to be a constant, as is the case for the commonly occurring condition of hydrostatic pressure loading.

2.3 General governing differential equation

Consider a shell curved about only one axis (e.g. cylindrical shell) here, and assume it is very long in this axis—designated as x-axis. The applied forces and boundary conditions are both uniform in x-direction, so the deformation is independent of x. And the assumption of $\varepsilon_x = 0$ is also taken here. Hence this shell can be analysed as a curved beam with unit width. Then from equations (2-7) and (2-8), the following equations can be obtained:

$$\begin{cases} N = A_{11}\varepsilon^0 + B_{11}\kappa \\ M = B_{11}\varepsilon^0 + D_{11}\kappa \end{cases} \tag{2-9}$$

where for the reason of clarification and unity with the expression in Figure 2.2b, the subscripts s in all related variables are omitted, and ε^0 is the in-plane strain in s-direction at mid-surface. Eliminating the term ε^0 in the first expression in equation (2-9), results in the second equation being written as:

$$M = \frac{B_{11}}{A_{11}}N + (D_{11} - \frac{B_{11}^2}{A_{11}})\kappa \tag{2-10}$$

According to the theory of curved surfaces and elastic shells, when considering the effect of in-plane deformation on the change of curvature of circular beam or cylindrical shell,

the relation between the lateral deflection w and curvature κ is as below (see Appendix B):

$$\kappa = v\frac{d^2\theta}{ds^2} - \frac{d^2w}{ds^2} - w\left(\frac{d\theta}{ds}\right)^2 \tag{2-11}$$

where v is the displacement in s-direction.

Substituting expression (2-11) in equation (2-10), the relation between bending moment M and lateral deflection w for a general curved beam can be known as

$$M = \frac{B_{11}}{A_{11}}N + D_{11}\left(1 - \frac{B_{11}^{\ 2}}{A_{11}}\right)\left[v\frac{d^2\theta}{ds^2} - \frac{d^2w}{ds^2} - w\left(\frac{d\theta}{ds}\right)^2\right] \tag{2-12}$$

and then substituting equation (2-12) in equation (2-6), the governing differential equation for general curved composite beam on an elastic foundation is finally obtained as follows:

$$\frac{d^4w}{ds^4} + \left(\frac{d\theta}{ds}\right)^2\frac{d^2w}{ds^2} + 4\frac{d\theta}{ds}\frac{d^2\theta}{ds^2}\frac{dw}{ds} + \left[2\frac{d\theta}{ds}\frac{d^3\theta}{ds^3} + 2\left(\frac{d^2\theta}{ds^2}\right)^2 + \frac{k}{D_{11}\left(1 - \frac{B_{11}^{\ 2}}{A_{11}}\right)}\right]w$$
$$= \frac{1}{D_{11}\left(1 - \frac{B_{11}^{\ 2}}{A_{11}}\right)}\left(q + \frac{B_{11}}{A_{11}}\frac{d^2N}{ds^2} + \frac{d\theta}{ds}N\right) + \frac{d^2\theta}{ds^2}\frac{d^2v}{ds^2} + 2\frac{d^3\theta}{ds^3}\frac{dv}{ds} + \frac{d^4\theta}{ds^4}v \tag{2-13}$$

For the case of curved isotropic beam on an elastic foundation, because B_{11}= 0, the above governing differential equation becomes

$$\frac{d^4w}{ds^4}+\left(\frac{d\theta}{ds}\right)^2\frac{d^2w}{ds^2}+4\frac{d\theta}{ds}\frac{d^2\theta}{ds^2}\frac{dw}{ds}+\left[2\frac{d\theta}{ds}\frac{d^3\theta}{ds^3}+2\left(\frac{d^2\theta}{ds^2}\right)^2+\frac{k}{D}\right]w$$
$$=\frac{1}{D}\left(q+\frac{d\theta}{ds}N\right)+\frac{d^2\theta}{ds^2}\frac{d^2v}{ds^2}+2\frac{d^3\theta}{ds^3}\frac{dv}{ds}+\frac{d^4\theta}{ds^4}v \tag{2-14}$$

Furthermore, if the shape of this isotropic curved beam is a circular arc, noting there is $\frac{d\theta}{ds}=\frac{1}{R}$ (constant), equation (2-13) then reduces to

$$\frac{d^4w}{ds^4}+\frac{1}{R^2}\frac{d^2w}{ds^2}+\frac{k}{D}w=\frac{1}{D}\left(q+\frac{N}{R}\right) \tag{2-15}$$

Differentiating equation (2-15) with respect to s and then substituting equations (2-2) and (2-3) into it to eliminate N, and also noting $s=R\theta$, the following differential equation for the case of circular isotropic beam on an elastic foundation is derived again

$$\frac{d^5w}{d\theta^5}+2\frac{d^3w}{d\theta^3}+\left(\frac{kR^4}{D}+1\right)\frac{dw}{d\theta}=\frac{R^4}{D}\frac{dq}{d\theta} \tag{2-16}$$

Analyses for this problem has been well documented (Hetenyi, 1946).

2.4 Circular composite beam on an elastic foundation

Consider the case of long cylindrical shell, which is the most usual case, in this section. Similarly to last section, assuming the deformation is independent of x, and $\varepsilon_x = 0$. Then this cylindrical shell can be considered as a circular composite beam with unit with, and assuming the radius of curvature of this circular beam is R. Hence, in equation (2-13) there is $\frac{d\theta}{ds}=\frac{1}{R}$ (constant) and $\frac{d^2\theta}{ds^2}=\frac{d^3\theta}{ds^3}=\frac{d^4\theta}{ds^4}=0$, and also noting $s=R\theta$. Then the differential equation (2-13) becomes:

$$\frac{d^4w}{d\theta^4}+\frac{d^2w}{d\theta^2}+\frac{kR^4}{D_{11}\left(1-\frac{B_{11}{}^2}{A_{11}}\right)}w=\frac{R^4}{D_{11}\left(1-\frac{B_{11}{}^2}{A_{11}}\right)}\left(q+\frac{B_{11}}{A_{11}}\frac{d^2N}{ds^2}+\frac{1}{R}N\right) \tag{2-17}$$

Differentiating equation (2-17) with respect to θ, and noting from equations (2-2) and (2-3), there is $\frac{dN}{d\theta}=\frac{1}{R}\frac{dM}{d\theta}$, and also substituting equation (2-12) in it, then the following governing differential equation for the problem of circular composite beam on an elastic foundation can be achieved.

$$\frac{d^5w}{d\theta^5}+2\frac{d^3w}{d\theta^3}+\left(\frac{kR^4}{D_{11}-\frac{B_{11}{}^2}{A_{11}}}+1\right)\frac{dw}{d\theta}=\frac{R^4}{D_{11}-\frac{B_{11}{}^2}{A_{11}}}\left(\frac{dq}{d\theta}+\frac{1}{R^2}\frac{B_{11}}{A_{11}}\frac{dN}{d\theta}+\frac{1}{R^2}\frac{B_{11}}{A_{11}}\frac{d^3N}{dx^3}\right) \tag{2-18}$$

Two conditions will be considered next.

1) N_0 = Constant

This is a common occurrence in the case of sandwich beams subjected to pure bending, where the axial force in the skin is a constant throughout the span. This, if coupled with the previous assumption of constant pressure q, leads to the right part of equation (2-18) being zero. The equation thus simplifies to be:

$$\frac{d^5w}{d\theta^5}+2\frac{d^3w}{d\theta^3}+\eta^{*2}\frac{dw}{d\theta}=0 \tag{2-19}$$

where:
$$\eta^*=\sqrt{\frac{R^4k}{D_{11}-\frac{B_{11}^2}{A_{11}}}+1} \tag{2-20}$$

The general solution of the homogeneous differential equation (2-19) is:

$$w = K_0 + (K_1 \cosh\alpha^*\theta + K_2 \sinh\alpha^*\theta)\cos\beta^*\theta + (K_3 \cosh\alpha^*\theta + K_4 \sinh\alpha^*\theta)\sin\beta^*\theta \tag{2-21}$$

where K_i are constants. From this, the reaction force of the elastic foundation can be deduced as:

$$p = \Lambda_0 + (\Lambda_1 \cosh\alpha^*\theta + \Lambda_2 \sinh\alpha^*\theta)\cos\beta^*\theta + (\Lambda_3 \cosh\alpha^*\theta + \Lambda_4 \sinh\alpha^*\theta)\sin\beta^*\theta \tag{2-22}$$

where
$$\begin{cases} \alpha^* = \sqrt{\dfrac{\eta^* - 1}{2}} \\ \beta^* = \sqrt{\dfrac{\eta^* + 1}{2}} \end{cases} \tag{2-23}$$

where $\Lambda_i = kK_i$, are also constants to be determined from boundary conditions.

2) $N = g_0 + g_1 \cos\theta$

This is the case when a curved sandwich beam is subjected to a pair of tension/compression forces at two ends. Again, the right hand side of equation (2-18) is zero again. Thus, the governing differential equation and solutions for the lateral deflection and reaction forces will be the same as (2-19), (2-21) and (2-22) respectively.

2.5 Circular mid-plane symmetric composite beam

For a laminate symmetric with respect to the midplane, the case becomes simpler, because there is no tension-bending coupling, i.e. $B_{ij} = 0$. Hence,

$$\begin{Bmatrix} M_x \\ M_s \\ M_{xs} \end{Bmatrix} = \begin{bmatrix} D_{11} & D_{12} & D_{16} \\ D_{12} & D_{22} & D_{26} \\ D_{16} & D_{26} & D_{66} \end{bmatrix} \cdot \begin{Bmatrix} \kappa_x \\ \kappa_s \\ \kappa_{xs} \end{Bmatrix} \tag{2-24}$$

Further, in the case of a special symmetric laminate whose material direction is the same as the principal direction, there is no bending-torsion coupling either, so D_{16} and D_{26} become zero. The above equation then turn to be:

$$\begin{Bmatrix} M_x \\ M_s \\ M_{xs} \end{Bmatrix} = \begin{bmatrix} D_{11} & D_{12} & 0 \\ D_{12} & D_{22} & 0 \\ 0 & 0 & D_{66} \end{bmatrix} \cdot \begin{Bmatrix} \kappa_x \\ \kappa_s \\ \kappa_{xs} \end{Bmatrix} \tag{2-25}$$

In such a case, and still considering a very long cylindrical shell and taking the assumption of the deformation independent of x, as in the above section about general laminate case, then:

$$\kappa = \frac{M}{D_{11}} \tag{2-26}$$

Substituting expression (2-11) in formula (2-26) and noting $\frac{d^2\theta}{ds^2}$:

$$D_{11}\left(\frac{d^2w}{dx^2} + \frac{w}{R^2}\right) = -M \tag{2-27}$$

Combining equation (2-6) with equation (2-27), and simultaneously making the substitution $s=R\theta$, the final differential equation can be obtained as:

$$\frac{d^5w}{d\theta^5} + 2\frac{d^3w}{d\theta^3} + \eta^2\frac{dw}{d\theta} = \frac{1}{D_{11}}\frac{1}{R}\frac{dq}{d\theta} \tag{2-28}$$

with: $$\eta = \sqrt{\frac{R^4 k}{D_{11}} + 1} \tag{2-29}$$

Again, noting that q is a constant, for a layered beam symmetric about its mid-plane the following differential equation is valid:

$$\frac{d^5 w}{d\theta^5} + 2\frac{d^3 w}{d\theta^3} + \eta^2 \frac{dw}{d\theta} = 0 \tag{2-30}$$

As can be seen, the form of equation (2-30) is the same as the form of equation (2-19). Only the coefficients η in (2-30) and η^* in (2-19) are different. As a consequence, the above equation (2-30) has the same form of solution:

$$w = K_0 + (K_1 \cosh \alpha\theta + K_2 \sinh \alpha\theta)\cos \beta\theta + (K_3 \cosh \alpha\theta + K_4 \sinh \alpha\theta)\sin \beta\theta \tag{2-31}$$

where again: $$\begin{cases} \alpha = \sqrt{\dfrac{\eta - 1}{2}} \\ \beta = \sqrt{\dfrac{\eta + 1}{2}} \end{cases} \tag{2-32}$$

The reaction force of the elastic foundation is:

$$p = kw = \Lambda_0 + (\Lambda_1 \cosh \alpha\theta + \Lambda_2 \sinh \alpha\theta)\cos \beta\theta + (\Lambda_3 \cosh \alpha\theta + \Lambda_4 \sinh \alpha\theta)\sin \beta\theta \tag{2-33}$$

The coefficients Λ_i in the above formula can also be determined from boundary conditions. If the curved beam is symmetric with respect to the axis $\theta = 0$, then in the equations (2-31) and (2-33), only even-function parts remain:

$$w = K_0 + K_1 \cosh\alpha\theta \cos\beta\theta + K_4 \sinh\alpha\theta \sin\beta\theta \tag{2-34}$$

$$p = \Lambda_0 + \Lambda_1 \cosh\alpha\theta \cos\beta\theta + \Lambda_4 \sinh\alpha\theta \sin\beta\theta \tag{2-35}$$

2.6 Distributions of bending moment and shear force

For a beam symmetric with respect to the axis $\theta = 0$, and from the geometry of the beam, it can be deduced that:

$$\begin{aligned} -\kappa &= \frac{1}{R^2}\frac{d^2w}{d\theta^2} + \frac{1}{R^2}w \\ &= \frac{1}{R^2}\left[\left(K_1\alpha^2 + 2K_4\alpha\beta - K_1\beta^2 + K_1\right)\cosh\alpha\theta\cos\beta\theta + \right. \\ &\quad \left.\left(K_4\alpha^2 - 2K_1\alpha\beta - K_4\beta^2 + K_4\right)\sinh\alpha\theta\sin\beta\theta + K_0\right] \end{aligned} \tag{2-36}$$

Noting the general form of the relationships in equations (2-20) and (2-23), the following relationships can be deduced:

$$\alpha^2 - \beta^2 = -1 \quad \text{and} \quad \alpha\beta = \sqrt{\frac{1}{2}\cdot\frac{R^4 k}{D_{11} - \frac{B_{11}^2}{A_{11}}}} \tag{2-37}$$

Combining equations (2-36) and (2-10) and using equation (2-37), the expression for bending moment becomes:

$$\begin{aligned} M = \frac{B_{11}}{A_{11}}N - \left(D_{11} - \frac{B_{11}^2}{A_{11}}\right)\frac{1}{R^2}\left[K_0 + 2K_4\alpha\beta\cosh\alpha\theta\cos\beta\theta \right. \\ \left. - 2\alpha\beta K_1 \sinh\alpha\theta\sin\beta\theta\right] \end{aligned} \tag{2-38}$$

From equation (2-3), and using the relationship for M from equation (2-38), the expression for Q becomes:

$$Q=\frac{B_{11}}{A_{11}}\frac{dN}{d\theta}\frac{1}{R}-\frac{1}{R^3}\left(D_{11}-\frac{B_{11}^{\ 2}}{A_{11}}\right)\cdot\left[\left(2K_1\alpha^2\beta-2K_4\alpha\beta^2\right)\cosh\alpha\theta\sin\beta\theta+\left(2K_1\alpha\beta^2-2K_4\alpha^2\beta\right)\sinh\alpha\theta\cos\beta\theta\right] \tag{2-39}$$

Also, from equations (2-2) and (2-39), the following relationship can be derived:

$$\frac{1}{R^2}\left(D_{11}-\frac{B_{11}^{\ 2}}{A_{11}}\right)\cdot\left[\left(2K_1\alpha^2\beta-2K_4\alpha\beta^2\right)\cosh\alpha\theta\sin\beta\theta+\left(2K_1\alpha\beta^2+2K_4\alpha^2\beta\right)\sinh\alpha\theta\cos\beta\theta\right]$$
$$=\left(\frac{B_{11}}{A_{11}}-R\right)\frac{dN}{d\theta} \tag{2-40}$$

When $N=N_0$, i.e. a constant, it can be seen that the above equation is satisfied under any value of θ only when: $K_1=K_4=0$. Thus, for constant $N=N_0$, the following results will hold true:

$$\begin{cases} M=\dfrac{B_{11}}{A_{11}}N_0-(D_{11}-\dfrac{B_{11}^{\ 2}}{A_{11}})\dfrac{K_0}{R^2} \\ N_0=RkK_0 \\ p=kK_0 \\ Q=0 \end{cases} \tag{2-41}$$

The above conclusion shows that even in a general case where: (a) tension-bending coupling occurs as a result of the laminate layer; and (b) the beam is subjected to in-plane forces N and bending moments M, the shear force Q still is zero. Consequently, the curved beam on elastic foundation can still be considered as the problem in which stresses are independent of polar angle.

2.7 The effect of tension-bending coupling in general laminate

By comparing formula (2-29) to formula (2-20), it is obvious that:

$$\eta^* > \eta \tag{2-42}$$

then, according to formula (2-32) and (2-23):

$$\alpha^* > \alpha \ ; \ \beta^* > \beta \tag{2-43}$$

Therefore, the existence of tension-bending coupling in curved layered composite beam results in a bit larger oscillation in the distributions of mechanical variables p, w and M, N etc. along the span of curved beam.

2.8 The solutions by taking into account the thickness of laminate

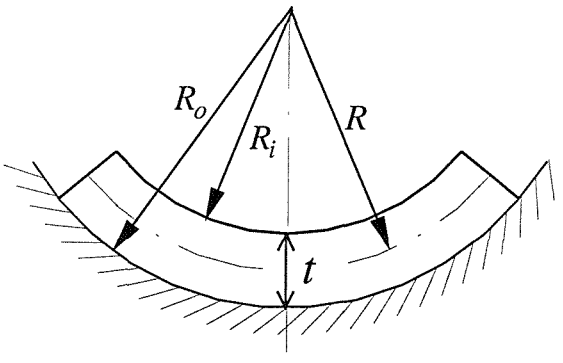

Figure 2.3 Curved beam with thickness of t on an elastic foundation

Thickness of the laminate can be incorporated into the equations. If the thickness of laminate t is taken into account, equilibrium condition in radial direction (2-1) becomes:

$$p(\frac{ds}{d\theta}+\frac{t}{2})d\theta - Nd\theta - q(\frac{ds}{d\theta}-\frac{t}{2})d\theta = dQ \tag{2-44a}$$

Thus equilibrium equation (2-6) changes to be:

$$k(1+\frac{t}{2}\frac{d\theta}{ds})w-(1-\frac{t}{2}\frac{d\theta}{ds})q-N\frac{d\theta}{ds}=\frac{d^2M}{ds^2} \tag{2-45a}$$

If it is an circular arch with constant curvature radius R, the above two equations (2-44a) and (2-45a) turn to be:

$$p(R+\frac{t}{2})d\theta - Nd\theta - q(R-\frac{t}{2})d\theta = dQ \tag{2-44b}$$

$$k(1+\frac{t}{2R})w-(1-\frac{t}{2R})q-\frac{N}{R}=\frac{d^2M}{ds^2} \tag{2-45b}$$

And also considering the existence of unidistributed pressure acting downwards on the inner surface of curved beam q_0, as well as constant $N = N_0$, by the similar deduction in the above subsections, following equations can be finally obtained:

$$\begin{cases} M=\dfrac{B_{11}}{A_{11}}N_0-(D_{11}-\dfrac{B_{11}^{\ 2}}{A_{11}})\cdot\dfrac{K_0}{R^2} \\ N_0=k(R+\dfrac{t}{2})K_0-q_0(R-\dfrac{t}{2}) \\ p=kK_0 \\ Q=0 \end{cases} \tag{2-46}$$

These results will be used in the following Chapters as force boundary conditions when an accurate general solution of orthotropic beam on an elastic foundation is obtained using a stress function approach.

Chapter 3 Estimation of Response Using Airy Stress Function Approach

A very long cylindrical shell is still considered here, and also the applied forces and boundary conditions are both assumed uniform in cylinder axial direction (x-direction), thus the deformation is independent of x. Therefore the present problem can be analysed as a generalised plane-strain problem.

3.1 Airy stress function and compatibility equation

By introducing the Airy stress function in polar coordinates $\Phi(r,\theta)$, the stresses can be written as (Timoshenko, 1934):

$$\begin{cases} \sigma_r = \dfrac{1}{r}\dfrac{\partial \Phi}{\partial r} + \dfrac{1}{r^2}\dfrac{\partial^2 \Phi}{\partial \theta^2} \\ \sigma_\theta = \dfrac{\partial^2 \Phi}{\partial r^2} \\ \tau_{r\theta} = -\dfrac{\partial}{\partial r}\left(\dfrac{1}{r}\dfrac{\partial \Phi}{\partial \theta}\right) \end{cases} \tag{3-1}$$

The above equation automatically satisfies the equilibrium equations. For the problem under consideration, the stress components do not depend on θ and, in addition, $\tau_{r\theta} \equiv 0$ (i.e. constant in-plane force and hydrostatic load).

For the cylindrical material anisotropy, a compatibility equation can be obtained as (Lekhnitskii, 1981):

$$\frac{d^4\Phi}{dr^4} + \frac{2}{r}\cdot\frac{d^3\Phi}{dr^3} - \frac{\lambda}{r^2}\cdot\frac{d^2\Phi}{dr^2} + \frac{\lambda}{r^3}\cdot\frac{d\Phi}{dr} = 0 \tag{3-2}$$

where $\lambda = \frac{E_2}{E_1}$ (3-3)

where E_1 and E_2 are the elastic moduli in the in-plane and through-thickness directions respectively, and λ is known as anisotropy ratio. As can be seen, the stress distribution in anisotropic material depends on the elastic constants of material, which is different from isotropic material.

3.2 General solution

The general solution to the ordinary differential equation (3-2) is:

$$\Phi = C_1 + C_2 r^2 + C_3 r^{1+\sqrt{\lambda}} + C_4 r^{1-\sqrt{\lambda}} \tag{3-4}$$

from which stress components can be obtained:

$$\begin{cases} \sigma_r = 2C_2 + (1+\sqrt{\lambda})C_3 \cdot r^{\sqrt{\lambda}-1} + (1-\sqrt{\lambda})C_4 \cdot r^{-\sqrt{\lambda}-1} \\ \sigma_\theta = 2C_2 + (1+\sqrt{\lambda})\sqrt{\lambda}C_3 \cdot r^{\sqrt{\lambda}-1} - (1-\sqrt{\lambda})\sqrt{\lambda}C_4 \cdot r^{-\sqrt{\lambda}-1} \end{cases} \tag{3-5}$$

where C_2, C_3 and C_4 are all constants which need to be determined.

3.3 Determination of coefficients in solution

In solving the problem, the coefficients C_2, C_3 and C_4 in the above expressions (3-5) can be determined from appropriate boundary conditions. Equations of (2-46) obtained in the previous chapter are then considered as the necessary boundary conditions here. From equations of (2-46) and the geometry and considering the direction of the forces, also according to St. Venant Principle, the following relationships can then be deduced:

$$\begin{cases} r = R + \dfrac{t}{2}: \quad \sigma_r = p_0 = -kK_0 \\ r = R - \dfrac{t}{2}: \quad \sigma_r = -q_0 \\ \int_{R-\frac{t}{2}}^{R+\frac{t}{2}} \sigma_\theta dr = N_0 = -k(R + \dfrac{t}{2})K_0 + q_0(R - \dfrac{t}{2}) \\ \int_{R-\frac{t}{2}}^{R+\frac{t}{2}} \sigma_\theta r d\theta = M_0 \end{cases} \tag{3-6}$$

Substituting the expressions of stress components (3-5) into the above boundary condition (3-6), then an equation group about the coefficients C_2, C_3 and C_4 can be obtained. In this equation group, there are four equations but only three unknown variables. However, it can be seen that the third equation is automatically satisfied when the first and second equations are both satisfied. This equation group can be solved to yield values of coefficients C_1, C_2 and C_3. For simplification of the solution the entity δ can be introduced:

$$\delta = \frac{R_i}{R_o} \tag{3-7}$$

Here: $R_i = R - \dfrac{t}{2}$ is the inner radius of curved beam. $R_o = R + \dfrac{t}{2}$ is the outer radius of curved beam. Also introducing Δ, Δ_3 and Δ_4 as:

$$\begin{aligned} \Delta &= \begin{vmatrix} \left(1+\sqrt{\lambda}\right)(1-\delta^{\sqrt{\lambda}-1}) & \left(1-\sqrt{\lambda}\right)(1-\delta^{-\sqrt{\lambda}-1}) \\ \left(\sqrt{\lambda}-1\right)(1-\delta^{\sqrt{\lambda}+1}) & \left(1+\sqrt{\lambda}\right)(\delta^{-\sqrt{\lambda}+1}-1) \end{vmatrix} \\ \Delta_3 &= \begin{vmatrix} -kK_0 + q_0 & \left(1-\sqrt{\lambda}\right)(1-\delta^{-\sqrt{\lambda}-1})R_o^{-2} \\ 2M_0 + kK_0R_o^{\,2} - qR_i^{\,2} & \left(1+\sqrt{\lambda}\right)(\delta^{1-\sqrt{\lambda}}-1) \end{vmatrix} \\ \Delta_4 &= \begin{vmatrix} \left(1+\sqrt{\lambda}\right)(1-\delta^{\sqrt{\lambda}-1})R_o^{-2} & -kK_0 + q_0 \\ \left(\sqrt{\lambda}-1\right)(1-\delta^{\sqrt{\lambda}+1}) & 2M_0 + kK_0R_o^{\,2} - qR_i^{\,2} \end{vmatrix} \end{aligned} \tag{3-8}$$

and denoting the relationships:

$$\begin{aligned}\overline{\Delta}_3 &= \frac{\Delta_3}{\Delta} \\ \overline{\Delta}_4 &= \frac{\Delta_4}{\Delta}\end{aligned} \tag{3-9}$$

The coefficients of the stress formulae can then be obtained as:

$$\begin{aligned}2C_2 &= -kK_0 - (1+\sqrt{\lambda})\overline{\Delta}_3 - (1-\sqrt{\lambda})\overline{\Delta}_4 \\ C_3 &= \overline{\Delta}_3 \cdot R_o^{\,1-\sqrt{\lambda}} \\ C_4 &= \overline{\Delta}_4 \cdot R_o^{\,1+\sqrt{\lambda}}\end{aligned} \tag{3-10}$$

Substituting them into equations (3-5), the corresponding solution of stresses σ_r and σ_θ are:

$$\begin{cases}\sigma_r = \left[-kK_0 - (1+\sqrt{\lambda})\overline{\Delta}_3 - (1-\sqrt{\lambda})\overline{\Delta}_4\right] + (1+\sqrt{\lambda})\overline{\Delta}_3\left(\frac{r}{R_o}\right)^{\sqrt{\lambda}-1} \\ \qquad\qquad + (1-\sqrt{\lambda})\overline{\Delta}_4\left(\frac{r}{R_o}\right)^{-\sqrt{\lambda}-1} \\ \sigma_\theta = \left[-kK_0 - (1+\sqrt{\lambda})\overline{\Delta}_3 - (1-\sqrt{\lambda})\overline{\Delta}_4\right] + (1+\sqrt{\lambda})\cdot\sqrt{\lambda}\cdot\overline{\Delta}_3\left(\frac{r}{R_o}\right)^{\sqrt{\lambda}-1} \\ \qquad\qquad - (1-\sqrt{\lambda})\cdot\sqrt{\lambda}\cdot\overline{\Delta}_4\left(\frac{r}{R_o}\right)^{-\sqrt{\lambda}-1}\end{cases} \tag{3-11}$$

3.4 Maximum value of σ_r

The location of the maximum value of σ_r, and consequently the most likely location for delamination in a laminate, is obtained using:

$$\frac{\partial \sigma_r}{\partial r} = 0 \tag{3-12}$$

Using the following notation:

$$r = R + \xi \quad ; \qquad -\frac{t}{2} \le \xi \le \frac{t}{2} \tag{3-13}$$

And substituting expression (3-11) into equation (3-12), then the solution can be obtained as:

$$\xi^* = \left[\left(-\frac{\overline{\Delta}_4}{\overline{\Delta}_3} \right)^{\frac{1}{2\sqrt{\lambda}}} - \frac{1+\delta}{2} \right] R_o \tag{3-14}$$

Then $r^* = R + \xi^*$

which indicates the radial location where the maximum through-thickness stress σ_r maybe exists.

Actually the result directly obtained from equation (3-14) is the location of stationary value of σ_r, as shown by equation (3-12). Sometimes it corresponds to the minimum value and sometimes its value ξ^* exceeds the thickness scale of the considered curved beam ($-\frac{t}{2} \le \xi \le \frac{t}{2}$). Therefore, the values of through-thickness tension stress at three locations should be calculated separately, as $\sigma_r\big|_{r=R_i}$, $\sigma_r\big|_{r=r^*}$ and $\sigma_r\big|_{r=R_o}$ by equation (3-11). And then denoting:

$$\sigma_{r\max} = Max(\sigma_r\big|_{r=R_i}, \sigma_r\big|_{r=r^*}, \sigma_r\big|_{r=R_o}) \tag{3-15}$$

which is the value of maximum through-thickness stress σ_r.

3.5 Corresponding results for curved isotropic beam

Here it should be noted that the above anisotropic solution cannot be extended to the isotropic case only taking $\lambda = \frac{E_2}{E_1} = 1$, though convergence to the isotropic solution can be achieved by putting λ close to 1. As is known, the isotropic material case of $\lambda = 1$ actually corresponds to a double root of the characteristic equation arising from the generalised differential equation (3-2), leading to the logarithmic term in the expression of stress components and stress function. In homogeneous isotropic materials, as to the problem of plane symmetrical about the axis, the stress distribution can be described as (Timoshenko, 1934):

$$\begin{cases} \sigma_r = \dfrac{a}{r^2} + b(1 + 2\ln r) + 2c \\ \sigma_\theta = -\dfrac{a}{r^2} + b(3 + 2\ln r) + 2c \\ \tau_{r\theta} = 0 \end{cases} \tag{3-16}$$

If same boundary conditions as in equation (3-6) are assumed, then the constants in the expressions (3-16) can be determined as:

$$\begin{cases} a = \dfrac{R_o^{\,2} R_i^{\,2}}{R_i^{\,2} - R_o^{\,2}} \left[(q_0 - p_0) - 2\ln\dfrac{R_o}{R_i} b \right] \\ b = \dfrac{2\left(R_i^{\,2} - R_o^{\,2}\right) M_0 - R_o^{\,2}\left(R_i^{\,2} - R_o^{\,2}\right) p_0 - 2R_o^{\,2} R_i^{\,2} \ln\dfrac{R_i}{R_o}(q_0 - p_0)}{4R_o^{\,2} R_i^{\,2} \ln^2\dfrac{R_o}{R_i} - \left(R_i^{\,2} - R_o^{\,2}\right)^2} \\ 2c = -p_0 - \dfrac{a}{R_o^2} - (1 + 2\ln R_o) b \end{cases} \tag{3-17}$$

Chapter 4: General Solution for Curved Laminates and Sandwich Beams

4.1 Introduction

Based on the solutions in Chapter 3, further analysis can be done to obtain a general solution for the problem of through-thickness stress in curved composite laminates and sandwich beams. A curved layered beam subjected to no-circumferential-dependence loads is considered in this chapter, as shown in Figure 4.1. This layered beam is composed of arbitrary number of layers among which each layer can be considered as an curved orthotropic beam or isotropic beam (e.g. 90° stacking laminae in laminate or core material in sandwich beam). Thus the solutions in Chapter 3 can be used here to analyse every layer in curved layered beam.

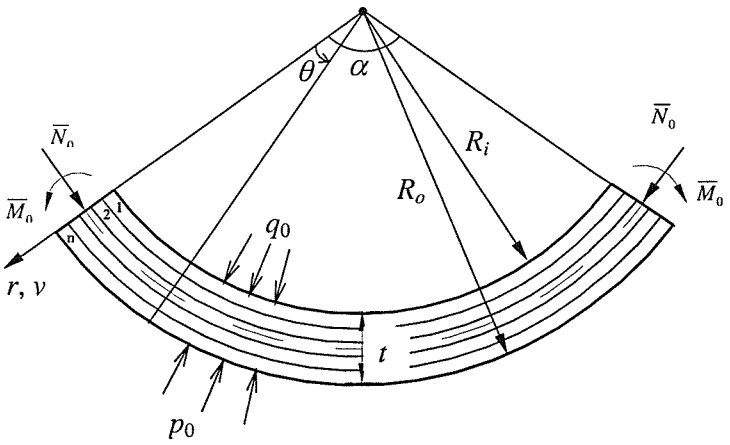

Figure 4.1 Typical curved composite beam under loads

4.2 Extension of solution for curved orthotropic beam to layered beam

Assuming there are n layers in curved composite beam, where every layer has the elastic coefficients:

$$E_1^{(i)},\ E_2^{(i)},\ \nu_{12}^{(i)} \text{ and } \nu_{21}^{(i)}$$

and where the superscript (i) means this variable is related to the ith layer. The boundary conditions to be satisfied in every layer are as follows:

$$\begin{cases} r = r_{i-1}: & \sigma_r = \sigma_r^{(i-1)} \\ r = r_i: & \sigma_r = \sigma_r^{(i)} \\ \int_{r_{i-1}}^{r_i} \sigma_\theta \cdot dr = N^{(i)} \\ \int_{r_{i-1}}^{r_i} \sigma_\theta \cdot r \cdot dr = M^{(i)} \end{cases} \tag{4-1}$$

where $\sigma_r^{(i)}$ is normal tension stress in the interface between ith layer and $(i+1)$th layer. In addition, following on from equation (2-46), there exist the following relations:

$$\begin{cases} N^{(i)} = \sigma_r^{(i)} \cdot r_i - \sigma_r^{(i-1)} \cdot r_{i-1} \\ M^{(i)} = \dfrac{B_{11}^{(i)}}{A_{11}^{(i)}} \cdot N^{(i)} - \left(D_{11}^{(i)} - \dfrac{B_{11}^{(i)2}}{A_{11}^{(i)}} \right) \cdot \dfrac{4C_0^{(i)}}{\left(r^{(i)} + r^{(i-1)}\right)^2} \end{cases} \tag{4-2}$$

where $C_0^{(i)}$ is assumed to be the radial displacement of ith layer in the global curved composite layered beam.

In fact, every layer in the curved composite beam can be considered as an orthotropic beam or isotropic beam, with the interaction forces between adjacent layers taken as the reaction force of a kind of "elastic foundation"$-p$ and the water pressure $-q$. This is because in a mathematical context, $\sigma_r^{(i-1)}$ and q, $\sigma_r^{(i)}$ and p have the same meaning. They are only constants in the formulae, under no-circumferential-dependence condition.

Then we analyse the plies of global laminate one by one. From boundary conditions for each ply--equations (4-1) and equations (3-11), the distributions of through-thickness stress-σ_r and in-plane stress-σ_θ in each ply can be expressed in form of functions of $\sigma_r^{(i)}\big|_{i=1,2,\cdots,n}$ and $C_0^{(i)}\big|_{i=1,2,\cdots,n}$, e.g. in the ith layer, they are:

$$\begin{cases} \sigma_r = \left[\sigma_r^{(i)} - (1+\sqrt{\lambda^{(i)}})\overline{\Delta}_3^{(i)} - (1-\sqrt{\lambda^{(i)}})\overline{\Delta}_4^{(i)}\right] + (1+\sqrt{\lambda^{(i)}})\overline{\Delta}_3^{(i)}(\frac{r}{r_i})^{\sqrt{\lambda^{(i)}}-1} \\ \qquad\qquad + (1-\sqrt{\lambda^{(i)}})\overline{\Delta}_4^{(i)}(\frac{r}{r_i})^{-\sqrt{\lambda^{(i)}}-1} \\ \sigma_\theta = \left[\sigma_r^{(i)} - (1+\sqrt{\lambda^{(i)}})\overline{\Delta}_3^{(i)} - (1-\sqrt{\lambda^{(i)}})\overline{\Delta}_4\right] + (1+\sqrt{\lambda^{(i)}})\sqrt{\lambda^{(i)}}\overline{\Delta}_3^{(i)}(\frac{r}{r_i})^{\sqrt{\lambda^{(i)}}-1} \\ \qquad\qquad - (1-\sqrt{\lambda^{(i)}})\sqrt{\lambda^{(i)}}\overline{\Delta}_4^{(i)}(\frac{r}{r_i})^{-\sqrt{\lambda^{(i)}}-1} \end{cases} \tag{4-3}$$

where the denotations of variables are all analogue to those in last section, among which $\overline{\Delta}_3{}^{(i)} = \dfrac{\Delta_3{}^{(i)}}{\Delta^{(i)}}$, $\overline{\Delta}_4{}^{(i)} = \dfrac{\Delta_4{}^{(i)}}{\Delta^{(i)}}$, and here are:

$$\begin{aligned} \Delta^{(i)} &= \begin{vmatrix} \left(1+\sqrt{\lambda^{(i)}}\right)(1-\delta^{(i)\sqrt{\lambda^{(i)}}-1}) & \left(1-\sqrt{\lambda^{(i)}}\right)(1-\delta^{(i)-\sqrt{\lambda^{(i)}}-1}) \\ \left(\sqrt{\lambda^{(i)}}-1\right)(1-\delta^{(i)\sqrt{\lambda^{(i)}}+1}) & \left(1+\sqrt{\lambda^{(i)}}\right)(\delta^{(i)-\sqrt{\lambda^{(i)}}+1}-1) \end{vmatrix} \\ \Delta_3{}^{(i)} &= \begin{vmatrix} \sigma_r^{(i)} - \sigma_r^{(i-1)} & \left(1-\sqrt{\lambda^{(i)}}\right)(1-\delta^{(i)-\sqrt{\lambda^{(i)}}-1})r_i^{-2} \\ 2M^{(i)} - \sigma_r^{(i)}r_i^{\,2} + \sigma_r^{(i-1)}r_{i-1}^{\,2} & \left(1+\sqrt{\lambda^{(i)}}\right)(\delta^{(i)1-\sqrt{\lambda^{(i)}}}-1) \end{vmatrix} \\ \Delta_4{}^{(i)} &= \begin{vmatrix} \left(1+\sqrt{\lambda^{(i)}}\right)(1-\delta^{(i)\sqrt{\lambda^{(i)}}-1})\cdot r_i^{-2} & \sigma_r^{(i)} - \sigma_r^{(i-1)} \\ \left(\sqrt{\lambda^{(i)}}-1\right)(1-\delta^{(i)\sqrt{\lambda^{(i)}}+1}) & 2M^{(i)} - \sigma_r^{(i)}r_i^{\,2} + \sigma_r^{(i-1)}r_{i-1}^{\,2} \end{vmatrix} \end{aligned} \tag{4-4}$$

where the superscript (i) means this variable is related to the i th layer.

As in the analysis for the curved orthotropic beam in the last chapter, here too the known boundary conditions at inner and outer surfaces of the curved layered beam can be imposed for the global curved layered beam:

$$\begin{cases} r = r_{i=0} = R_i : & \sigma_r = -q_0 \\ r = r_{i=N} = R_o : & \sigma_r = -p_0 \end{cases} \tag{4-5}$$

Therefore, in the analysis of the whole laminate, there exist unknown variables $\sigma_r^{(i)}\big|_{i=1,2,\cdots,n-1}$ and $C_0^{(i)}\big|_{i=1,2,\cdots,n}$. The number of these variables is $n+(n-1)=2n-1$ in all.

4.3 The displacement compatibility conditions on the interfaces

Following the above section, the task left is to determine these variables by appropriate conditions. The displacement compatibility conditions on the interface can then be used to achieve this goal. Because of the plane-strain assumption, the equations of Hooke's Law of anisotropic material (see Appendix A) can be expressed.

$$\begin{cases} \varepsilon_r = \dfrac{1}{E_2'} \cdot \sigma_r - \dfrac{\nu_{12}'}{E_1'} \cdot \sigma_\theta \\ \varepsilon_\theta = -\dfrac{\nu_{21}'}{E_2'} \cdot \sigma_r + \dfrac{1}{E_1'} \cdot \sigma_\theta \\ \varepsilon_{r\theta} = \dfrac{1}{2\mu_{12}} \cdot \tau_{r\theta} \end{cases} \tag{4-6}$$

where:

$$E_1' = \frac{E_1}{1-\nu_{13}\nu_{31}}, \qquad E_2' = \frac{E_2}{1-\nu_{23}\nu_{32}}$$

$$\nu_{12}' = \frac{\nu_{12}+\nu_{13}\nu_{32}}{1-\nu_{13}\nu_{31}}, \qquad \nu_{21}' = \frac{\nu_{21}+\nu_{23}\nu_{31}}{1-\nu_{23}\nu_{32}} \tag{4-7}$$

Combining equation (4-3), (4-6) and (4-7) with the relationship between strain components and displacement components in polar coordinates:

$$\varepsilon_r = \frac{\partial u_r}{\partial r}\ ,\ \varepsilon_\theta = \frac{u_r}{r} + \frac{1}{r}\cdot\frac{\partial u_\theta}{\partial \theta}\ ,\ \gamma_{r\theta} = \frac{1}{r}\cdot\frac{\partial u_r}{\partial \theta} + \frac{\partial u_\theta}{\partial r} - \frac{u_\theta}{r} \tag{4-8}$$

By integrating the above equations and noting the relation: $\frac{\nu'_{12}}{E'_1} = \frac{\nu'_{21}}{E'_2}$, $\lambda = \frac{E'_2}{E'_1}$, the solution of displacement in ith layer can be finally obtained as:

$$\begin{aligned} u_r = & \left(\frac{1}{E_1'^{(i)}} - \frac{\nu_{21}'^{(i)}}{E_2'^{(i)}}\right)\cdot\left[\sigma_r^{(i)} - (1+\sqrt{\lambda^{(i)}})\overline{\Delta}_3^{(i)} - (1-\sqrt{\lambda^{(i)}})\overline{\Delta}_4^{(i)}\right]\cdot r + \\ & \frac{R_o}{\sqrt{\lambda^{(i)}}}\cdot\left[\left(1+\sqrt{\lambda^{(i)}}\right)\cdot\frac{1}{E_1'^{(i)}} - \left(\sqrt{\lambda^{(i)}}+\lambda^{(i)}\right)\cdot\frac{\nu_{21}'^{(i)}}{E_2'^{(i)}}\right]\cdot\overline{\Delta}_3^{(i)}\cdot\left(\frac{r}{R_o}\right)^{\sqrt{\lambda^{(i)}}} - \\ & \frac{R_o}{\sqrt{\lambda^{(i)}}}\cdot\left[\left(1-\sqrt{\lambda^{(i)}}\right)\cdot\frac{1}{E_1'^{(i)}} + \left(\sqrt{\lambda^{(i)}}-\lambda^{(i)}\right)\cdot\frac{\nu_{21}'^{(i)}}{E_2'^{(i)}}\right]\cdot\overline{\Delta}_4^{(i)}\cdot\left(\frac{r}{R_o}\right)^{-\sqrt{\lambda^{(i)}}} + f^{(i)}(\theta) \\ u_\theta = & \left(-\frac{1}{E_1'^{(i)}} + \frac{1}{E_2'^{(i)}}\right)\cdot\left[\sigma_r^{(i)} - (1+\sqrt{\lambda^{(i)}})\overline{\Delta}_3^{(i)} - (1-\sqrt{\lambda^{(i)}})\overline{\Delta}_4^{(i)}\right]\cdot r\theta - \int f^{(i)}(\theta)d\theta \end{aligned} \tag{4-9}$$

where the superscript (i) means this variable is related to the i th layer. The arbitrary function $f^{(i)}(\theta)$ in the above equations can be determined by the end displacement boundary conditions of individual layer of global curved composite beam. We assume that these arbitrary functions $f^{(i)}(\theta)$ corresponding to every layer are all the same in the whole layered beam, provided that there are no delamination or considerable shear slide on interfaces in this curved composite beam being considered.

Known from Chapter 3, also the above anisotropic solution of displacement cannot be extended to the isotropic case by only taking $\lambda = \frac{E_2}{E_1} = 1$. In homogeneous isotropic materials, as to the same problem, the displacement distribution in the jth layer (here it is

assumed that the jth layer can be considered as isotropic case, for example, the core in sandwich beam or 90° stacking laminae) is:

$$\begin{cases} u_r = \dfrac{1}{E^{(j)}}[-\dfrac{1}{r}(1+\nu)a^{(j)} + 2(1-\nu)b^{(j)} r\ln r - (1+\nu)b^{(j)} r + 2(1-\nu)c^{(j)} r] + g^{(j)}(\theta) \\ u_\theta = \dfrac{4b^{(j)} r\theta}{E^{(j)}} - \int g^{(j)}(\theta)d\theta \end{cases} \tag{4-10}$$

Similarly to the anisotropic case, the arbitrary function $g^{(j)}(\theta)$ in the above expression can also be determined by end boundary conditions of this analysed layer. And here we still assume that arbitrary functions $g^{(j)}(\theta)$ or $f^{(i)}(\theta)$ are all the same, if there is no delamination or considerable shear slide occurring on interfaces in the whole layered beam. According to equation (4-1), then the constants in the above expressions (4-10) can be determined as:

$$\begin{cases} a^{(j)} = \dfrac{r_i^2 r_{i-1}^2}{R_i^2 - r_i^2}\left[\left(\sigma_r^{(i)} - \sigma_r^{(i-1)}\right) - 2\ln\dfrac{r_i}{R_i}b^{(j)}\right] \\ b^{(j)} = \dfrac{2\left(r_{i-1}^2 - r_i^2\right)M^{(j)} + r_i^2\left(r_{i-1}^2 - r_i^2\right)\sigma_r^{(i)} - 2r_i^2 r_{i-1}^2 \cdot \ln\dfrac{r_{i-1}}{r_i}\cdot\left(\sigma_r^{(i)} - \sigma_r^{(i-1)}\right)}{4r_i^2 r_{i-1}^2 \ln^2\dfrac{r_i}{r_{i-1}} - \left(r_{i-1}^2 - r_i^2\right)^2} \\ 2c^{(j)} = \sigma_r^{(i)} - \dfrac{a^{(j)}}{r_i^2} - b^{(j)}\left(1 + 2\ln r_i\right) \end{cases} \tag{4-11}$$

The displacement compatibility conditions on the interfaces can be represented as:

$$\begin{cases} u_r^{(i+1)}(r_i) = u_r^{(i)}(r_i) & i = 1,2,\cdots,n-1 \\ u_\theta^{(i+1)}(r_i) = u_\theta^{(i)}(r_i) & i = 1,2,\cdots,n-1 \end{cases} \tag{4-12}$$

$u_r^{(i)}(r), u_\theta^{(i)}(r)$ are as expressed in equations (4-9), or equation (4-10), according to that this layer is orthotropic beam or isotropic beam under consideration.

4.4 The global force boundary condition

Apart from these, for the case of curved beam on an elastic foundation under no-circumferential-dependence condition, as shown in Figure 4.2a, there is the global force boundary condition:

$$\sum_{i=1}^{n} N^{(i)} = \overline{N}_0 = kR_o C_0^{(n)} - q_0 R_i \tag{4-13a}$$

where $p_0 = kC_0^{(n)}$

And for the case of curved beam subjected to pure bending, as shown in Figure 4.2b because there is no axial force $\overline{N}_0$, another global force boundary condition is provided according to the global equilibrium by equation (2-41):

$$\overline{M}_0 = \frac{B_{11}}{A_{11}} \cdot \overline{N}_0 - \left(D_{11} - \frac{B_{11}^{\ 2}}{A_{11}} \right) \cdot \frac{4C_0^{(n)}}{\left(R_i + R_o\right)^2} = -\left(D_{11} - \frac{B_{11}^{\ 2}}{A_{11}} \right) \cdot \frac{4C_0^{(n)}}{\left(R_i + R_o\right)^2} \tag{4-13b}$$

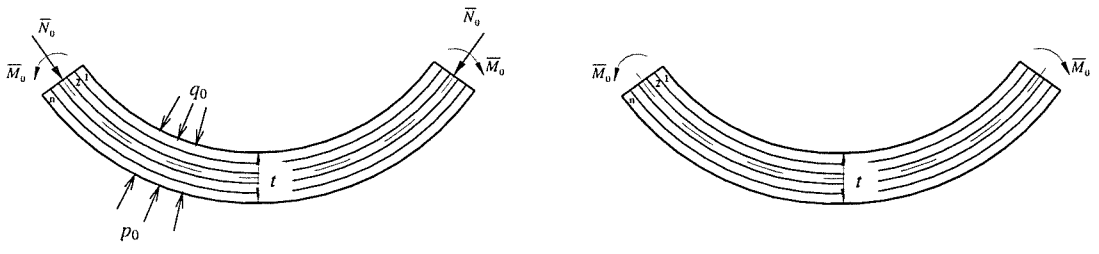

Figure 4.2 Curved layered beam under different load condition

As can be seen, there are: $2\times(n-1)+1 = 2n-1$ equations altogether, just the same as the number of unknown variables. Thus the problem can be solved. Consequently, the

through-thickness tensile/compressive stress-σ_r and in-plane tensile/compressive stress-σ_θ in the present curved composite laminate can both be obtained. However, it should be noted that this general solution for curved layered composite beam on elastic foundation is under no-circumferential-dependence condition. Note also that $\sigma_r^{(i)}\big|_{i=1,2,\cdots,n}$ are the tensile through thickness stresses between every two adjacent layers – interface tension stress, which many researchers and engineers are concerned.

The application and discussion of the theoretical approach developed in this chapter will be shown in chapters 7 and 9.

Chapter 5: Stability of Curved Beam on an Elastic Foundation

5.1 Background

The background of the presented problem is the local instability of skin of curved sandwich beam.

5.2 Problem statement

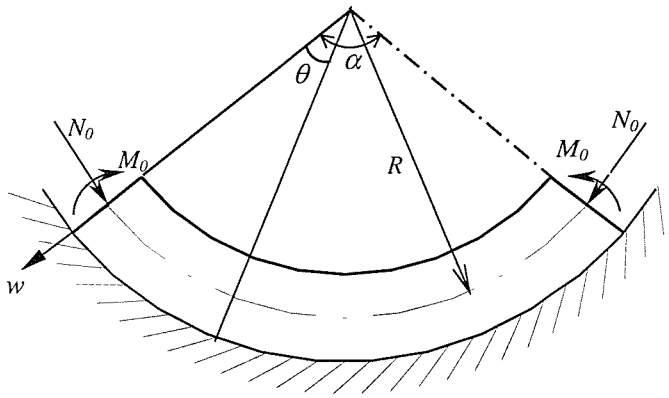

Figure.5.1 Curved laminate on an elastic foundation

Consider a curved beam lying on an elastic foundation which is subjected to compressed axial force and bending moment. It also possesses the possibility of instability, analogue to the problem of buckling of straight bar on an elastic medium which was first discussed by S.Timoshenko (1936). However, the geometry curvature of the beam make the problem more complicated. Here the Winkler hypothesis (Selvadurai, 1979) is still assumed, which means that the reaction of the elastic foundation, at each cross section of

the beam, is proportional to the normal deflection at that cross section and in the normal (i.e. radial) direction.

In the usual case of a curved sandwich beam subjected to pure bending, for example, closing bending moment, its inner face is then under compression and buckling or wrinkling are possible to occur. In this Chapter, the core is considered as elastic foundation and the skin is considered as a curved composite beam lying on elastic foundation. In this section, we still denote the radial displacement as w, the coordinates are all the same as before. Therefore this problem is just the above problem of instability of curved composite beam on an elastic foundation as shown in Figure 5.1.

5.3 Approach for solution

5.3.1 General Solution

Assuming the buckling deflection of curved beam lying on an elastic foundation is based on the equilibrium place, then the actual radial deflection of curved beam is:

$$w = w_0 + \delta w \tag{5-1}$$

Where w_0 is the radial displacement of the static equilibrium state (see Chapter 2) and δw is a small perturbation. In the present problem, because axial force N in the curved composite beam (skin of sandwich beam) is constant N_0, w_0 is also a constant N_0 / k (k is the elastic stiffness of foundation), through the whole span of this curved beam.

Then it is assumed that δw can be expressed by Fourier series according to the simply supported boundary condition:

$$\delta w = \sum_{i=1}^{\infty} a_i \sin \frac{i\pi\theta}{\alpha} \tag{5-2}$$

In the case of symmetric stacking laminate, there is the following relationship (Chapter 2):

$$M = D \cdot \kappa$$
$$\kappa = \frac{1}{R^2}\frac{d^2 w}{d\theta^2} + \frac{w}{R^2} \tag{5-3a}$$

where κ, M, D are curvature change, bending moment and flexural rigidity of beam respectively. According to equations (5-1) and (5-2), the above equation turns to be:

$$M = \frac{D}{R^2}\left\{ w_0 + \left[1 - \left(\frac{\pi}{\alpha}\right)^2\right] a_1 \sin\frac{\pi\theta}{\alpha} + \left[1 - \left(\frac{2\pi}{\alpha}\right)^2\right] a_2 \sin\frac{2\pi\theta}{\alpha} + \cdots \right\}$$
$$\kappa = \frac{1}{R^2}\left\{ w_0 + \left[1 - \left(\frac{\pi}{\alpha}\right)^2\right] a_1 \sin\frac{\pi\theta}{\alpha} + \left[1 - \left(\frac{2\pi}{\alpha}\right)^2\right] a_2 \sin\frac{2\pi\theta}{\alpha} + \cdots \right\} \tag{5-3b}$$

The strain energy change of bending of the beam due to the small perturbation δw is:

$$\Delta V_1 = \frac{1}{2} R \int_0^\alpha M \kappa d\theta - V_1 \tag{5-4a}$$

where $V_1 = \frac{D}{2R^3} v_0^2 \alpha$ is the strain energy of bending of the bean at static equilibrium state.

Substitute equation (5-3b) into the above, and noting: $\int_0^\alpha \sin\frac{i\pi\theta}{\alpha}\sin\frac{j\pi\theta}{\alpha} d\theta = 0$ $(i \neq j)$ and $\int_0^\alpha \sin^2\frac{i\pi\theta}{\alpha} d\theta = \frac{\alpha}{2}$, the following result can then be obtained:

$$\Delta V_1 = \frac{1}{4}\frac{D}{R^3}\sum_{n=1}^{\infty}\left[1 - \left(\frac{n\pi}{\alpha}\right)^2\right]^2 a_n^2 + \frac{2Dw_0}{R^3}\frac{\alpha}{\pi}\sum_{n=1,3,5,\cdots}^{\infty}\left[1 - \left(\frac{n\pi}{\alpha}\right)^2\right]\frac{a_n}{n} \tag{5-4b}$$

Analogously the deformation energy change of the elastic foundation due to the small perturbation δw is:

$$\begin{aligned}\Delta V_2 &= \frac{1}{2}kR\int_0^{\alpha} w^2 d\theta - \frac{1}{2}kw_0{}^2 R\alpha \\ &= 2kw_0 R\left(\sum_{n=1,3,5\cdots}^{\infty} a_n\left(\frac{\alpha}{n\pi}\right)\right) + \frac{1}{4}k\alpha R\left(\sum_{n=1}^{\infty} a_n{}^2\right)\end{aligned} \tag{5-5}$$

Meanwhile, the change of the length of curved beam in circumferential direction is:

$$\delta l = \int_0^{\alpha} \frac{1}{2}\frac{1}{R}\left(\frac{dw}{d\theta}\right)^2 d\theta = \frac{\pi^2}{4R\alpha}\sum_{n=1}^{\infty} a_n{}^2 n^2 \tag{5-6}$$

The relative change of the angle between two end cross sections of curved beam is:

$$\begin{aligned}\delta\beta &= \frac{1}{R}\frac{dw}{d\theta}\Big|_0^{\alpha} \\ &= -\frac{2\pi}{\alpha}\frac{1}{R}\left(\sum_{n=1,3,5,\cdots}^{\infty} n a_n\right) + \frac{\pi^2}{4\alpha R^2}\left(\sum_{n=1}^{\infty} n^2 a_n^2\right)\end{aligned} \tag{5-7}$$

And using the relations (Chapter 2):

$$N_0 = kRw_0, \qquad M_0 = \frac{Dw_0}{R^2} \tag{5-8}$$

where M_0 is the bending moment of this curved beam at the static equilibrium state, which is also a constant in present problem as N_0.

Then the work done by all external forces during the period of small perturbation is:

$$\Delta T = N_0 \delta l + M_0 \delta \beta$$
$$= \frac{\pi^2 w_0}{4\alpha}\left(k + \frac{D}{R^4}\right)\left(\sum_{n=1}^{\infty} n^2 a_n^2\right) - \frac{2\pi}{\alpha}\frac{D w_0}{R^3}\left(\sum_{n=1,3,5,\cdots}^{\infty} n a_n\right) \tag{5-9}$$

From the principle of virtual displacement (Timoshenko, 1934 and 1936):

$$\Delta V_1 + \Delta V_2 = \Delta T \tag{5-10}$$

Substituting equations (5-4b), (5-5) and (5-9) into it, and also using the relation (5-8) again, the following result can finally be obtained:

$$N_0 = \frac{\frac{D\alpha}{R^3}\left\{\sum_{n=1}^{\infty}\left[1-\left(\frac{n\pi}{\alpha}\right)^2\right]^2 a_n^2\right\} + kR\alpha\left(\sum_{n=1}^{\infty} a_n^2\right)}{\frac{\pi^2}{R\alpha}\left(1+\frac{D}{kR^4}\right)\left(\sum_{n=1}^{\infty} n^2 a_n^2\right) - \frac{8D}{kR^4}\left\{\frac{\alpha}{\pi}\sum_{n=1,3,5,\cdots}^{\infty}\left[1-\left(\frac{n\pi}{\alpha}\right)^2\right]\frac{a_n}{n} + \frac{\pi}{\alpha}\sum_{n=1,3,5,\cdots}^{\infty} n a_n\right\} - \frac{8\alpha}{\pi}\sum_{n=1,3,5,\cdots}^{\infty}\frac{a_n}{n}} \tag{5-11}$$

In order to determine the critical value of the load N_0, it is necessary to find such a relation between the coefficient $a_1, a_2, \cdots, a_n$ as to make the above expression a minimum. This result can be approached by making all coefficients, except one, equal to zero.

When n is even, the above expression is simplified as:

$$N_0 = \frac{\frac{D\alpha}{R^3}\left[1-\left(\frac{n\pi}{\alpha}\right)^2\right]^2 a_n^2 + kR\alpha a_n^2}{\frac{\pi^2}{R\alpha}\left(1+\frac{D}{kR^4}\right) n^2 a_n^2} = \frac{\alpha^2}{\pi^2}\frac{\frac{D}{R^2}\left[1-\left(\frac{n\pi}{\alpha}\right)^2\right]^2 + kR^2}{\left(1+\frac{D}{kR^4}\right) n^2} \qquad (n=2,\ 4,\ 6,\ldots) \tag{5-12}$$

If n is odd, analogously, making all coefficients, equal to zero, except a_n, then the following equation can be obtained from equation (5-12):

$$N_0 = \frac{\alpha^2}{\pi^2} \frac{\frac{D}{R^2}\left(1-n^2\right)^2 a_n^2 + kR^2 a_n^2}{\left(1+\frac{D}{kR^4}\right) n^2 a_n^2 - \frac{8}{\pi}\frac{a_n}{n}\left(\frac{D}{kR^3}\frac{\alpha^2}{\pi^2}+R\right)} \qquad (n=3,5,7,\ldots) \qquad (5\text{-}13)$$

So a_n can be solved out as:

$$a_n = \frac{\frac{8N_0}{n\pi}\left(\frac{D}{kR^3}+\frac{\pi^2}{\alpha^2}R\right)}{N_0\left(1+\frac{D}{kR^4}\right)\frac{\pi^2}{\alpha^2}n^2 - \left[\frac{D}{R^2}\left(1-n^2\right)^2 + kR^2\right]} \qquad (n=3,5,7,\ldots) \qquad (5\text{-}14)$$

a_n will become infinite in the above expression (that just leads to the unstable state of the being considered curved beam on an elastic foundation) if:

$$N_0 = \frac{\alpha^2}{\pi^2} \frac{\frac{D}{R^2}\left(1-n^2\right)^2 + kR^2}{\left(1+\frac{D}{kR^4}\right) n^2} \qquad (n=3,5,7,\ldots) \qquad (5\text{-}15)$$

As can be seen, the result of odd n case is the same as that of even n.

Obviously, N_{0min} is dependent not only on the values α, k, D, R, n but also the relations between them. For n being both odd and even the same conclusion is achieved from equations (5-12) and (5-15):

$$N_0 = \frac{\alpha^2}{\pi^2} \frac{1}{1+\frac{D}{kR^4}} \left[\left(\frac{D}{R^2}+kR^2\right)\frac{1}{n^2} - 2\frac{D}{R^2}\left(\frac{\pi}{\alpha}\right)^2 + \frac{D}{R^2}\left(\frac{\pi}{\alpha}\right)^4 n^2\right] \qquad (n=2,3,4,\ldots) \qquad (5\text{-}16)$$

The number of half-waves n in which the curved beam subdivides at buckling can now be determined from the condition that the above expression should be a minimum. Provided

that N_0 is continuous function of variable n (and the other variables in the above are all constants), the minimum value of N_0 then can be achieved, if and only if:

$$\left(\frac{D}{R^2}+kR^2\right)\frac{1}{n^2}=\frac{D}{R^2}\left(\frac{\pi}{\alpha}\right)^4 n^2$$

leading to: $$n=\frac{\alpha}{\pi}\sqrt[4]{1+\frac{kR^4}{D}} \tag{5-17a}$$

However, because n is an integer, not a continuous variables, the real result of n should be rounded off to the closest integer from the above value. It should be pointed out that, because n = 1 corresponding to the displacement of curved beam as a rigid body, the smallest number of half-waves n in which the beam subdivides at buckling is n = 2. From the above, as can be seen, if k is very small or D is very big (which means that the foundation is very soft or the flexural rigidity of curved beam is very big), then always n = 2, that is the minimum number of half-waves at buckling. On the contrary, if the elastic foundation is relatively hard or the curved beam is flexural, then the buckling of this curved beam will occur in more than two half-waves.

Above all, once coefficient k, R, D are all given, the critical buckling load of the curved beam on an elastic foundation can then be determined:

$$N_{cr} = Min[N_0(n)] \qquad (n=2,3,4,\ldots) \tag{5-18}$$

The number of half-waves in which the curved beam is most likely to occur buckling can also be determined simultaneously, as is expressed in the above.

5.3.2 Flexural beam or hard foundation case

In the following, the condition of relatively small D or relatively large k will be considered first.

If $\frac{kR^4}{D} >> 1$, then equation (5-17a) turn to be:

$$n \approx \frac{\alpha}{\pi}\sqrt[4]{\frac{kR^4}{D}} \tag{5-17b}$$

When n is very large, there occurs wrinkling or rippling.

Noting $l=R\alpha$, then:

$$\frac{l}{n} = \sqrt[4]{\frac{\pi^4 D}{k}} \tag{5-19}$$

which is the length of one half-wave. As can be seen, the wrinkling wavelength is independent of both arch angle α and the curvature radius R, which is just expected. From equations (5-16), (5-17a), and (5-18), we have:

$$N_{cr} = \frac{1}{1+\frac{D}{kR^4}} \cdot \frac{2D(\frac{\pi^2}{\alpha^2}n^2 - 1)}{R^2} \tag{5-20}$$

If $\frac{kR^4}{D} >> 1$, then combining equations (5-17b), (5-19) and (5-20), the following conclusion is obtained:

$$N_{cr} \cong \frac{2\pi^2 D}{(l/n)^2} \tag{5-21}$$

Noting that, the critical value of the compressive force for wrinkling of a flat bar on an elastic foundation is (Timoshenko, 1936):

$$P_{cr} = \frac{2\pi^2 EIn^2}{l^2} \tag{5-22}$$

If a curved beam made from isotropic material is concerned, there is $D = EI$. It can be found that, equation (5-21) is just the same as equation (5-22), which means that the critical load value for wrinkling of curved beam on an elastic foundation is nearly identical to that for a flat bar case (the result for curved beam is only very little smaller). Therefore, under the same condition (and the elastic foundation is hard enough to make wrinkling rather than buckling occur), the curved beam on an elastic foundation has nearly the same possibility to lose its stability and result in wrinkling as the flat one. When $R \to \infty$, $N_{cr} \to \frac{2\pi^2 D}{(l/n)^2}$, which means the result for curved beam converges to that for straight one.

The equation (5-21) can also be rewritten as a very brief expression by substituting equation (5-19) into equation (5-21):

$$N_{cr} = 2\sqrt{Dk} \tag{5-23}$$

However, it should be noted that, this formula is only fit for the case of wrinkling, in which the number of buckling half waves must be large enough.

5.3.3 Stiff beam or soft foundation case

If the foundation is not very hard or the curved beam is not very flexible, n should be given as 2 or more according to equation (5-17a), and then equations (5-16) and (5-18) should be used to calculate the critical load for buckling which is the function of arch angle α and curvature radius R . The calculation for results becomes more complicated than the above case. And the critical value is not similar to that of straight beam case any longer. Another extreme case is considered in the following.

If the condition is that D is relatively very big or k is relatively very small, which means the beam is very stiff or foundation is very soft. Then, according to previous conclusion, there is $n = 2$. From equation (5-16) and Noting $l=R\alpha$, the following result is true:

$$\begin{aligned} N_{cr}' &= \frac{1}{1+\frac{D}{kR^4}}\left[\frac{1}{4}\left(\frac{D}{R^2}+kR^2\right)\left(\frac{\alpha}{\pi}\right)^2 - 2\frac{D}{R^2}+\frac{4D}{R^2}\left(\frac{\pi}{\alpha}\right)^2\right] \\ &= \frac{\pi^2 D}{l^2}\cdot\frac{1}{1+\frac{D}{kR^4}}\left[4-\frac{2}{\pi^2}\left(\frac{l}{R}\right)^2+\frac{1}{4\pi^4}\left(1+\frac{kR^4}{D}\right)\left(\frac{l}{R}\right)^4\right] \end{aligned} \tag{5-24}$$

As can be seen, the critical value of buckling load depends on not only the length of beam and foundation modulus, but also the curvature radius under this condition. Noting that the buckling load for a flat bar on an elastic foundation is (Timoshenko, 1936):

$$P_{cr}' = \frac{\pi^2 D}{l^2}\left(n^2+\frac{kl^4}{n^2\pi^4 D}\right) \tag{5-25}$$

By comparing the above two equations, it can be found that when $R \to \infty$, equation (5-24) converges to equation (5-25) of case that $n = 2$. However, under the condition of big D or small k, the critical value of buckling load for a flat bar on an elastic foundation is calculated by equation (5-25) in which $n = 1$ (Timoshenko, 1936). Therefore, the buckling critical force for curved beam on an elastic foundation does not converge to that for flat bar case by only let $R \to \infty$.

5.3.4 "Unstable length"

Now equation (5-24) is considered again. Assuming that the curvature radius is a constant, then critical force value will achieve a minimum if it happens that

$$\alpha = \frac{2\pi}{\sqrt[4]{1+\frac{kR^4}{D}}} \tag{5-26}$$

and then $$l_{cr} = \frac{2\pi R}{\sqrt[4]{1+\frac{kR^4}{D}}} \tag{5-27}$$

Here is an interesting phenomenon. It is due to the existence of elastic foundation and the geometry curvature, under some conditions there exists an "unstable length"-- l_{cr} with which the beam has the minimum buckling critical load value. At this time, the shorter means the safer which is understandable, but the longer maybe also means the safer to some extent. That – we can say -- is the characteristic phenomenon for the curved beam on an elastic foundation.

Chapter 6: The Effects of Key Parameters on Flexural Behaviour Pattern

As an application of the theoretical analyses given in Chapter 2 and 3, the effects of some key material- and geometry-related variables on stresses and displacements will be examined. In this section, we chiefly investigate the effects of λ, δ, R, k which is respectively anisotropy ratio of the material, ratio of outer radius to inner radius, curvature radius of the beam and stiffness of elastic foundation, and also the Poisson's ratio $\nu(\nu_{12})$ of the material of beam is studied.

The model considered here is a curved orthotropic beam lying on an elastic foundation, as shown in Figure 6.1:

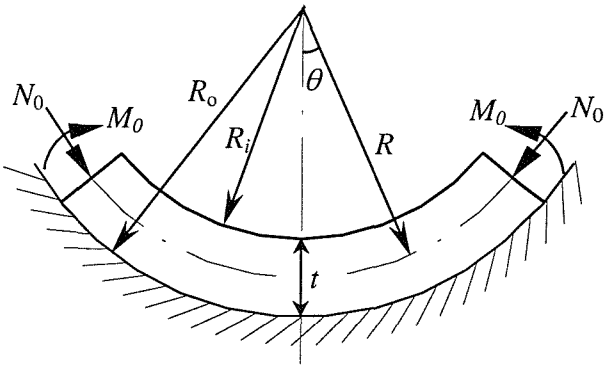

Figure 6.1 Curved orthotropic beam on an elastic foundation

From equations (3-14) and (3-11), the maximum through-thickness stress σ_r and its location can then both be determined. Figure 6.2 shows the variation of ξ with respect to δ, which is the ratio of inner radius to outer radius of a curved beam. ξ^* indicates the

location of the maximum normal, through-thickness stress; the distance is measured from the midplane axis. The result for the anisotropic beam without foundation is obtained from equation (3-14) by setting k to equal zero. Here we take: R_o= 1 (unit), anisotropy ratio $\lambda = E_2/E_1 = 0.25$ (which corresponds to typical glass fibre/epoxy composites), and assume $k/E_2 = 0.25$. As can be seen, when δ approaches 1.0, i.e. the thickness of curved beam is very small compared to its curvature radius, the point of maximum σ_r approaches the midplane. In the curved beam with anisotropy, this point is closer to the midplane, and owing to elastic foundation, this deviation become smaller.

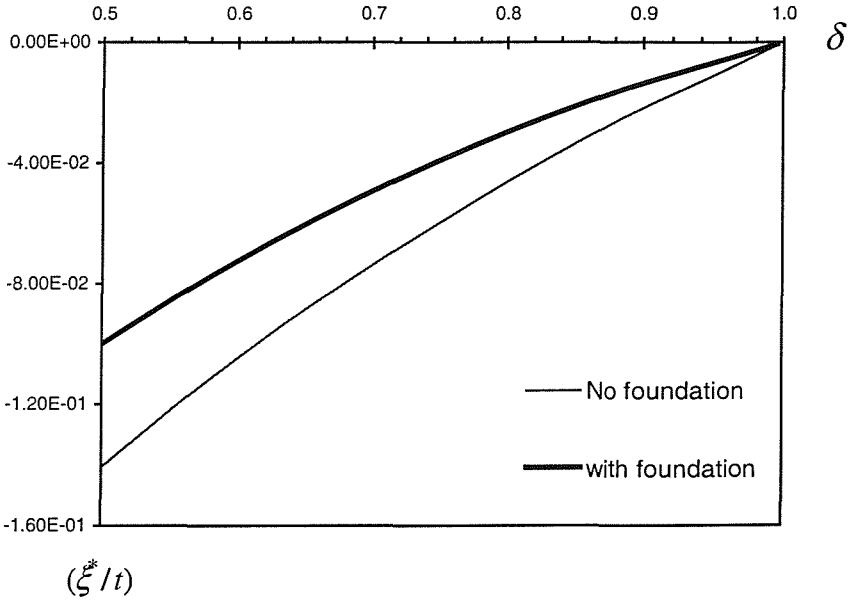

Figure 6.2 Effect of foundation on the location of maximum through thickness stress

Figure 6.3 shows the variation of ξ^* and maximum radial stress σ_r as functions of δ. The variables are normalised, $N_0/t = \sigma_0$ is the base stress. Here, again: R_o= 1 and anisotropy ratio $\lambda = E_2/E_1 = 0.25$. It can be seen that if the foundation is very hard, the absolute value of maximum σ_r become smaller when δ becomes bigger. However, if foundation is soft, the absolute values of maximum σ_r first increase, and then steadily

decrease. Note that as δ approaches 1.0, there is no big difference between the two cases-this is to be expected.

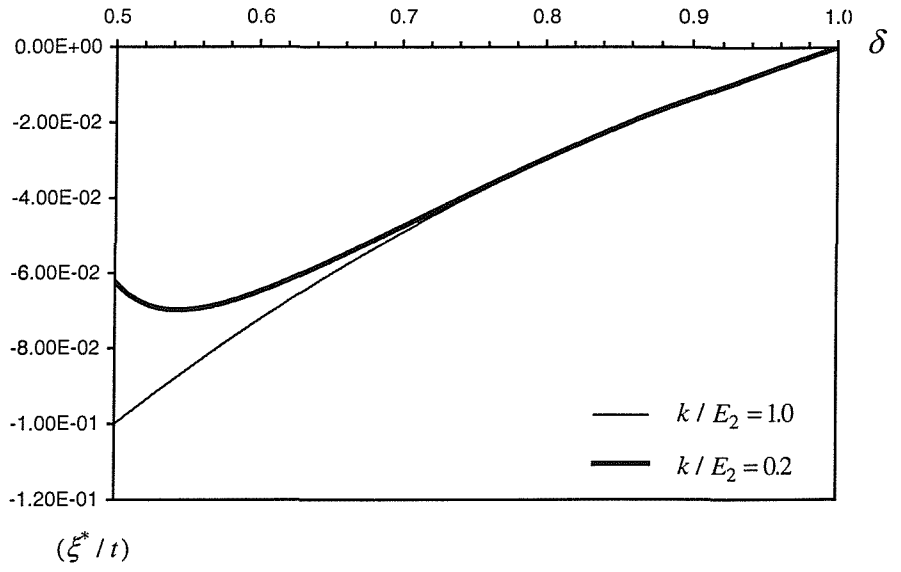

Figure 6.3a Effect of δ on the location of maximum σ_r

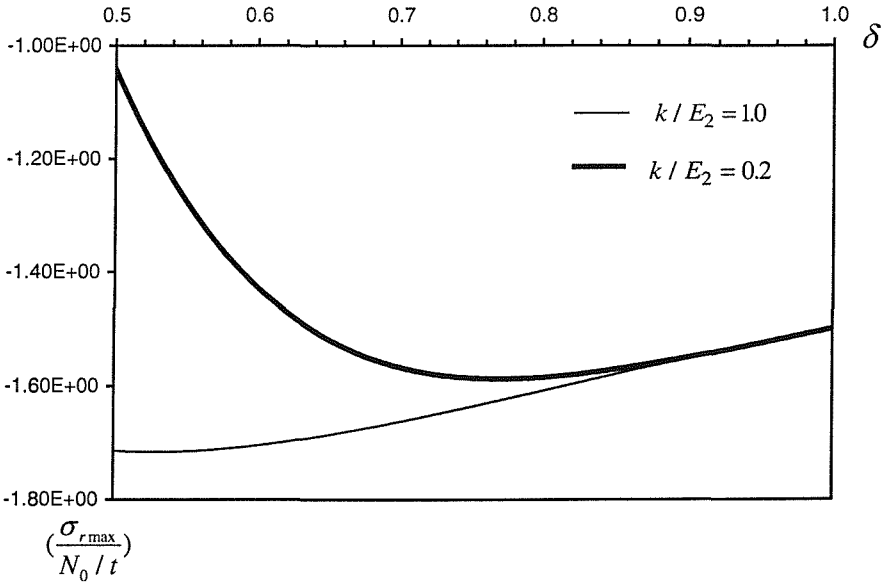

Figure 6.3b Effect of δ on the value of maximum σ_r

Figure 6.3 Effect of δ (ratio of inner radius to outer radius)

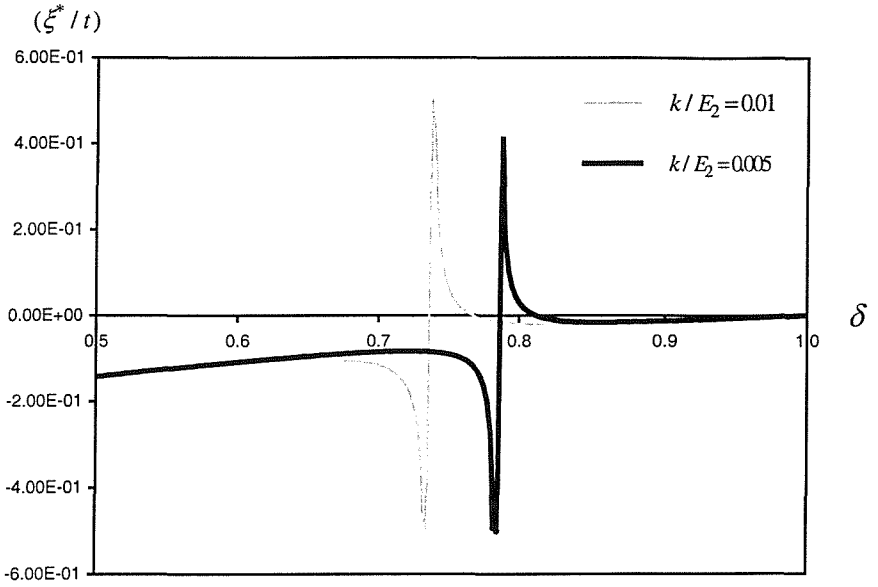

Figure 6.4 Effect of δ on the location of maximum σ_r -- very soft foundation

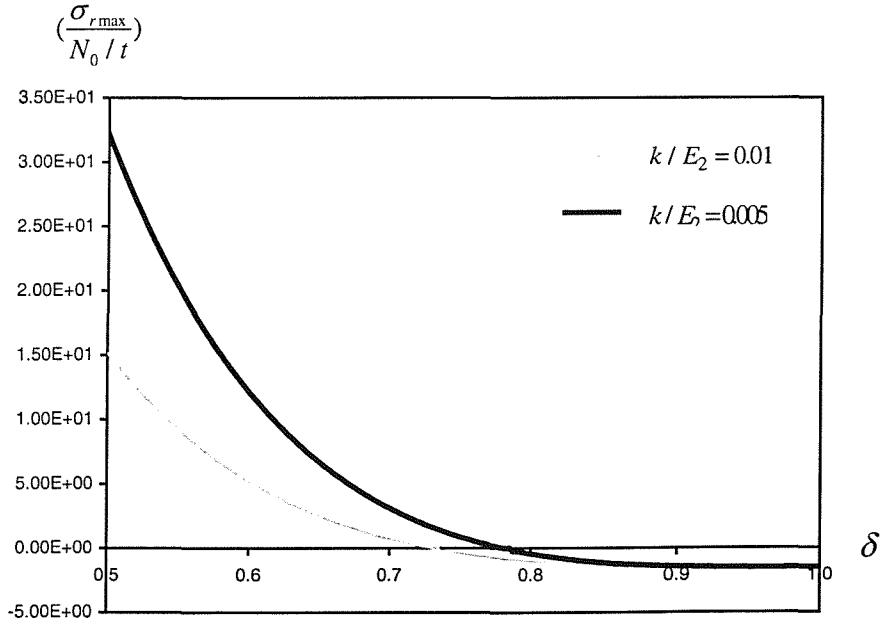

Figure 6.5 Effect of δ on the value of maximum σ_r -- very soft foundation

If the foundation is extremely soft, the results shown in Figure 6.4 and Figure 6.5 are quite different from the above results shown in Figure 6.3.

As can be noticed, when elastic foundation is very soft, with $k/E_2 = 0.01, 0.005$ (such as the foam core of a sandwich), then the value of maximum σ_r decreases steeply at first and gradually approaches to a constant when δ becomes bigger and gradually approaches to 1.0. There is an abrupt change in the curves of Figure 6.4 showing the location of maximum σ_r. It can be noted that the point of this abrupt change corresponds to the point at which value of normal tension stress nearly equals zero (i.e. $\sigma_r = 0$) in Figure 6.5. Therefore, it is understandable that ξ^* varies very abruptly in the small local of this singular point.

In order to investigate this singular point of ξ^* and confirm it is not due to numerical artefact, Figures 6.6a~6.6f show the distribution of through thickness stress along with thickness for those cases where the values of δ lie in the vicinity of this "singular point". In Figures 6a~6f, the anisotropy ratio $\lambda = 0.25$, and $k/E_2 = 0.01$. As described in Chapter 3, ξ^* from equation (3-14) is actually the location of stationary value of σ_r. From Figures 6.6a~6.6f, we can see the trend of changes of location where the stationary value exists. In the very small region of $\delta \in (0.73, 0.74)$, the location of stationary value of σ_r changes from very close to inner face to very close to outer face of the curved beam. That is the abrupt change of ξ^*.

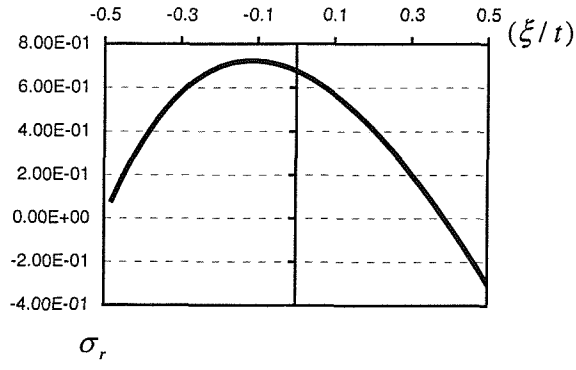

Figure 6.6a δ=0.70

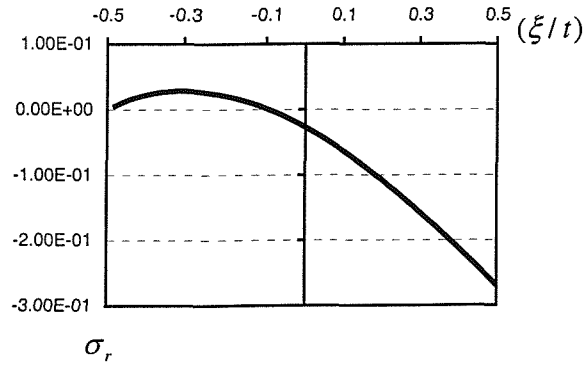

Figure 6.6b δ=0.73

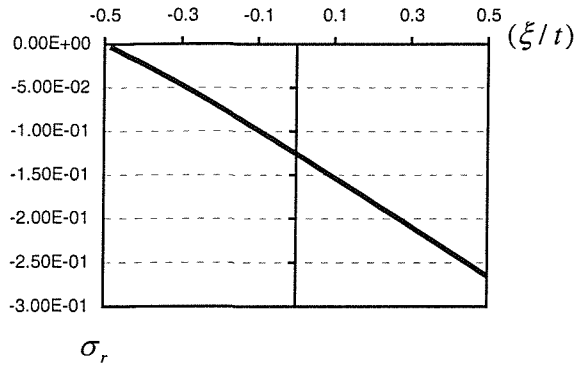

Figure 6.6c δ=0.735

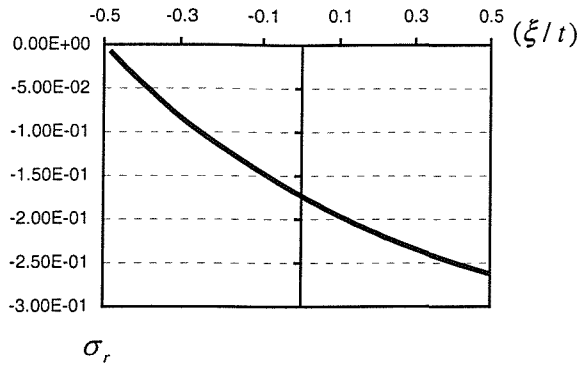

Figure 6.6d δ=0.7375

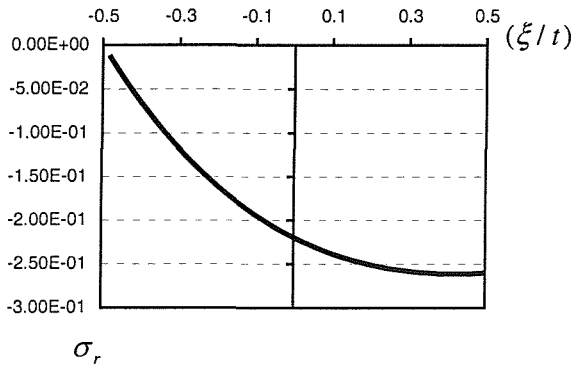

Figure 6.6e δ=0.74

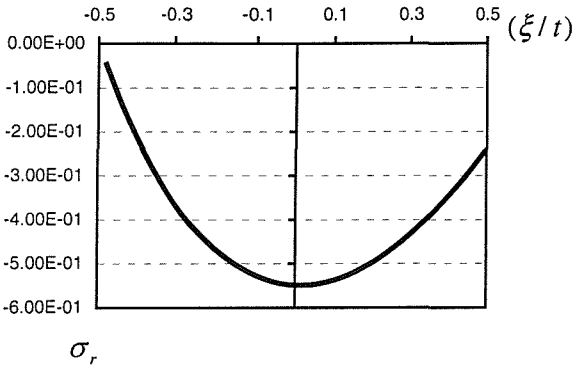

Figure 6.6f δ=0.76

Figure 6.6 The distribution of σ_r through the thickness of the beam

The above results (Figures 6.4 and 6.5) also show that if the foundation is very soft, then an "optimal thickness" of the curved beam can be specified which can make delamination stress--σ_r be very small.

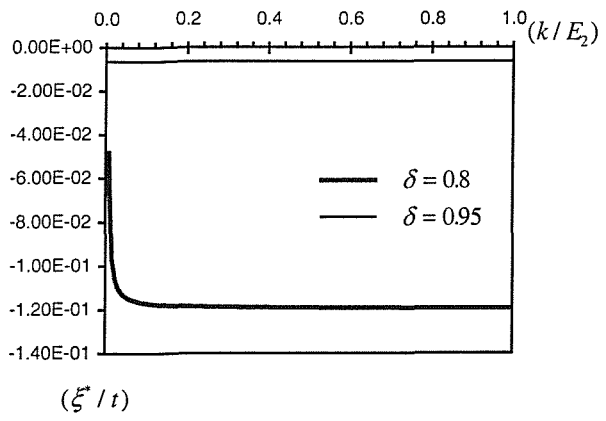

Figure 6.7a Effect on the location of $\sigma_{r\max}$

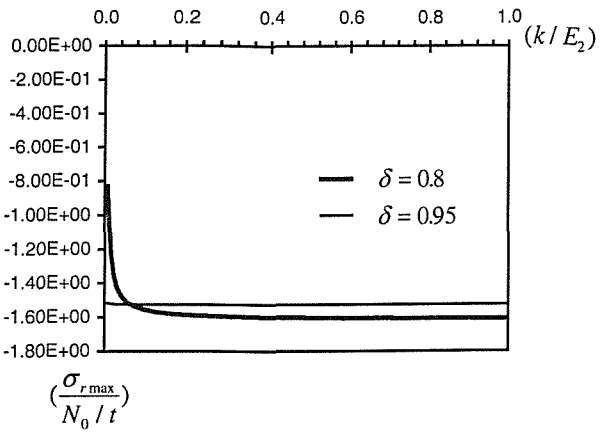

Figure 6.7b Effect on the value of $\sigma_{r\max}$

Figure 6.7 Effect of the elastic modulus of foundation

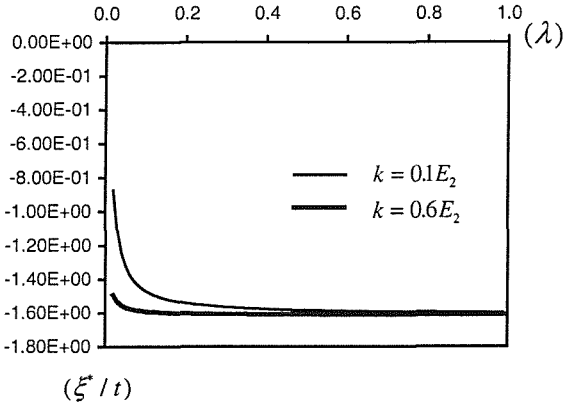

Figure 6.8a Effect on the location of $\sigma_{r\max}$

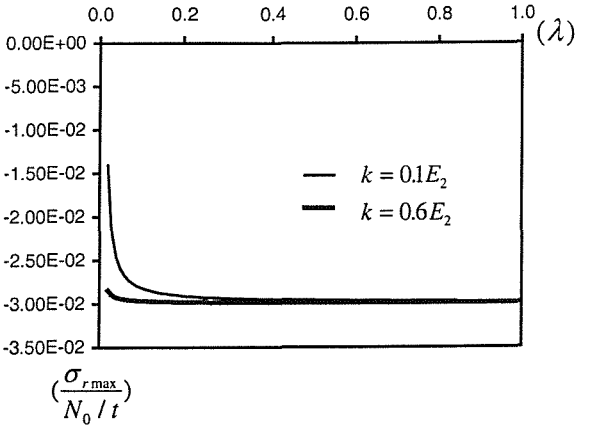

Figure 6.8b Effect on the value of $\sigma_{r\max}$

Figure 6.8 Effect of the anisotropy ratio of beam

Figure 6.7 and Figure 6.8 show the effect of foundation stiffness k and the effect of anisotropy ratio $\lambda = E_2/E_1$ separately. It can be seen that λ nearly has no effect on the location of maximum σ_r in the most of the regions, but does have an effect on the value of maximum σ_r. When λ becomes bigger, the absolute value of maximum σ_r also

becomes bigger, and gradually approaches to a constant. If δ is close to 1.0 (for example $\delta = 0.95$ in Figure 6.7), k also has no effect on the location of maximum σ_r, and even has no effect on the value of maximum σ_r. Nevertheless, if δ is not close to 1.0, k also has effects on the location of maximum σ_r, and the value of maximum σ_r especially in the region of small k value, *e.g.* when the foundation is very soft.

Figures 6.9, 6.10 and 6.11 show the effect of radius of curvature under different conditions. In Figures 6.9 and 6.10, the value of outer radius R_o is taken as x-axis, the thickness of beam t equals 0.1; in Figure 6.11, R_o/t is taken as x-axis, and t equals 0.01.

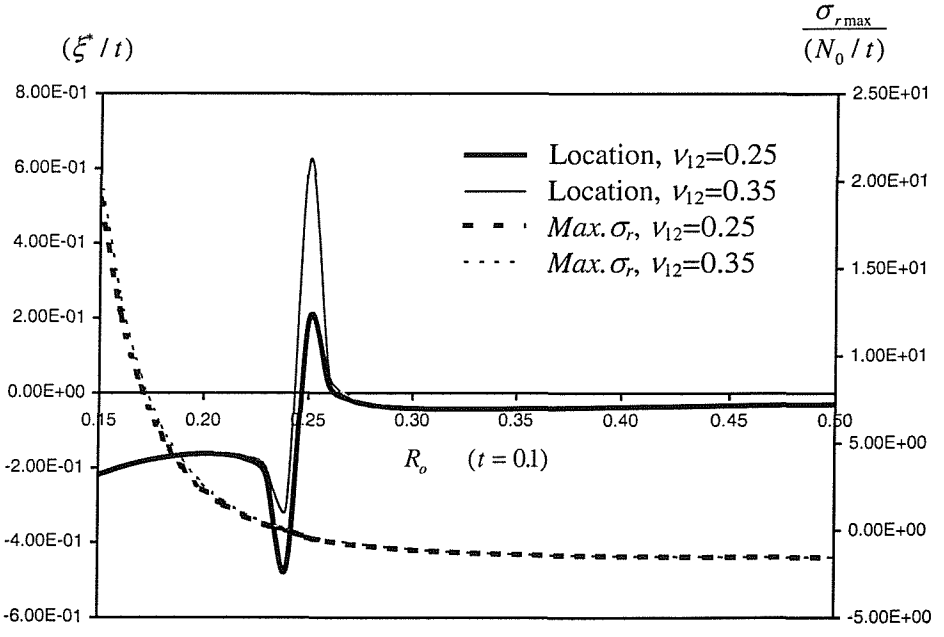

Figure 6.9 Effects of radius and Poisson Ratio with $k / E_2 = 0.2$

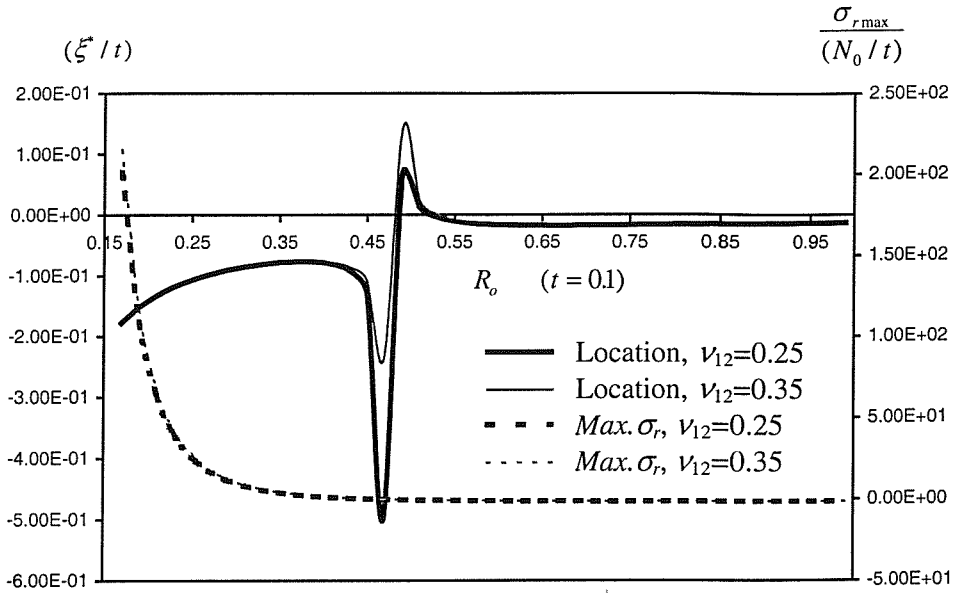

Figure 6.10 Effects of radius and Poisson Ratio with $k / E_2 = 0.01$

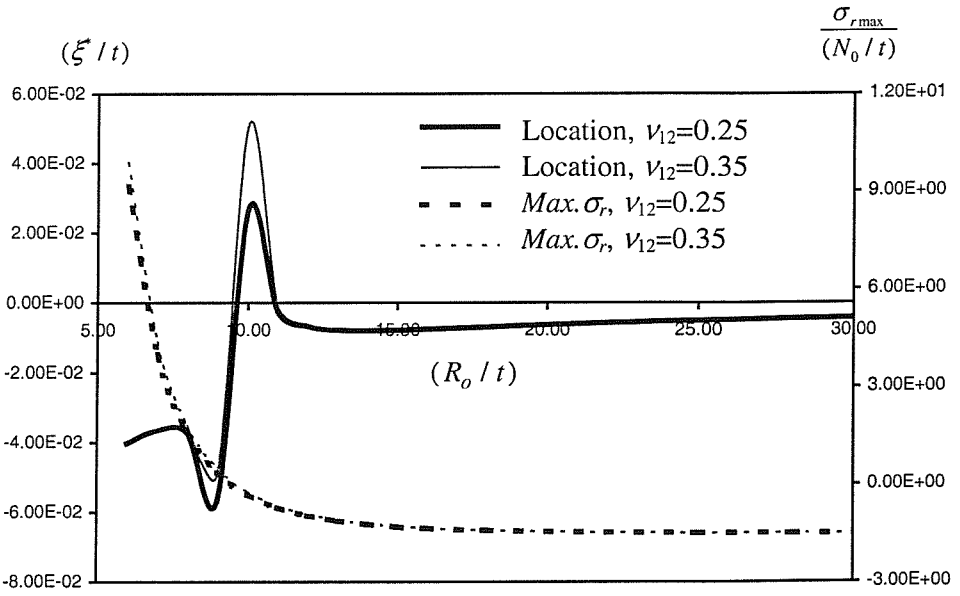

Figure 6.11 Effects of radius and Poisson Ratio with $k / E_2 = 0.005$

As can be seen, the radius of curved beam has big effect on the value of maximum σ_r, especially when R_o/t is not very big. The value of maximum σ_r decreases considerably

initially when R_o becomes bigger, although gradually this effect becomes less. For example, in Figure 6.11, after the point $R_o/t = 20$, the radius of curved beam nearly has no effect on the value of maximum σ_r. There also exists a "singular point" about the location of maximum σ_r, which corresponds to the point of σ_r being zero. This is in conformity with what has been discussed above and is consistent with earlier finite element analysis based results (Shenoi & Hawkins, 1995). The location of maximum σ_r changes very much in the beginning then approaches the midplane of beam with R_o becoming bigger.

In contrast, in Figures 6.9, 6.10 and 6.11, Poisson's Ratio ν has little effect on the present delamination research.

Chapter 7: Through-Thickness Stresses in Curved Composite Beams

7.1 Introduction

The effects of material- and geometry-related variables of a single-layer curved orthotropic beam and the elastic foundation on stresses and displacements have been examined in Chapter 6. In this Chapter, the effects of the stacking sequence of curved layered composite beam and the thickness of skin in curved sandwich on stress distributions along through-thickness direction are studied and examined based on the approach developed in Chapter 4.

7.2 Effect of laminate stacking sequence on stresses

The model considered here is a curved layered beam subjected to pure bending, as shown in Figure 7.1:

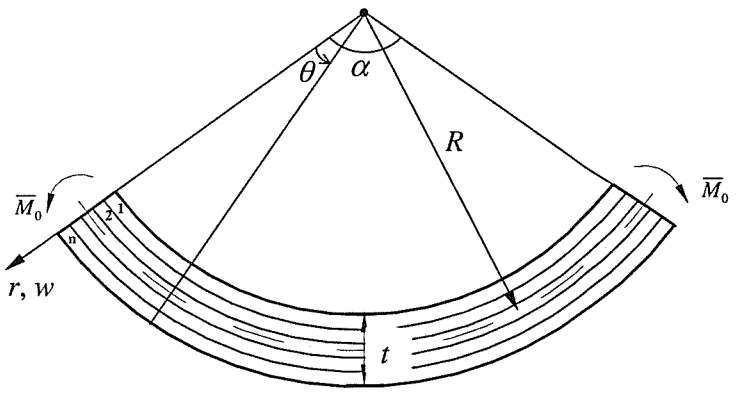

Figure 7.1 Typical curved composite beam under loads

In order to investigate the effects of stacking sequence of layered composite beam, an individual layer of unidirectional fibrous composite material is considered to possess the following properties (corresponding to a general E-glass/epoxy composite):

$E_L = 38.6\,\text{GPa}$ $E_T = 8.27\,\text{GPa}$ $G_{LT} = 4.14\,\text{GPa}$ $G_{TT} = 2.76\,\text{GPa}$

$\nu_{LT} = 0.26$ $\nu_{TT} = 0.5$

$V_f = 0.45$

Where L signifies the direction parallel to the fibres, T the transverse direction, and ν_{LT} is the Poisson ratio measuring strain in the transverse direction under uniaxial normal stress in the L direction. And it is assumed that the material characteristics through thickness direction are the same as those in the transverse direction totally. These properties are used in appropriate contexts in the equations for calculating stresses and displacements (3-3), (4-7) and (4-10). For example, for a UD ply with 0° orientation, then $E_1 = E_L$ and $E_2 = E_T$; for a ply with 90° orientation, $E_1 = E_T$ and $E_2 = E_T$, which means isotropic in the $y-z$ plane, thus $E=E_T$. Similar analogies can be given for other properties or for other layups.

Several separate stacking configurations are considered, namely:

(1) [0°/0°] and [90°/90°] – Describing orthortropic and isotropic beam respectively.

(2) [0°/90°] and [90°/0°] – Two bidirectional (coupled) laminates with the layers being of equal thickness.

(3) [0°/90°/0°] – A symmetric 3-ply laminate with cross-ply stacking ratio $m = 1.0$

(4) [0°/90°/0°/90°] and [90°/0°/90°/0°] – Two antisymmetric 4-ply laminates both with $m = 1.0$.

(5) [0°/90°/0°/90°/0°] – A symmetric 5-ply laminate with the layers being of equal thickness.

In each case, the curved beams have the same curvature radius: $R_i = 30$ mm, $R_o = 36$ mm, so the thickness of the beam is $t = 6$ mm. The curved beam is subjected to pure bending, the bending moment is $M = -1000$ N·m.

The functions of prime interest in the present case are radial stress σ_r (the through-thickness stress of the curved layered composite beam) and circumferential stress σ_θ (the in-plane stress of the curved layered composite beam). Under the no-circumferential-dependence condition, shear stress equals zero. Based on the approach developed in Chapter 4, the solutions for σ_r and σ_θ are calculated and illustrated in Figures 7.3-7.7. In each figure, abscissa is the value of stress and ordinate is the normalized thickness $\bar{z} = z/t$.

The stresses distribution in [0°/0°] layered beam are shown in Figure 7.3. The results of [90°/90°] layered beam are very similar to Figure 7.3. This correspond to the result for curved orthotropic beam on an elastic foundation (Chapter 6), which showed that anisotropy ratio λ has no significant effect on the stress distribution in the curved beam. The maximum through-thickness stress occurs on the inner side of the midplane of beam, very close to the midplane. Its value is 7.60 MPa.

Figure 7.4 gives the results for [0°/90°] and [90°/0°] – two bidirectional (coupled) laminate cases. In each case, the layers are of equal thickness. The results show that there is a big difference between these two coupled laminates, not only in the distribution of through-thickness stress and in-plane stress, but also in their values. The maximum absolute values of σ_r and σ_θ in [0°/90°] case are both more than 10% higher than those in [90°/0°] case separately. This difference will become bigger as the ratio $\delta(=R_i/R_o)$ decreases. In a flat layered composite beam, this distinguishing difference does not exist. In these two laminates, the maximum through-thickness stresses are both occur in the 0° layer.

A similar result can also be found in the analyses of [0°/90°/0°], [0°/90°/0°/90°] and [90°/0°/90°/0°] laminates. The stresses distribution in these case are showed in Figures 7.5 and 7.6. Three laminates have the same stacking ratio ($m = 1.0$). It is reasonable that the stress distributions are different among these cases due to their different stacking

sequence, but the maximum absolute values of stress in each laminate are quite different. The maximum values of through-thickness and in-plane stress are respectively 6.79 MPa and 192 MPa in [0°/90°/0°] laminate, 8.54 MPa and 261 MPa in [0°/90°/0°/90°] laminate, 8.11 MPa and 240 MPa in [90°/0°/90°/0°] laminate each. The maximum through-thickness stresses in three cases all occur in the 90° layer and close to the midplane of laminate.

Figure 7.7 shows the results for symmetric 5-ply stacking case. The value of maximum through-thickness stress in [0°/90°/0°/90°/0°] laminate curved beam is close to that in [0°/90°/0°] case, only very a little higher.

The above results indicate that the stacking sequence of layered composite beam does have an effect on stresses. In two-ply (coupled) case, stacking sequence [90°/0°] is "better" than [0°/90°]; in 4-ply case, stacking [90°/0°/90°/0°] is "better" than [0°/90°/0°/90°]. Under the condition of the same stacking ratio, apparently the [0°/90°/0°] is the "best" stacking sequence among the above stacking cases. It should also be noticed that in theory a unidirectional (UD) stacking is not a better one; the maximum value of through-thickness stress(7.60 MPa) in the UD case is more than 10% higher than that of [0°/90°/0°] case, although its maximum value of in-plane stress is lower(178 MPa). This indicates the possibility of identifying an "optimal stacking sequence" for a curved layered composite beam.

7.3 Through-thickness stresses in curved sandwich beams

In order to investigate the stress distribution in curved sandwich beams, two separate geometrical configurations are considered first:

(1) Thick skin-sandwich panel with $t_s / t_c = \frac{1}{4}$

(2) Thin skin-sandwich panel with $t_s / t_c = \frac{1}{10}$

The skin is a unidirectional cylindrical shell with the fibres oriented in the circumferential direction. The other geometrical variables of curved sandwich beam are the same as those of curved layered composite beam studied in the previous section. The material properties of the skin are the same as the above. The elastic constants of the isotropic core material of sandwich beam are:

E= 1.103 GPa $\nu = 0.3$

The curved sandwich beam is also subjected to pure bending, similar to the model in above section. The bending moment is also:

M = -1000 N·m

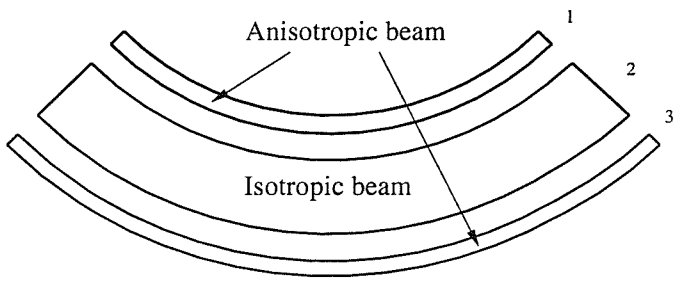

Figure 7.2 Three individual parts in the global sandwich beam

In our analyses, skins and core are considered as cylindrical anisotropic beam and isotropic beam respectively, as shown in Figure 7.2. Also using the approach developed in Chapter 4, the radial stress (Through-thickness stress) and circumferential stress in both skins and core can then be obtained. Because in our investigated samples, the inner skin and outer skin are the same, then there is $B_{11} \approx 0$ in equation (4-13b). Therefore, this global boundary condition involved in solution becomes: $\overline{M}_0 = D_{11} \cdot \dfrac{4C_0^{(3)}}{(R_i + R_o)^2}$

Figure 7.8 shows the results for these two kinds of curved sandwich beam. As can be seen, a significant through-thickness stress gradient exists in the skin, but the maximum

through-thickness stress occurs in the core. It is sometimes at the interface between core and the inner skin, sometimes in the core but near to that interface (as shown in Figure 7.8a). It can also be noted that the through-thickness stress changes only very slightly in the core; it keeps a high level nearly through the whole thickness of the core. This explains why in Gibson and Chandler's experiment (1994), delamination sometimes was seen to occur between either skin or core, and sometimes between both skins and the core.

From the trends in Figures 7.8a and 7.8b, it is known that in a thin-skin sandwich beam, there is a smaller through-thickness stress than that in a thick-skin sandwich beam, but a bigger in-plane stress exists also in the thin-skin sandwich beam, which is reasonable.

In order to investigate the effect of radius of the curved beam on stresses, another geometrical configuration of the curved layered composite beam is studied: R_i = 18 mm, R_o = 24 mm. The thickness of the beam is still h = 6 mm. The curved beam is still subjected to pure bending, the bending moment is $M = -1000$ N·m. Here the [0°/90°/0°] stacking sequence is again considered. The results are as follows as shown in Figure 7.5.

As would be expected, the radius of curved beam has big effect on the stresses, especially on the value of through-thickness stress, which is similar to the result for curved orthotropic beam (Chapter 6). As can be seen, when the thickness is stable and outer radius becomes a third smaller, the maximum of through-thickness stress in beam increases by 50%, simultaneously the maximum in-plane stress becomes a little bigger.

7.4 Summary

The effect of stacking sequence and radius of curvature of a curved layered composite beam on the distribution and value of through-thickness stress is chiefly investigated. Curved sandwich beams with thin and thick skin are also studied. The results show that the stacking sequences have a significant effect on the delamination and in-plane tensile

failure to some extent. The radius of curvature of the beam also has a large effect on the through-thickness stress, which is consistent with the results for a single layer curved orthotropic beam. The biggest through-thickness stress in a curved sandwich beam always occurs at the interface between inner skin and core or in the core but very close to that interface.

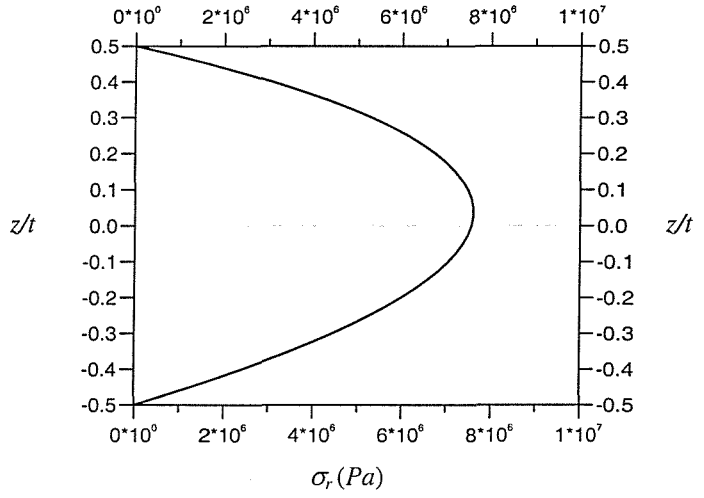

Figure 7.3a Through Thickness Stress Distribution

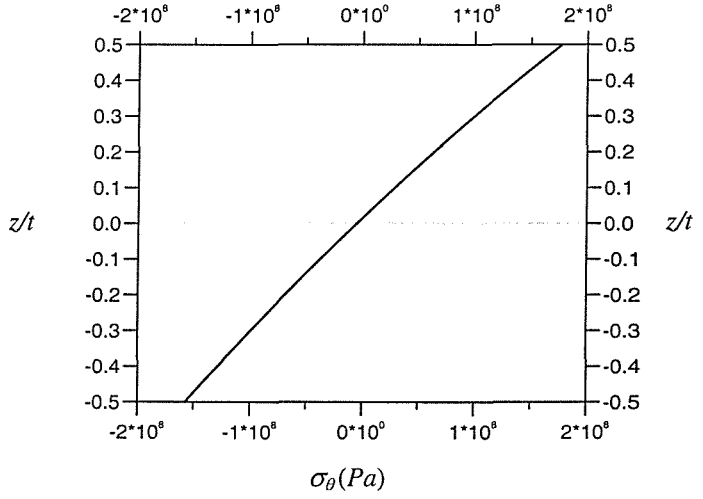

Figure 7.3b In-plane Tension Stress Distribution

Figure 7.3 Stresses Distribution Along Thickness in Unidirectional Laminate

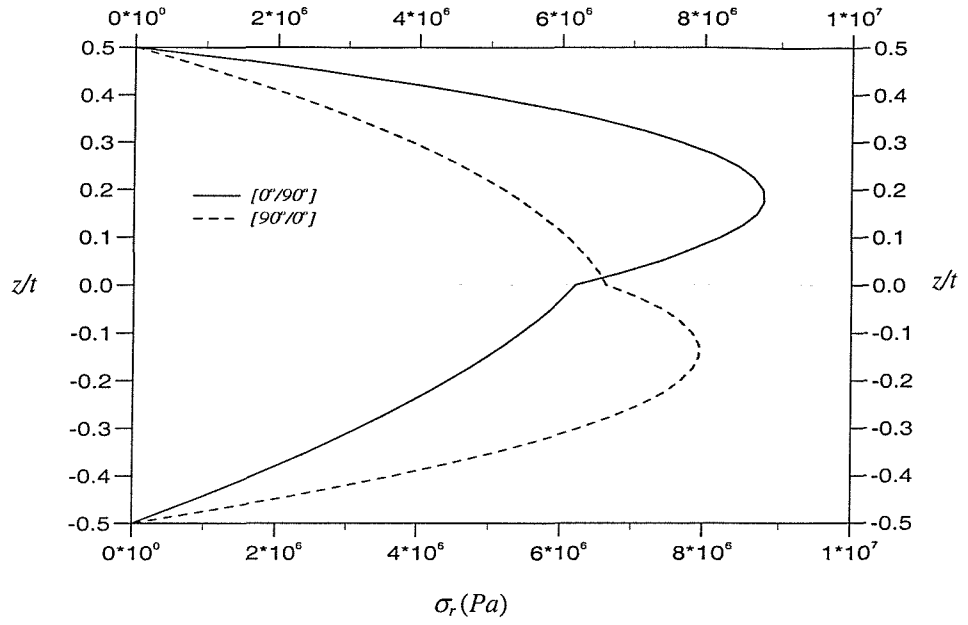

Figure 7.4a Through-Thickness Stress Distribution

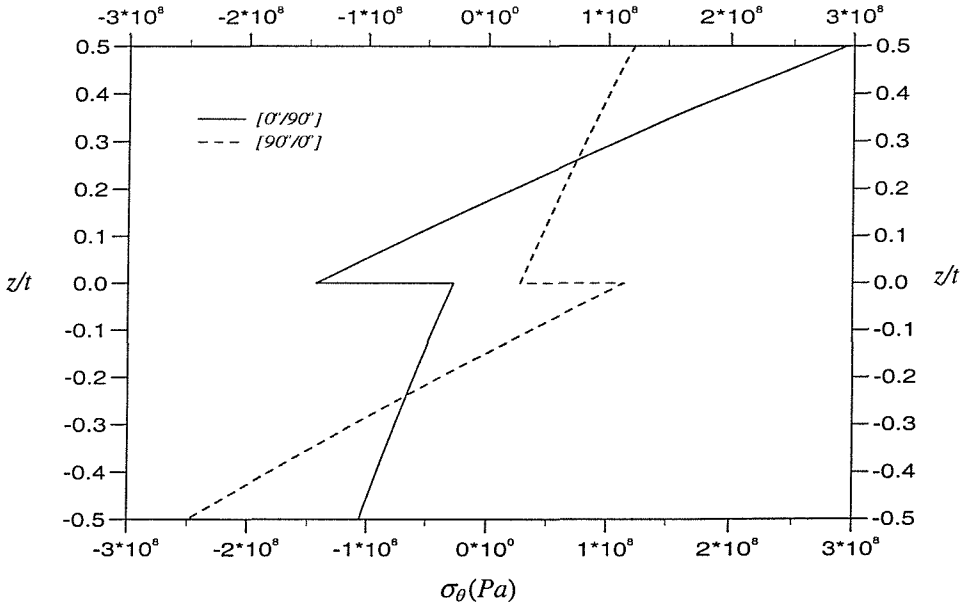

Figure 7.4b In-plane Tension Stress Distribution

Figure 7.4 Stresses Distribution Along Thickness in Cross-Ply Laminate

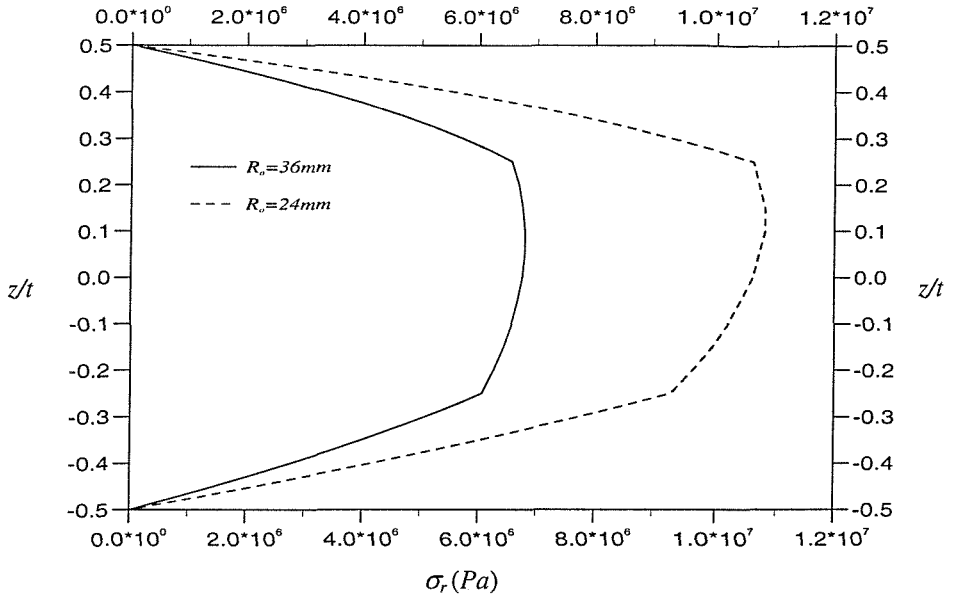

Figure 7.5a Through-Thickness Stress Distribution

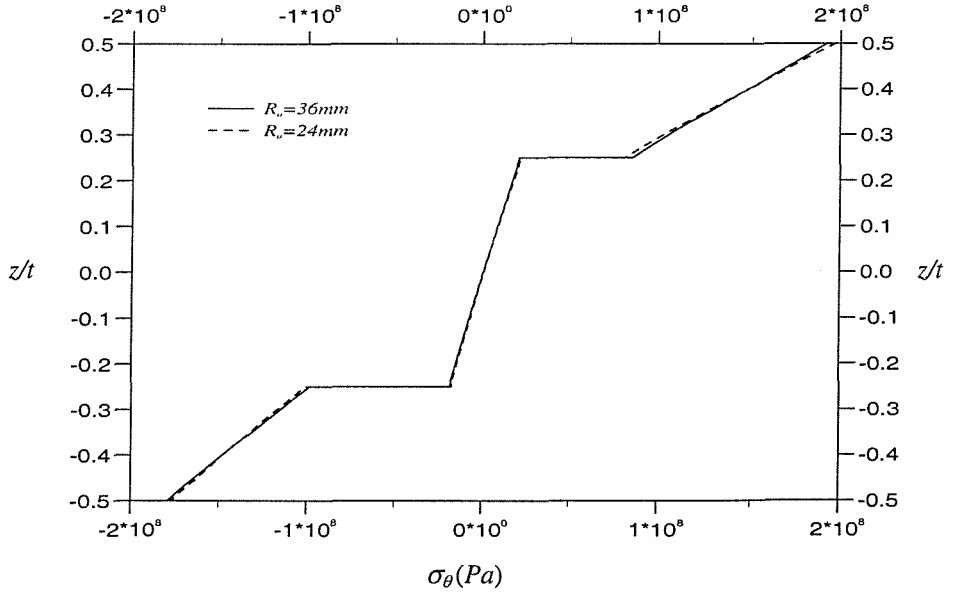

Figure 7.5b In-plane Tension Stress Distribution

Figure 7.5 Stresses Distribution Along Thickness in Symmetric 3-ply Laminate

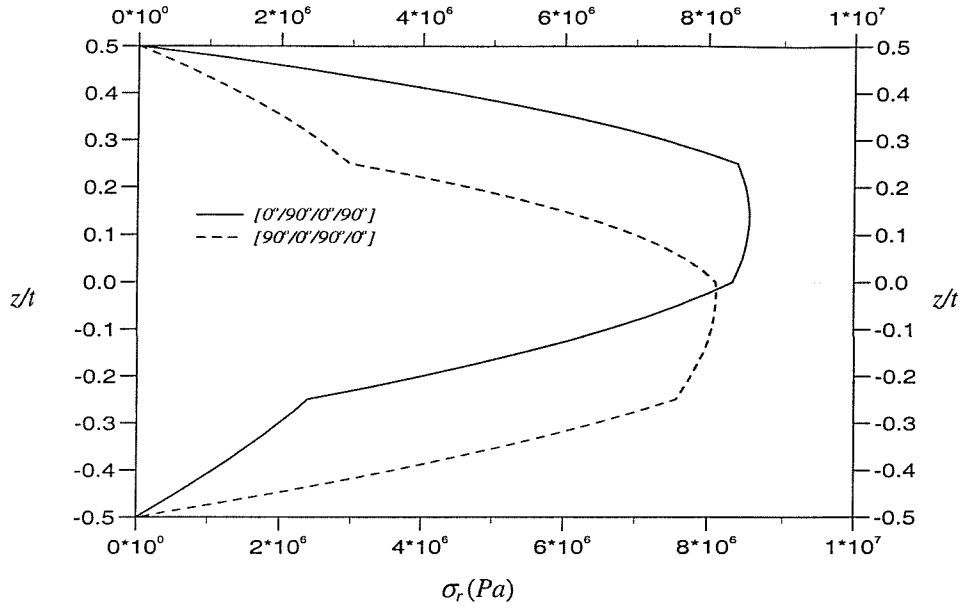

Figure 7.6a Through-Thickness Stress Distribution

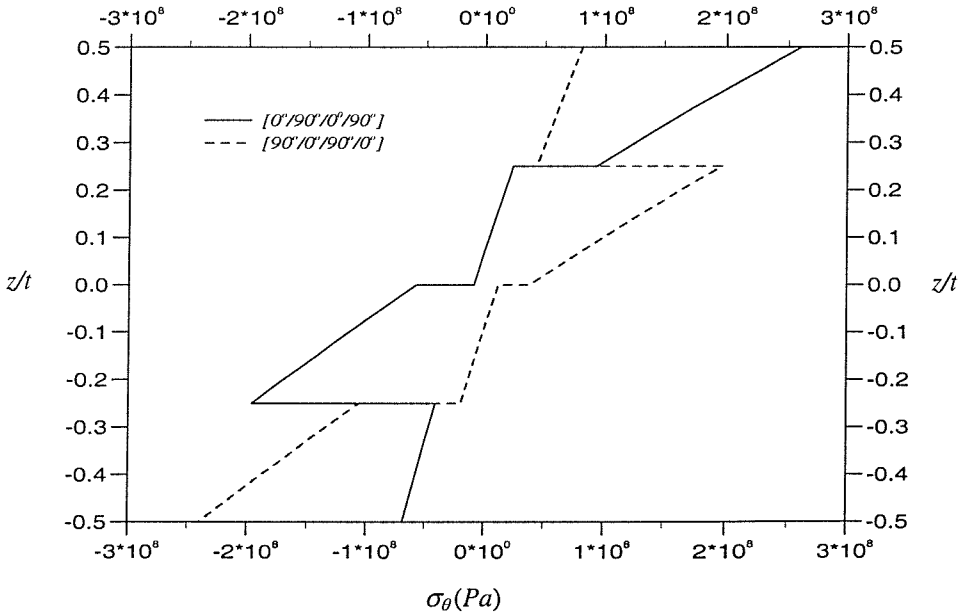

Figure 7.6b In-plane Tension Stress Distribution

Figure 7.6 Stresses Distribution Along Thickness in Antisymmetric 4-ply Laminate

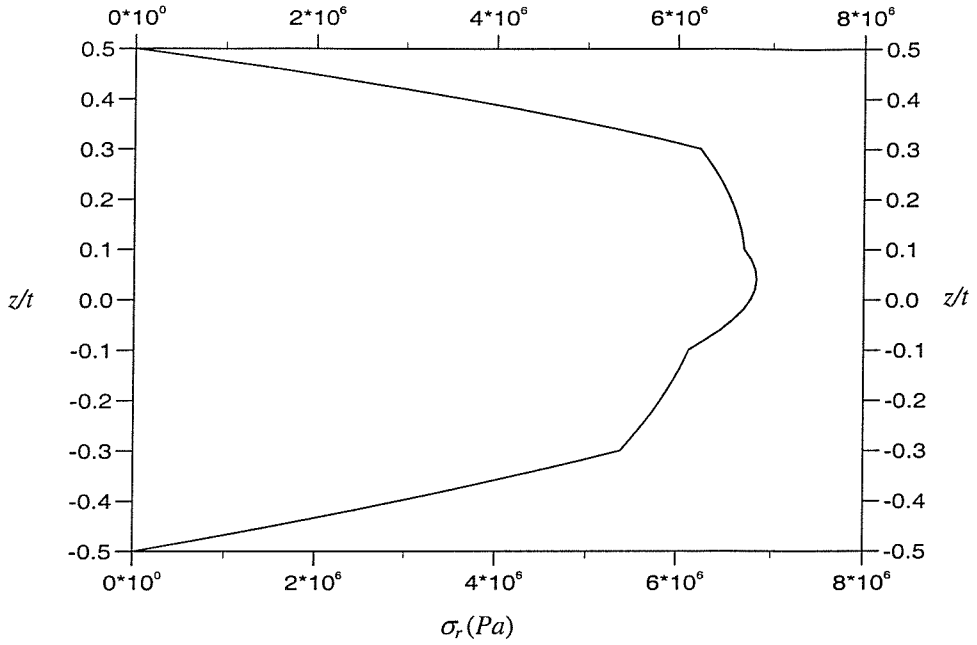

Figure 7.7a Through-Thickness Stress Distribution

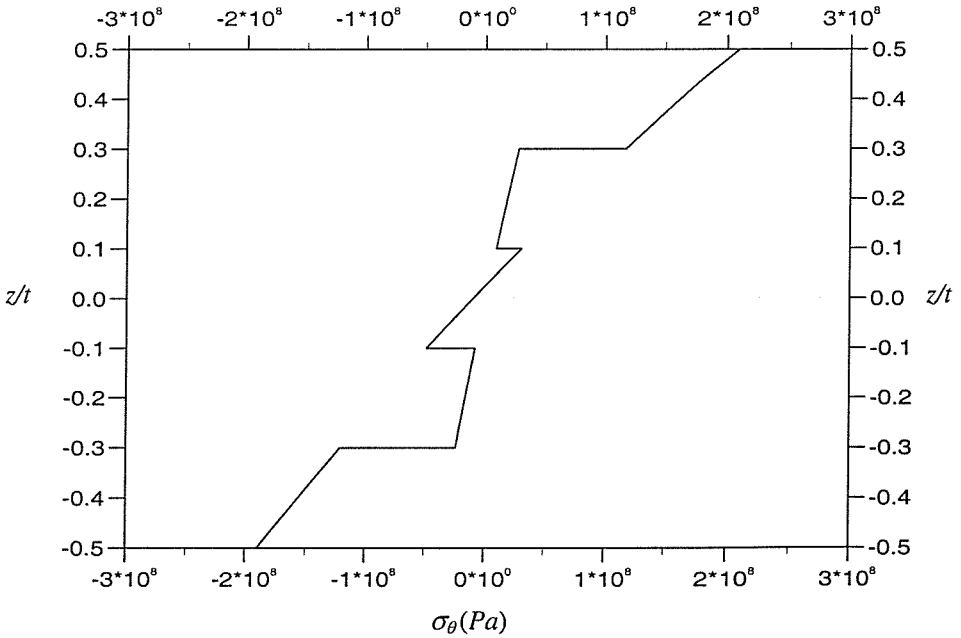

Figure 7.7b In-plane Tension Stress Distribution

Figure 7.7 Stresses Distribution Along Thickness—Stacking Sequence [0°/90°/0°/90°/0°]

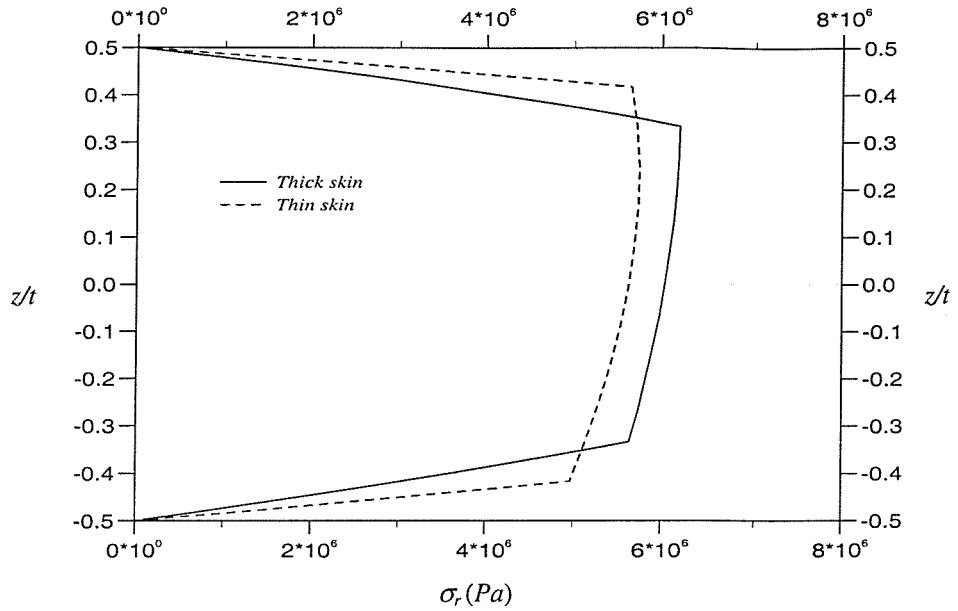

Figure 7.8a Through-Thickness Stress Distribution

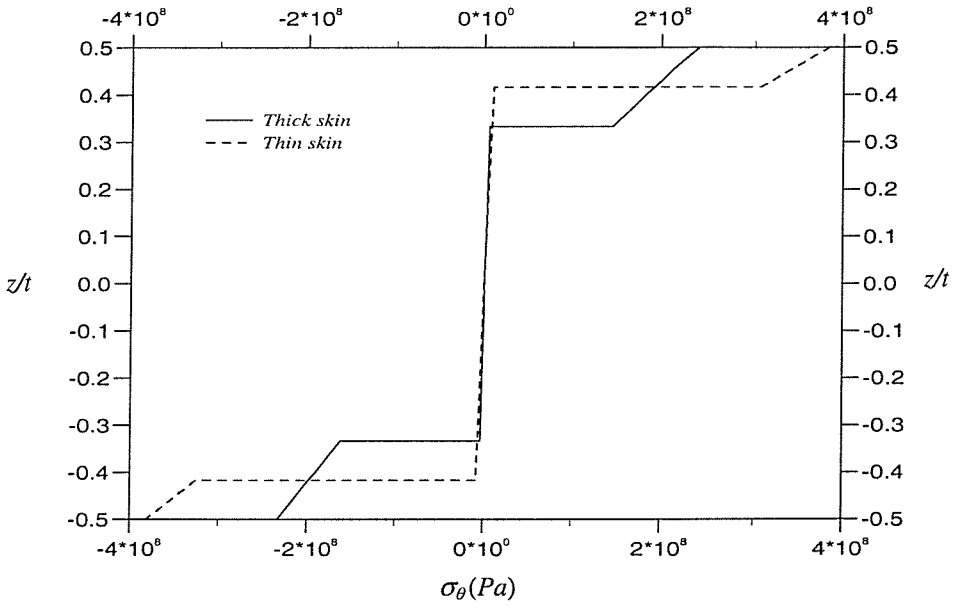

Figure 7.8b In-plane Tension Stress Distribution

Figure 7.8 Stresses Distribution Along Thickness in Sandwich Panel

Chapter 8: Delamination and Local Instability Damage Estimation of Curved Sandwich Beam

8.1 Introduction

Sandwich construction is widely used in industries where weight considerations have become important and has become an alternative in many new applications. In many such cases, curved sandwich panels or beams are needed. The geometry curvature in the structure results in not-so-insignificant through-thickness tensile stresses. These can significantly affect the performance of the structures due to the low values of through-thickness tensile strength. For example, the delamination of the skin in curved sandwich beam is more likely to occur in such cases. The analyses on this kind of failure mode are given in Chapters 4 and 7. The effects of some geometry related variables such as thickness of skin and geometry curvature of the sandwich beam on through-thickness stress leading to delamination are also investigated in Chapter 7.

One other feature of the curvature is the effect it has on the buckling/wrinkling characterisation of the face in compression. If the compression in the face of sandwich beam exceeds a critical load, this compressed face is then subject to a particular kind of instability which is either column/global buckling or local wrinkling/rippling. The local instability problem of straight sandwich beam can be studied by considering a long strut supported by a continuous elastic isotropic medium (Allen, 1969). However, as far as the curved sandwich beam is concerned, this problem becomes a little more complicated. In this chapter, the core material is still considered as elastic foundation and the Winkler Hypothesis is assumed. The theoretical solution achieved in Chapter 5 for critical value

of instability of a curved composite beam on an elastic foundation is then used to analyse the bending strength limit of a curved sandwich beam in the buckling/wrinkling failure of compressed skin.

8.2 Problem statement and approach for solution

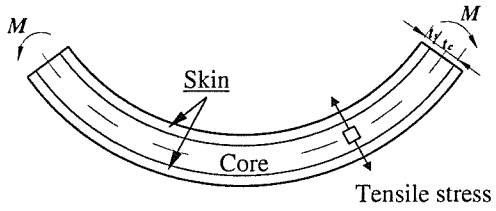

Figure 8.1a Opening bending moment

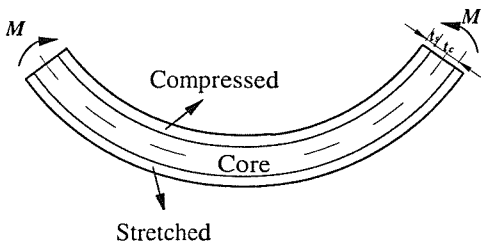

Figure 8.1b Closing bending moment

Figure 8.1 Typical curved sandwich beam under different loads

For flat sandwich beams a bending moment is transferred to the structure as compressive and tensile forces, while the core is subjected to very small through-thickness normal stress which can be neglected. The situation is different for curved sandwich beams. Through-thickness stresses occur due to the curved geometry in the structure. When a curved sandwich beam is subjected to an opening bending moment, as shown in Figure 8.1a, this stress is tensile. This tensile through-thickness stress could directly result in delamination. If, on the other hand this curved sandwich beam is subjected to a closing bending moment, as shown in Figure 8.1b, the stress is compressive. Under this condition, delamination is not so likely to occur as in the previous case. However, because the inner face of sandwich beam is compressed then instability becomes the cause of concern. These two cases are studied separately in the following paragraphs.

8.2.1 MODEL A: Curved sandwich beam with opening bending moment

According to the approach developed in Chapter 4, the through-thickness tensile stress distribution can be obtained, as has been shown in Chapter 7. Consequently, the opening bending strength limit can also be determined, provided that the through-thickness strengths of skin and core material and the adhesive strength of interface are all known. And also we can predict the occur of delamination in curved sandwich beam

8.2.2 MODEL B: Curved sandwich beam with closing bending moment

Consider a curved sandwich beam subjected to a closing bending moment. Its inner face is then under compression and instability becomes the cause of concern. In this section, the core is considered as an elastic foundation and the Winkler hypothesis (Selvadurai, 1979) is assumed. The compressed skin is considered as a curved composite beam lying on an elastic foundation. The critical load for buckling/wrinkling of the compressed skin can then be derived under this condition that curved sandwich is subjected to pure bending by curved beam theory and virtual displacement principle, as derived in Chapter 5. Thus the critical bending moment of curved sandwich beam can also be determined consequently in the failure of local instability (buckling/wrinkling) of compressed skin.

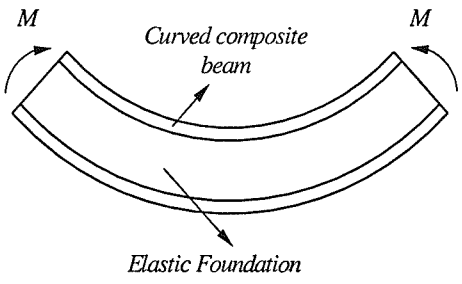

Figure 8.2a Global sketch

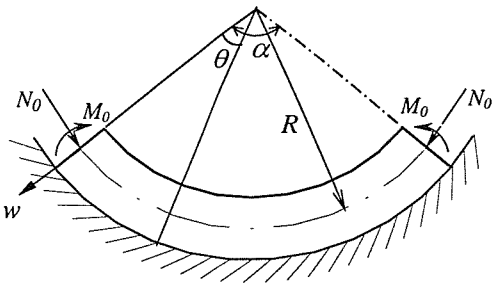

Figure 8.2b Local sketch

Figure 8.2 Sketches to analyse Model B

In calculating the critical bending moment, the following approximate formula is adapted to the thin skin sandwich sample:

$$M_{cr} = N_{cr} t_c b \tag{8.1}$$

where N_{cr} is the critical value of buckling/wrinkling of skin which can be obtained from the theoretical solution in Chapter 5, and in the analyses, the elastic stiffness of foundation – k is calculated by the approximation (Allen, 1969):

$$k = E_c / t_c \tag{8.2}$$

As far as thick skin curved sandwich beam is concerned, formula (8.1) is not suitable any longer. Meanwhile, the determination of critical value of skin N_{cr} is not very simple. The problem then becomes more complicated.

8.3 Application and comparison with numerical and experimental results

8.3.1 Through-thickness stress in curved sandwich beam with opening bending moment

In order to investigate the stress distribution in curved sandwich beams, the approach developed in Chapter 4 about through-thickness stress is applied to analyse two samples once used in Smidt's research work (Smidt, 1993 and 1996). The theoretical results are compared with corresponding numerical results and other approximate analytical results.

The magnitudes and material properties of curved sandwich beam sample are as follows:

Width b = *95* mm,	Inner radius of core R=*166* mm
Skin thickness t_f= *2* mm, *10* mm	Core thickness t_c=*50* mm
Young's modulus of skin:	In plane--E_1 = *18.1* GPa;
	Through thickness--E_2= *9.05* GPa (assumed)
Young's modulus of core:	E_c = *55* MPa
Poisson's ratio of skin:	ν_{12}=*0.4*, ν_{21} = *0.2* (assumed)
Poisson's ratio of core:	ν = *0.3*

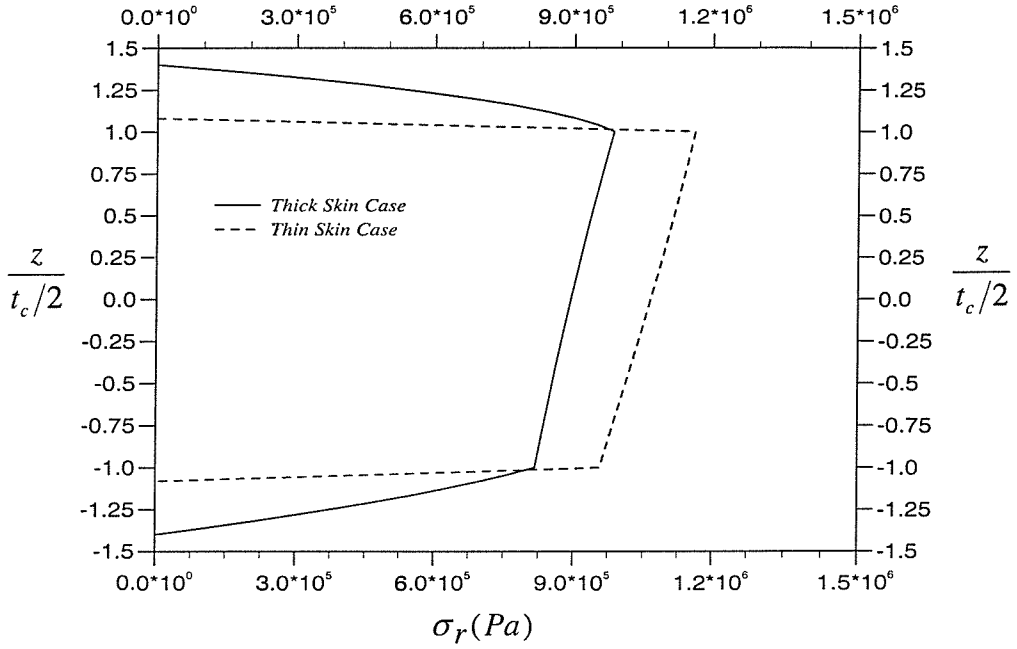

Figure 8.3 Through-thickness tensile stress distribution in curved sandwich beam

Figure 8.3 shows the results for these two curved sandwich beam samples. In this figure, abscissa is the value of through-thickness stress and ordinate is the normalised thickness $\bar{z} = \frac{z}{t_c/2}$, where t_c is the thickness of core. As can be seen again, a significant through-thickness stress gradient exists in the skin, and the maximum through-thickness stress generally occurs at the interface between core and the inner skin (sometimes in the core

but near to that interface). It can also be noted that the through-thickness stress changes only very slightly in the core; it keeps a high level nearly through the whole thickness of the core. This explains why in Gibson and Chandler's experiment (Gibson et al, 1994), delamination sometimes was seen to occur between either skin or core, and sometimes between both skins and the core.

Comparing the trends in thin skin case and thick skin case, although in a thick-skin sandwich beam, there is a smaller through-thickness stress than that in a thin-skin sandwich beam, it should be noted that the thickness of thick skin is five times of the thin skin and the distance between the centrelines of the faces increased up to 15.4%, which lead to bigger general bending stiffness of sandwich beam and much bigger weight of course. If the total thickness of sandwich beam is kept constant, then thick skin structure pose the bigger through-thickness stress which has been shown in Chapter 7.

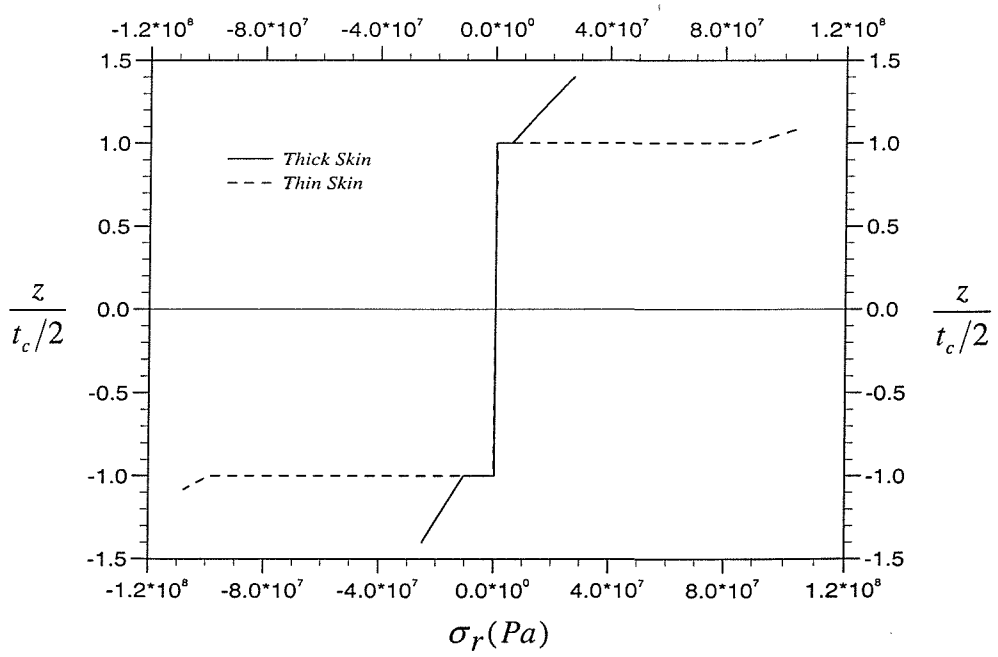

Figure 8.4 In-plane tensile stress distribution in curved sandwich beam

The results for in-plane tensile stress are shown in Figure 8.4. The largest value of in-plane stress in thin skin sandwich beam is as 3.93 times big as that in thick skin one (Noting that the thickness of thick skin is five times of the thin skin, and both samples have the same thickness of core).

Here it should also be pointed out that Gibson et al (1994) and Smidt (1993) once gave an approximation separately for calculating the maximum through-thickness stress in curved sandwich panel with thin skin which can both be expressed as:

$$Max.\sigma_r = \frac{-M}{Rt} \tag{8.3}$$

where in Gibson's formula R is the curvature radius of mid-plane of core and t is the total thickness of sandwich panel, while in Smidt's formula R is the inner radius of core and t is the thickness of core (which is later optimised to the distance between the centrelines of the faces (Smidt, 1996)).

Applying the formula for the above sandwich beams, Gibson's approximation underestimates maximum through-thickness stress considerably, especially to the sandwich panel with a thick skin, meanwhile Smidt's approximation overestimates maximum through-thickness stress.

Smidt also studied and examined the stresses distribution in these two sample and effects of material- and geometry-related variables of curved sandwich beam by FEM. In the numerical analyses (Smidt, 1993 and 1996), the maximum values of through-thickness stresses are 1.14 MPa and 0.95 MPa respectively, which are both located at the inner interface. As can be seen, the theoretical results—of about 1.16 MPa and 0.985 MPa—coincide well with the numerical results.

The radius of curved sandwich beam also has big effect on the stress, especially to the thick-skin sandwich beam. In the third case, the thicknesses of core and skin are both the

same as the above ones, only the inner radius decrease from 166 mm to 116 mm. The result for this case is shown in Figure 8.5. In this figure, ordinate is the normalised thickness *z/t*. As can be seen, the maximum of through-thickness stress increases significantly.

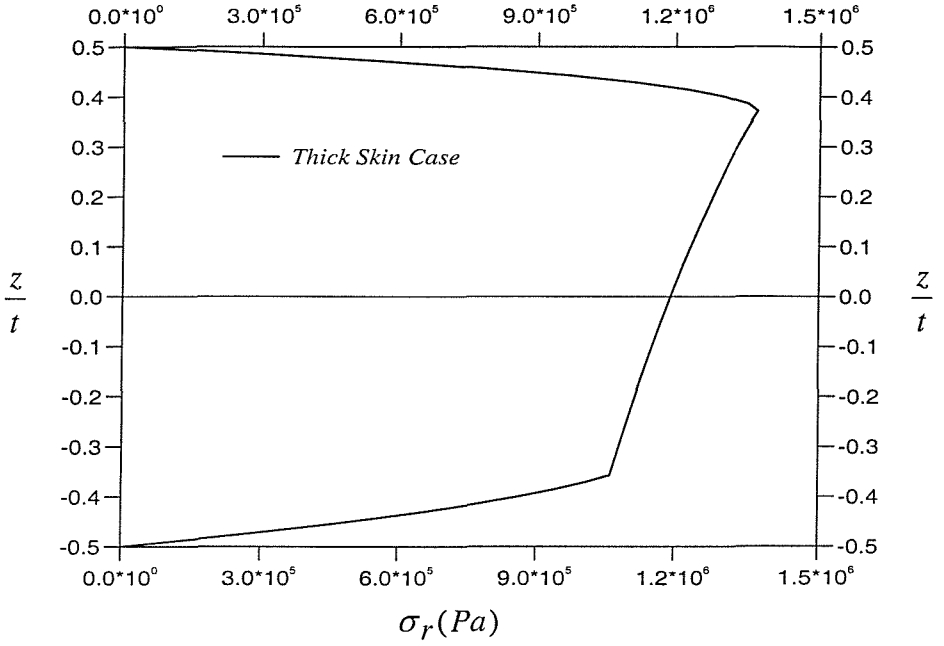

Figure 8.5 Through-thickness tensile stress distribution in curved sandwich beam with small radius

8.3.2 Strength of curved sandwich beam with closing bending moment compared to experimental results

As an application example of theoretical solution for instability of curved composite beam on an elastic foundation, the experimental results by S. Smidt (1993) are quoted and compared with the theoretical analyses.

Many sets of experiments on curved sandwich beams were designed and completed by Smidt, much part of which were investigation on the failure of curved sandwich beam under pure bending load. When the curved sandwich beam is subject to a critical closing bending moment, buckling in inner skin of sandwich beam will arise from compression. This is obviously local instability of the general beam. Thus the inner face and the core of the sandwich beam will then be considered as curved beam and elastic foundation respectively in the theoretical analyses.

It should also be pointed here that Smidt's typical sample is composed of straight part and curved part; and in some experiments, the buckling occurs in the straight part of the beam or very close to the transition between curved part and straight part. Therefore, these experiment results should be neglected. Three sets of tests are chosen here for comparision. The magnitudes of the curved part of the sample are as follows (Smidt, 1993):

Width $b = 95$ mm, Inner radius $R=166$ mm

Skin thickness $t_f=2$ mm, Core thickness $t_c=50$ mm

The material property of the core:

H60 : Density-$\rho=60$ kg/m^3; Young's Modulus-$E_c=55$ MPa

H130: Density-$\rho=130$ kg/m^3; Young's Modulus-$E_c=140$ MPa

The Young's moduli for the faces were *12* GPa (Woven roving laminates) and *18.1* GPa (Knitted cloth laminates).

Results from tests are then compared to calculation results from the above theoretical analyses. In theoretical analyses, the critical value of local instability of the skin is obtained from the approach presented in Chapter 5, and the critical bending moment is then calculated by formula (8.1) because the samples considered in this section are all thin skin samples. Both the theoretical results and experimental results are shown in Table 1. It could be seen from Table 1 that the theoretical results in all cases qualitatively agree with the experiment results respectively.

Table 8.1 Strength of curved sandwich beams with closing moment compared to theoretical results

Face	Core	Failure Load (experimental) [Nm]	Critical Load (theoretical) [Nm]
GRP(biaxial)	H60/60 Heat formated	754	921
GRP(triaxial)	H60/130* Heat formated	1875	1803
GRP(triaxial)	H130/130 Heat formated	2011	1803

- H60/130 means the core material in the straight part of sandwich beam H60, and in the curved part H130. H60/60 and H130/130 in the same column have the similar implication.

8.4 Summary

An elasticity-theory-based approach is used for studying through-thickness tension in curved sandwich beam whose behaviour is referred to under pure bending load condition. Since the solutions are exact within the assumptions of linear elasticity, there need be no strict distinction between thick and thin skin curved sandwich beam. The biggest through-thickness stress generally exists at the interface between core and inner face. The results from theoretical analyses satisfy well with the numerical results by other researchers, and are compared to two simply approximation formulae.

The critical bending moment for local instability of curved sandwich beam is also presented. The solution is based on consideration for buckling/wrinkling of curved laminate on an elastic foundation by beam theory and virtual displacement principle. Analyses for three samples give qualitative agreement with the experimental results in the literature.

The approaches presented in this thesis can therefore be used as a simple design tool for estimating ultimate limit state capability of a curved sandwich beam.

Chapter 9: Application to Tee Joint Structures

9.1 Introduction

The developed approach could be applicable in practical contexts involving the design and characterisation of tee joints, for example. A typical tee joint, with variables influencing the design, is shown in Figure 9.1. Currently such structures are analysed using physical (Hawkins et al, 1993; Shenoi and Hawkins, 1992) or numerical modelling (Shenoi and Hawkins, 1992; Dodkins et al, 1994). Much of the experimental (and FEA) work relates to a 45° pull-off condition, where the tee piece is clamped on the two flanges and a load (at 45°) is applied to the tip of the web, as shown in Figure 9.2. In most of the work it has been shown that the performance of the joint is dependent on the strength of the boundary angle. A critical condition determining performance is the value of through-thickness inter-laminar tensile stresses, which induce the first delamination in the overlaminate or boundary angle and thus lead to eventual failure of the joint. Currently such conclusions can only be drawn after comprehensive and detailed numerical modelling.

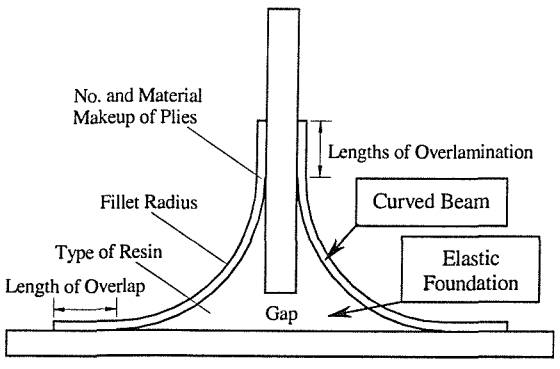

Figure 9.1 A typical tee-joint configuration

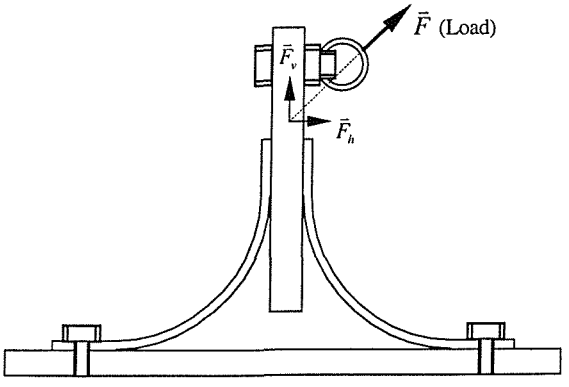

Figure 9.2 Boundary conditions

9.2 Application

The analytical approach developed in this paper is amenable for a relatively simple application to the boundary angle in the tee joint. Table 9.1 lists the design particulars of four different joint designs – all subjected to a 17.23kN pull-off load shown in Figure 9.2.

Table 9.1 Design details of the tee joints

Sample	Boundary angle thickness (mm)	Fillet radius (mm)	Fillet overlay	Resin	Edge gap (mm)
B	15	50	---	CR1200	20
F	2	75	2WR*	CR1200	15
K	2	50	2WR	CR1200	15
L	2	75	2WR+CSM+	polyester	15

- * WR – woven roving;
- + CSM – chopped strand mat

Table 9.2 Comparison of FEA with curved beam model results

Sample	Numerical Result [24,25] Maximum T-T Stress (MPa)	Theoretical Result	
		Maximum T-T Stress (MPa)	Location
B	10.85	Very large (>50.00)	Near midplane
F	2.79	5.79	interface
K	9.10	14.28	interface
L	8.05	8.09	interface

In the brief theoretical analyses for these samples, it is assumed that in the transition part of tee joint the load is totally sustained by the overlaminates and the shear forces in the overlaminates are neglected. By dividing load into vertical and horizontal components, $\bar{F}_v$ and $\bar{F}_h$, as shown in Figure 9.2, the axial force and bending moment in every

overlaminate can then be approximately calculated. The left overlaminate obviously posses the bigger axial force, thus it was taken as the object to be analysed by the approach in Chapter 3. It should be noticed here that the practical load condition actually does not coincide with the load condition required in the theoretical approach which is no-circimferential-dependence. Therefore the analyses presented here will give only relatively approximate results but can provide qualitative trend in a series of samples.

The inter-laminar tensile stresses calculated from the curved beam model are listed in Table 9.2 and compared with values deduced from previous FEA analyses (Shenoi and Hawkins, 1992; Dodkins et al, 1994). As can be observed, there is close qualitative agreement of results in all cases. Importantly the trend is consistent. The reasons for the differences are two-fold. Firstly, deducing the boundary conditions at the edge of the boundary angles for purposes of analytical calculations proved difficult. Therefore some simplifications had to be made regarding the fixity and rigidity of the root region of the joint. These assumptions led to increased apparent stiffness in the boundary angle, leading to increased stresses. Secondly, the numerical analyses were carried out with a geometrical non-linearity option whereas the curved beam analytical model is based on inherent geometric and material linearities. This again would tend to increase (deflection, strains and thus) stresses. Such simple closed form, curved beam analyses can thus be used as a quick design reference to check for adequacy in a load-bearing context.

9.3 Summary

The approach for treating curved orthotropic beams resting on an elastic foundation and subjected to flexural loading has been also used to analyse four tee joint samples. The analytical results show close qualitative agreement with the results of FEM in all cases. The trend is consistent with the conclusion of numerical analyses or experiments. The approach is simple enough to be used for both qualitative and quantitative evaluation at design stages of practical structures.

Chapter 10: Delamination Buckling of Curved Composite Beam

10.1 Introduction

As is known, delamination can significantly reduce the load-bearing capacity of composite structures. Delamination in curved composite laminates is more likely to be introduced during operational life as well as during the manufacturing process. One of the primary causes for delamination during operational life is the not-so-insignificant through-thickness tensile stress in curved laminates. One of the ways in which early structural failure can be caused is by delamination buckling. Local delamination can be considered as a crack in the interlaminar bond. Under buckling there appears a high interlaminar stress level at crack tip which leads to the crack process. Delamination growth can also lead to structural instability.

In recent years the problem of delamination buckling has been studied by some researchers, both experimentally and theoretically. However, it is noticeable that most of the work concerns straight laminated beams.

The delamination buckling in curved composite beam is investigated in this chapter. Based on linear and non-linear curved beam theory coupled with fracture mechanics concepts, two theoretical approaches are developed respectively for linear and nonlinear problems of delamination buckling which are concerned in the cases of normal delamination buckling and snap buckling. The general solutions are also applied to analyse some special cases e.g. delamination occurring at midplane and very close to surface of the beam. The effects of the arc angle of delamination crack and the radius of curvature of the beam etc. on the critical load in each case are also evaluated.

10.2 Problem Statements

The proposed problem deals with a circular arc shaped composite beam subjected to pure bending. This can be sub-divided into two cases.

Firstly, consider the case of a curved beam with pre-induced delamination in the middle of the whole span under the action of opening bending moment, as shown in Figure 1a. Here, in the middle part which contains delamination, the outer ply is subjected to compression and bending, while the inner ply is subjected to tension and bending. Upon further loading, the delamination crack will be opened and the outer ply may buckle to some extent. If the load—couple M_0 exceeds a limit, then the crack will progress. Actually this is a problem of coupled delamination and delamination induced buckling.

Secondly, consider the case of a curved beam with or without pre-induced delamination under the action of a closing bending moment. Thus the inner layer is subjected to compression and bending. When this compression reaches a critical value, the inner layer will suddenly transfer to a new equilibrium state by a snap mechanism, as shown in Figure 1b. Even if there is no pre-induced delamination, due to the weak interlaminar strength, this kind of snap buckling is also likely to occur in the inner thin film.

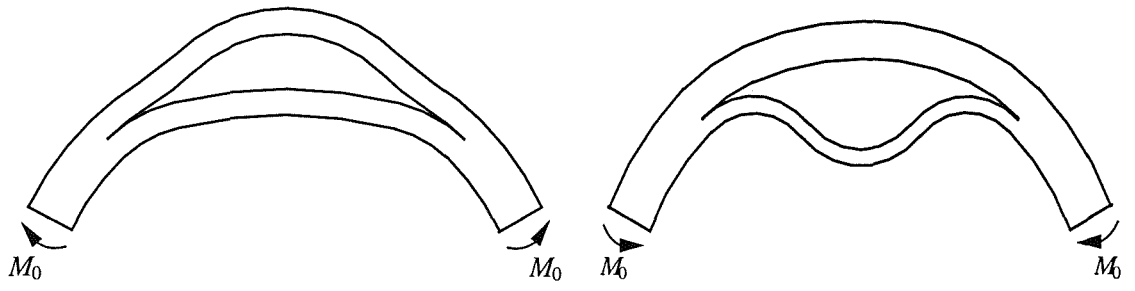

(a) Opening bending moment (b) Closing bending moment

Figure 10.1 curved composite beam subjected to pure bending

These cases will be investigated separately in the following two sections. Further, it is assumed that the delaminated part or potentially delaminated part is in the middle of global beam. Then owing to symmetry, only half the global beam need be considered. Actually because the curved beam is subjected to pure bending, the length of undelaminated part does not affect the mechanical characteristics of global beam.

10.3 Linear Problem—Delamination and Delamination Induced Buckling

10.3.1 General solution

As described above, in the case of a curved beam with delamination in the middle part and under the action of an opening bending moment, The problem is one of coupled delamination and delamination induced buckling. Here it is assumed that the new equilibrium form of delaminated part is close to the equilibrium form before deformation. Hence this problem is still considered as linear problem and linear theory is used for analysis.

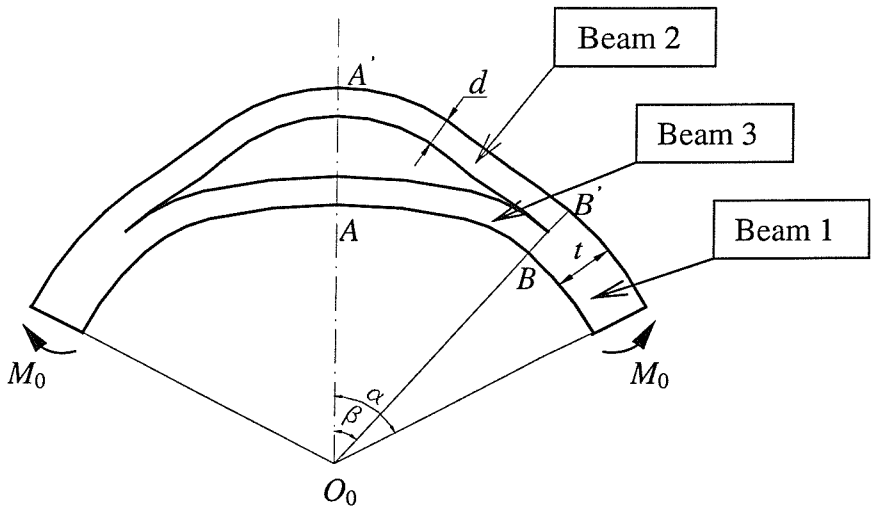

Figure 10.2 Delamination buckling in curved beam subjected to opening bending

The model sketch is shown in Figure 2. Assume the delamination is located exactly in the middle of the beam. The whole span is then symmetric. Hence in the following analysis, only the half span is analysed. Appropriate boundary conditions are placed at the symmetry cross section AA'. The delaminated curved beam is further divided into three parts, the normal undelaminated part is designated as beam 1, the outer layer of delaminated part is designated as beam 2, the inner layer is beam 3, as shown in Figure 2. The load applied on each beam and the respective boundary condition are shown in Figure 10.3(a).

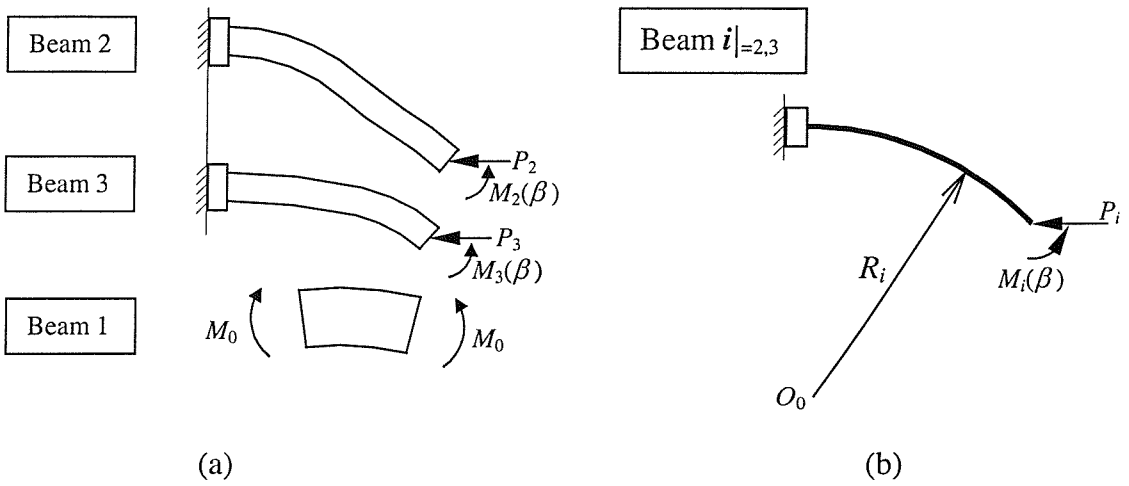

Figure 10.3 Model sketch for every part in the global beam

The general bending equation for a curved beam with a radius of curvature R is

$$\frac{d^2w}{d\theta^2} + w = -\frac{M(\theta)\cdot R^2}{D} \tag{10-1}$$

where D is the flexural rigidity of the beam and M is taken to be positive when it produces a decrease in the curvature.

It should be noted that a curved beam without any other restriction (e.g. foundation etc.) can only undertake pure bending or a pair of forces applied along the line linking the two

applied points. Therefore, the direction of forces acting on beams 2 and 3 can be known, which according to the considered conditions should be in the horizontal direction as shown in Figure 10.3a. Beams 2 and 3 can be described uniformly by Figure 10.3b, and the internal bending moment at any cross section of the beam can consequently be expressed uniformly as:

$$M_i(\theta) = M_i(\beta) - P_i\left(R_i\cos\theta - R_i\cos\beta\right), \qquad i = 2,3 \tag{10-2}$$

Substituting this into the bending equation (10-1), the following equation can then be obtained

$$\frac{d^2w_i}{d\theta^2} + w_i = \frac{P_i \cdot R_i^3}{D_i}\cos\theta - \frac{R_i^2}{D_i}\left[M_i(\beta) + P_iR_i\cos\beta\right], \qquad i = 2,3 \tag{10-3}$$

The solution of this differential equation is

$$w_i = A_i\cos\theta + B_i\sin\theta - \frac{R_i^2}{D_i}\left[M_i(\beta) + P_iR_i\cos\beta\right] + \frac{P_iR_i^3}{2D_i}\theta\sin\theta, \quad i = 2,3 \tag{10-4}$$

Beam I is subjected to pure bending, and its displacement can be solved directly by equation (10-1) and where the $M(\theta)$ is replaced by constant M_0

$$w_1 = A_1\cos\theta + B_1\sin\theta - \frac{M_0R^2}{D} \tag{10-5}$$

Noting the symmetry condition, $B_i = 0$ (i = 1, 2 and 3). Then the radial displacement in each part beam is:

$$\begin{cases} w_1 = A_1\cos\theta - \dfrac{M_0R^2}{D} \\ w_2 = A_2\cos\theta - \dfrac{R_2^2}{D_2}[M_2(\beta) + P_2R_2\cos\beta] + \dfrac{P_2R_2^3}{2D_2}\theta\sin\theta \\ w_3 = A_3\cos\theta - \dfrac{R_3^2}{D_3}[M_3(\beta) + P_3R_3\cos\beta] + \dfrac{P_3R_3^3}{2D_3}\theta\sin\theta \end{cases} \tag{10-6}$$

where

$$\begin{cases} R_2 = R + \dfrac{t-d}{2} \\ R_3 = R - \dfrac{d}{2} \end{cases}$$

Thus there are seven unknown variables in the above results: A_1, A_2, A_3, M_2, M_3, P_2, P_3. Here it is assumed:

$$w_1|_{\theta=0} = 0 \tag{10-7}$$

The displacement compatibility in the cross section of $\theta = \beta$ leads to:

$$\begin{aligned} w_1|_{\theta=\beta} &= w_2|_{\theta=\beta} \\ w_1'|_{\theta=\beta} &= w_2'|_{\theta=\beta} \\ w_1|_{\theta=\beta} &= w_3|_{\theta=\beta} \\ w_1'|_{\theta=\beta} &= w_3'|_{\theta=\beta} \end{aligned} \tag{10-8}$$

where $w_1' = \dfrac{1}{R_1}\dfrac{dw_1}{d\theta}, w_2' = \dfrac{1}{R_2}\dfrac{dw_2}{d\theta}, w_3' = \dfrac{1}{R_3}\dfrac{dw_3}{d\theta}$.

Further, according to the equilibrium condition at cross section BB' in Figure 2, there are the following relations hold true:

$$\begin{aligned} &P_2 + P_3 = 0 \\ &M_2(\beta) + M_3(\beta) + P_2\frac{t-d}{2}\cos\beta - P_3\frac{d}{2}\cos\beta = M_0 \end{aligned} \tag{10-9}$$

As can be seen, there are just seven equations altogether—equations (10-7)~(10-9). Thus the coefficients in the above result expressions (10-5) can be all solved out by these equations as follows:

$$A_1 = \frac{M_0 R^2}{D} \tag{10-10}$$

$$P_2 = -P_3 = \frac{4M_0}{t} \frac{1 - \frac{R}{D}\left(\frac{D_2}{R_2} + \frac{D_3}{R_3}\right)\cos\beta - \frac{R^2}{D}\left(\frac{D_2}{R_2^2} + \frac{D_3}{R_3^2}\right)(1-\cos\beta)}{\frac{\beta}{\sin\beta} + \cos\beta} \tag{10-11}$$

$$\begin{aligned} A_2 &= \frac{M_0 R}{D} R_2 + \frac{P_2 R_2^3}{2D_2}(1 + \beta\cot\beta) \\ A_3 &= \frac{M_0 R}{D} R_3 + \frac{P_3 R_3^3}{2D_3}(1 + \beta\cot\beta) \end{aligned} \tag{10-12}$$

$$\begin{aligned} M_2(\beta) &= A_2 \frac{D_2}{R_2^2}\cos\beta + P_2 R_2\left(\frac{1}{2}\beta\sin\beta - \cos\beta\right) + M_0 \frac{R^2}{R_2^2}\frac{D_2}{D}(1-\cos\beta) \\ M_3(\beta) &= A_3 \frac{D_3}{R_3^2}\cos\beta + P_3 R_3\left(\frac{1}{2}\beta\sin\beta - \cos\beta\right) + M_0 \frac{R^2}{R_3^2}\frac{D_3}{D}(1-\cos\beta) \end{aligned} \tag{10-13}$$

Consequently the bending moment in beams 1, 2 and 3 respectively are:

$$\begin{aligned} M_1(\theta) &= M_0 \\ M_2(\theta) &= M_2(\beta) + P_2 R_2\cos\beta - P_2 R_2\cos\theta \\ M_3(\theta) &= M_3(\beta) + P_3 R_3\cos\beta - P_3 R_3\cos\theta \end{aligned} \tag{10-14}$$

The consequential strain energies in the beams are:

$$\begin{aligned} U_1 &= \int_\beta^\alpha \frac{1}{2D} M_1^2(\theta) R d\theta = \frac{M_0^2 R}{2D}(\alpha - \beta) \\ U_2 &= \int_0^\beta \frac{1}{2D_2} M_2^2(\theta) R_2 d\theta \\ U_3 &= \int_0^\beta \frac{1}{2D_3} M_3^2(\theta) R_3 d\theta \end{aligned} \tag{10-15}$$

The total strain energy in the global curved beam is then obtained:

$$U = U_1 + U_2 + U_3 \tag{10-16}$$

From the Griffith's criterion of fracture, the following relation is true:

$$\frac{\partial U}{\partial(R^*\beta)} = 2\Gamma \tag{10-17}$$

where $R^* = R + \frac{t}{2} - d$ which is the curvature radius of delamination crack, and Γ is surface energy (energy required to form a unit of a new surface in the body). Substituting all the related equations into the above relation, the external bending couple M_0 can then be finally solved out as a function of half arc angle of delamination crack β, given that other parameters are all fixed.

Obviously the expression of this solution for the general case is very complex, so it is not given here for reasons of saving space. Two usual important cases will be considered in detail in the following sections as examples for the above analytical approach.

10.3.2 Delamination occurs at the midplane of curved beam

According to previous work (e.g. Shenoi & Wang, 2001), the maximum through-thickness tension stress in curved orthotropic beam always exists in a location very close to midplane; so delamination is most likely to occur there. Also the occurrence and growth of the delamination is assumed to be in its own plane in keeping with the laminate character of layered composite. We note that the delaminated layers may not possess the same properties of the original perfect beam. Such material behaviour change can be readily dealt with at the expense of introducing additional parameters into the problem, as shown in the above. However neither the physical principles involved in the analyses nor the general character of the results will change, hence attention to these details will be omitted here and in the following parts. For simplicity reasons the properties of the curved beam are assumed homogeneous, linearly elastic, and the same before and after

delamination. Further, it is assumed here that delamination is exactly at the midplane so as to simplify the problem, with $d = t/2$, leading to $D_2 = D_3 = D/8$.

Let $\delta = t/R$. Assume $\delta << 1$, so $(t-d)/R$ and $d/R << 1$ too. Then

$$P_2 = -P_3 \approx \frac{M_0}{t} \frac{3 - \frac{\delta}{4}\cos\beta}{\frac{\beta}{\sin\beta} + \cos\beta} \tag{10-18}$$

Substitute this into expressions (10-12) and (10-13). Further, because $\delta << 1$, for the reasons of simplification the approximation: $R_2 \approx R_3 \approx R$ holds true. A_2, A_3, M_2 and M_3 can all be determined then:

$$\begin{aligned} A_2 &= \frac{M_0 R^2}{D} + \frac{4R^3}{D}\frac{M_0}{t}\frac{\left(3 - \frac{\delta}{4}\cos\beta\right)(\sin\beta + \beta\cos\beta)}{\beta + \sin\beta\cos\beta} \\ A_3 &= \frac{M_0 R^2}{D} - \frac{4R^3}{D}\frac{M_0}{t}\frac{\left(3 - \frac{\delta}{4}\cos\beta\right)(\sin\beta + \beta\cos\beta)}{\beta + \sin\beta\cos\beta} \end{aligned} \tag{10-19}$$

$$\begin{aligned} M_2 &= \frac{M_0}{8} + \frac{3}{2}\frac{M_0 R}{t} - 3\frac{M_0 R}{t}\frac{\sin\beta\cos\beta}{\beta + \sin\beta\cos\beta} \\ M_3 &= \frac{M_0}{8} - \frac{3}{2}\frac{M_0 R}{t} + 3\frac{M_0 R}{t}\frac{\sin\beta\cos\beta}{\beta + \sin\beta\cos\beta} \end{aligned}$$

The equations (10-15) can then be simplified as

$$\begin{aligned} U_1 &= \frac{M_0^2 R}{2D}(\alpha - \beta) \\ U_2 &= \frac{4R}{D}\int_0^\beta M_2{}^2(\theta)d\theta \\ U_3 &= \frac{4R}{D}\int_0^\beta M_3{}^2(\theta)d\theta \end{aligned} \tag{10-20}$$

and the relation (10-17) can be simplified as:

$$\frac{\partial U}{\partial \beta} = 2R\Gamma \tag{10-21}$$

By substituting equation (10-19) into equations (10-15) and (10-16), and then using the relation (10-20), the final solution can be deduced:

$$M_0^* = \sqrt{\frac{2D\Gamma}{g(\beta)}} \tag{10-22}$$

where M_0^* is the critical value of M_0 for the progress of delamination crack, and:

$$g(\beta) = 18\left(\frac{R}{t}\right)^2 f(\beta) - \frac{3}{8}$$

$$f(\beta) = \left(\frac{\beta - \sin\beta\cos\beta}{\beta + \sin\beta\cos\beta}\right)^2 + \frac{\beta^2 \sin\beta\cos\beta - \beta\sin^2\beta\cos^2\beta}{(\beta + \sin\beta\cos\beta)^2}\left(\frac{2\sin^2\beta}{\beta + \sin\beta\cos\beta} - \beta\right) \tag{10-23}$$

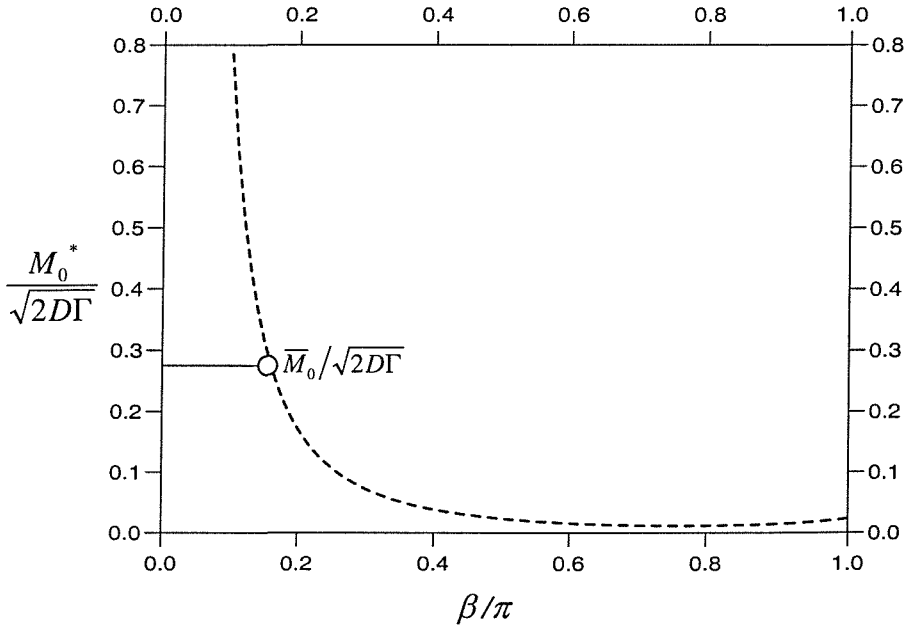

Figure 10.4 Dimensionless critical load with respect to half arc angle of delamination

According to equations (10-22) and (10-23), the trend of normalised critical bending moment $\frac{M_0^*}{\sqrt{2D\Gamma}}$ with respect to normalised half delamination arc angle β/π is shown in Figure 10.4 as a dashed line under the condition that R/t=10.

If β is large enough, compared with the first term in the right side of expression of $g(\beta)$, the second term is usually small enough to be neglected, then the result can be further simplified:

$$\frac{M_0^*}{\sqrt{D\Gamma}} = \frac{\delta}{3}\frac{1}{\sqrt{f(\beta)}} \tag{10-24}$$

Considering the extreme condition of $\beta = 0$, which means there is no delamination in curved beam at first: $\lim_{\beta\to 0} f(\beta) = 0$. Then the critical value of M_0 from equation (10-24) at this condition becomes infinite, which is expected:

$$M_0^*|_{\beta=0} = \infty \tag{10-25}$$

However it should be pointed out that when β is small, the value from equation (10-24) is always quite larger than the value (designated as $\overline{M}_0$) which induces through-thickness tensile stress exceeding the interface strength of curved composite beam and leading to delamination. Therefore, as far as the critical value of bending couple for curved composite beam with delamination crack is concerned, it should be the smaller of these two value (M_0^* and $\overline{M}_0$)—designated as $\overline{M}_0^*$:

$$\overline{M}_0^* = Min\{M_0^*, \overline{M}_0\} \tag{10-26}$$

Therefore as shown in Figure 10.4, $\overline{M}_0^* = \overline{M}_0$ when β is small and $\overline{M}_0^* = M_0^*$ for large β.

In order to investigate the effect of curvature radius on the critical load for delamination buckling, equation (10-24) is rewritten, noting $\delta=t/R$ and $L=R\beta$

$$\frac{M_0^*}{\sqrt{D\Gamma}} = \frac{t}{3L} \cdot \frac{\beta}{\sqrt{f(\beta)}} \tag{10-27}$$

where L is the half length of delamination

As can be seen, if L and t – the length and thickness of delamination -- are both constant, the value of critical load is only subject to the value of function $\frac{\beta}{\sqrt{f(\beta)}}$. The variation of function $\frac{\beta}{\sqrt{f(\beta)}}$ is shown in Figure 10.5. The abscissa represents the normalised half arc angle of delamination and ordinate represents the value of the function.

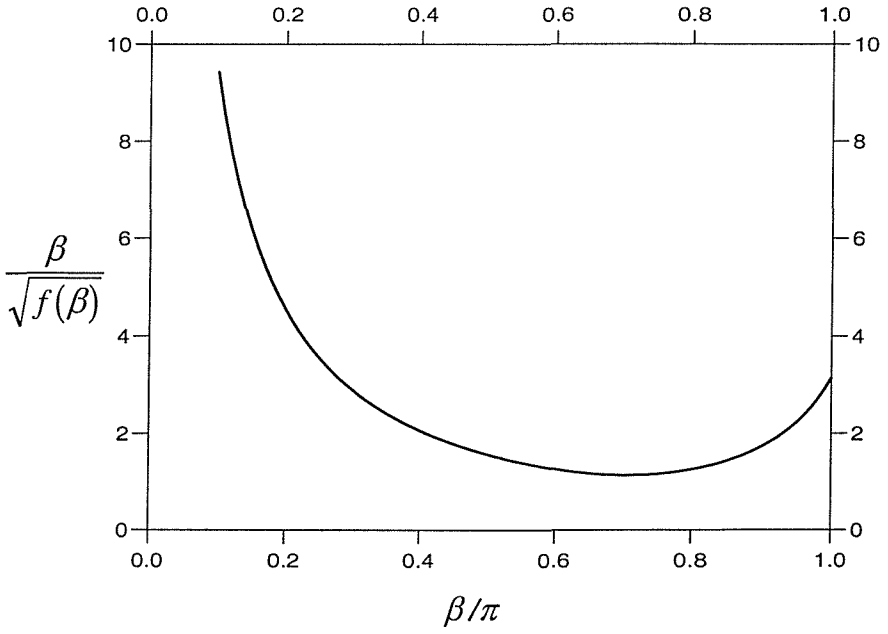

Figure 10.5 Variation of function $\frac{\beta}{\sqrt{f(\beta)}}$

When β increases, the function firstly decreases and then increases. It reaches minimum value at $\beta = 0.71\pi$. Noting that $\beta=L/R$ and L is assumed to be constant, that means when R decreases, the value of critical bending moment firstly decreases and then increases, and it reaches minimum if $L= 0.71\pi R$. Also note that when R is very large, the value of critical load is not calculated from equation (10-27) but is subject to the value of $\overline{M}_0$ (equation (10-26)).

It should also be noted that $\overline{M}_0$ is not the same for different beam geometries. Our previous research work (Shenoi & Wang, 2001) shows that radius of curvature R has a major effect on the maximum through-thickness tension stress consequently $\overline{M}_0$. From the previous work, it can be known that larger R leads to a smaller through-thickness tensile stress which results in larger critical bending moment – provided that other parameters are all constant. Therefore, above all, after the point $R=L/0.71\pi$ increasing curvature radius R results in an increased value of the critical load.

10.3.3 Delamination occurs very close to the surface of considered curved beam

Sometimes delamination exists close to the surface of the beam. Assuming here delamination occurs very close to outer surface, which means $d << t$, it is called thin film delamination. Based on this assumption, we have:

$$\frac{D_2}{D} \approx 0 \text{ and}$$

$$\frac{D_3}{D} = \left(\frac{t-d}{t}\right)^3 \approx 1-3\frac{d}{t} \qquad (10\text{-}28)$$

Then from equation (10-11), and also taking the similar assumption with $\delta = t/R << 1$:

$$P_2 = -P_3 \approx \frac{12M_0 d}{t^2}\frac{\sin\beta}{\beta+\sin\beta\cos\beta} \tag{10-29}$$

Using the approach in the preceding subsection, substituting this into equations (10-12) and (10-13), and also using the approximation: $R_2 = R_3 = R$, A_2, A_3, M_2 and M_3 can then be determined again:

$$\begin{aligned}
A_2 &= \frac{M_0 R^2}{D} + \frac{6R^3}{D_2}\frac{M_0 d}{t^2}\frac{\sin\beta+\beta\cos\beta}{\beta+\sin\beta\cos\beta} \\
A_3 &= \frac{M_0 R^2}{D} - \frac{6R^3}{D_3}\frac{M_0 d}{t^2}\frac{\sin\beta+\beta\cos\beta}{\beta+\sin\beta\cos\beta} \\
M_2 &\approx 6\frac{M_0 Rd}{t^2}\frac{\beta-\sin\beta\cos\beta}{\beta+\sin\beta\cos\beta} \\
M_3 &= \frac{D_3}{D}M_0 - 6\frac{M_0 Rd}{t^2}\frac{\beta-\sin\beta\cos\beta}{\beta+\sin\beta\cos\beta}
\end{aligned} \tag{10-30}$$

Let $\eta = \frac{d}{t}$, so $D_2 = \eta^3 D$. Substituting all the above equations (10-29) and (10-30) into equation (10-15) to estimate strain energies with three beams, then into (10-16) to estimate total strain energy with system and then into relation (10-21) for the Griffith's criterion, the final solution for the case of thin film delamination can be deduced:

$$\frac{\hat{M}_0^*}{\sqrt{D\Gamma}} = \frac{\delta}{3}\frac{\sqrt{\eta}}{\sqrt{\hat{f}(\beta)}} \tag{10-31}$$

where $\hat{M}_0^*$ is the critical value for the case of thin film delamination, and

$$\hat{f}(\beta) = \left(\frac{\beta-\sin\beta\cos\beta}{\beta+\sin\beta\cos\beta}\right)^2 + 2\frac{\beta^2\sin\beta\cos\beta-\beta\sin^2\beta\cos^2\beta}{(\beta+\sin\beta\cos\beta)^2}\left(\frac{2\sin^2\beta}{\beta+\sin\beta\cos\beta}-\beta\right) \tag{10-32}$$

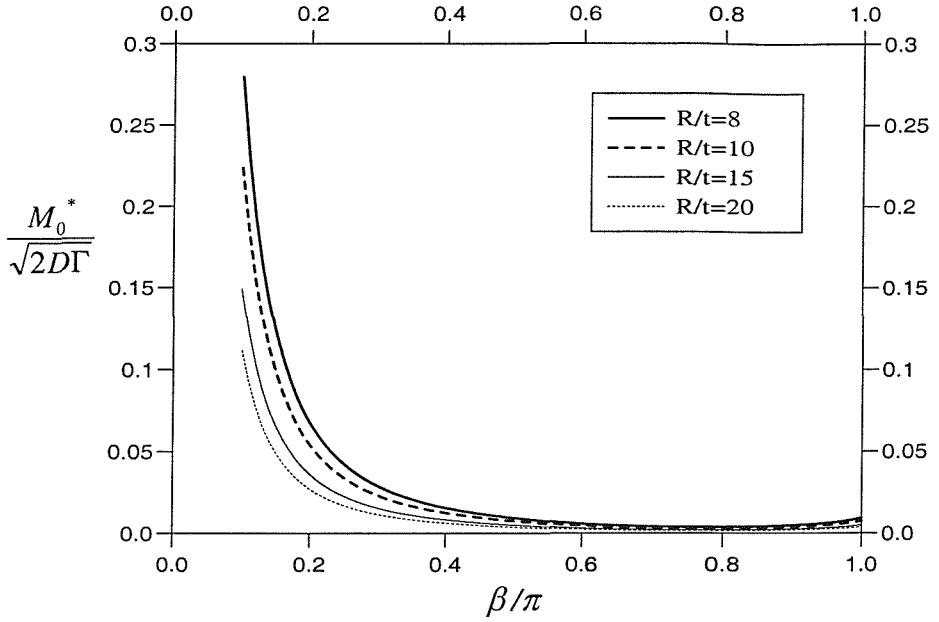

Figure 10.6 Dimensionless critical loads corresponding to different *R/t*

The results for four cases of different *R/t* (equal to 8, 10, 15, 20 respectively) are shown in Figure 10.6. Here the abscissa still represents the normalised half arc angle of delamination β/π, and the ordinate represents the normalised critical load value $\frac{M_0^*}{\sqrt{2D\Gamma}}$, the same as in Figure 10.5, for the reason of comparision. Comparing the case of *R/t*=10 with Figure 10.5, it can be seen that the values in Figure 10.6 are smaller than corresponding values in Figure 10.5. This is mostly due to the existence of $\sqrt{\eta}$ in equation (10-31) compared with equation (10-24). This result shows that delamination buckling is more likely to occur close to the surface in curved composite beam. That can explain to some extent why in some samples delamination occurs and progress very close to the surface although the maximum through-thickness tensile stress usually exists at midplane of global curved beam (Shenoi & Hawkins, 1992).

It should be noted that equations (10-31) and (10-32) are both deduced from the assumption of thin film delamination. If we extend it to general cases, it will probably

bring errors to some extent. For example, if it is used to analyse the case of delamination at midplane, in this case $\eta = 1/2$. The right side of equation (10-31) is not only $\sqrt{2}$ times right side of equation (10-24), but $f(\beta)$ of equation (10-22) is obviously different from $\hat{f}(\beta)$ of equation (10-32). The comparison of function $f(\beta)$ with $\hat{f}(\beta)$ is shown in Figure 10.7.

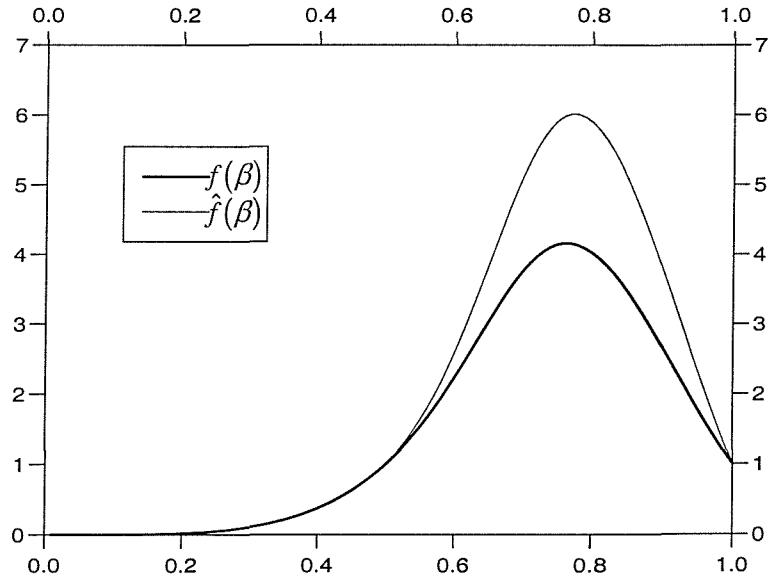

Figure 10.7 $f(\beta)$ and $\hat{f}(\beta)$

However, as can be seen from Figure 10.7, there is only very little difference between functions $f(\beta)$ and $\hat{f}(\beta)$ in the scope of $\beta \in \left(0, \frac{\pi}{2}\right)$. Therefore if the delamination arc is smaller than a semi-circle, which is the usual case, an approximate formula based on the interpolation of these two cases can be provided to analyse the general case

$$\frac{\hat{M}_0^*}{\sqrt{D\Gamma}} = \frac{\delta}{3}\frac{\eta'}{\sqrt{\hat{f}(\beta)}} \tag{10-33}$$

where $\eta' = \left[-\left(\sqrt{2}-1\right)(2\eta-1)^2+\sqrt{2}\right]\sqrt{\eta} \qquad (0<\eta<1)$

As in the last subsection, the effect of radius of curvature R on the value of the critical load in the case that delamination buckling occurs very close to the surface can be analysed by the variation of function $\frac{\beta}{\sqrt{\hat{f}(\beta)}}$, as shown in Figure 10.8. The trend of it is very similar to function $\frac{\beta}{\sqrt{f(\beta)}}$.

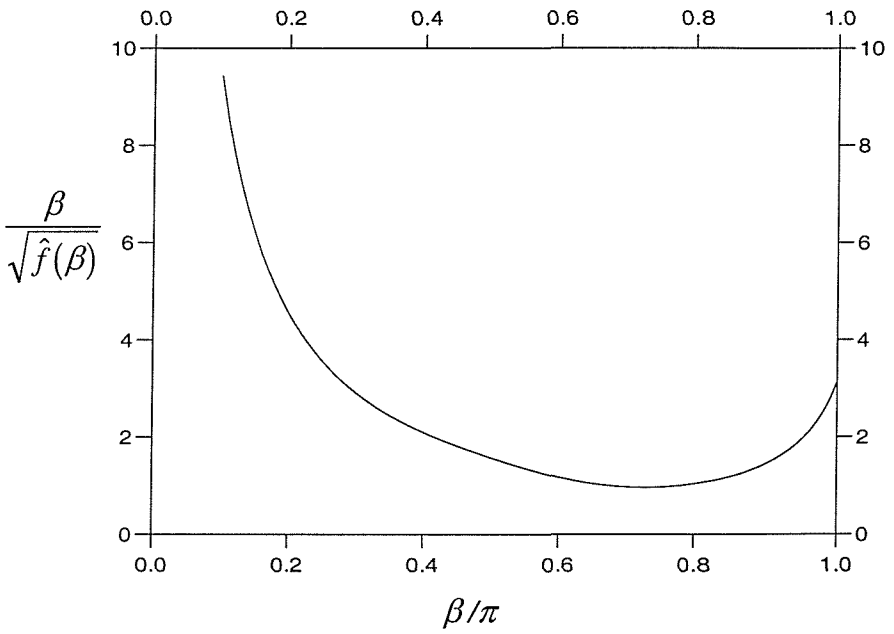

Figure 10.8 Variation of function $\frac{\beta}{\sqrt{\hat{f}(\beta)}}$

10.4 Nonlinear Problem-Snap Buckling

In this section the problem of a curved composite beam under a closing bending moment will be considered. Under this condition, the layer next to the inner surface of the beam is then subjected to compressive stress. If this stress is high enough, snap buckling of

internal layer arises due to the relatively low strength of the inter-laminar bond in the layered composite beam. If there already exists a delamination in this curved beam before the load is applied, then snap buckling of the inner layer is certainly more likely to occur, and progress of this delamination crack becomes of considerable concern.

In this case, the new equilibrium state is not close to the initial one. Therefore this problem is a nonlinear problem. The general solution of this problem can be found by the nonlinear analyses on deformation of the flexible beam.

10.4.1 General solution

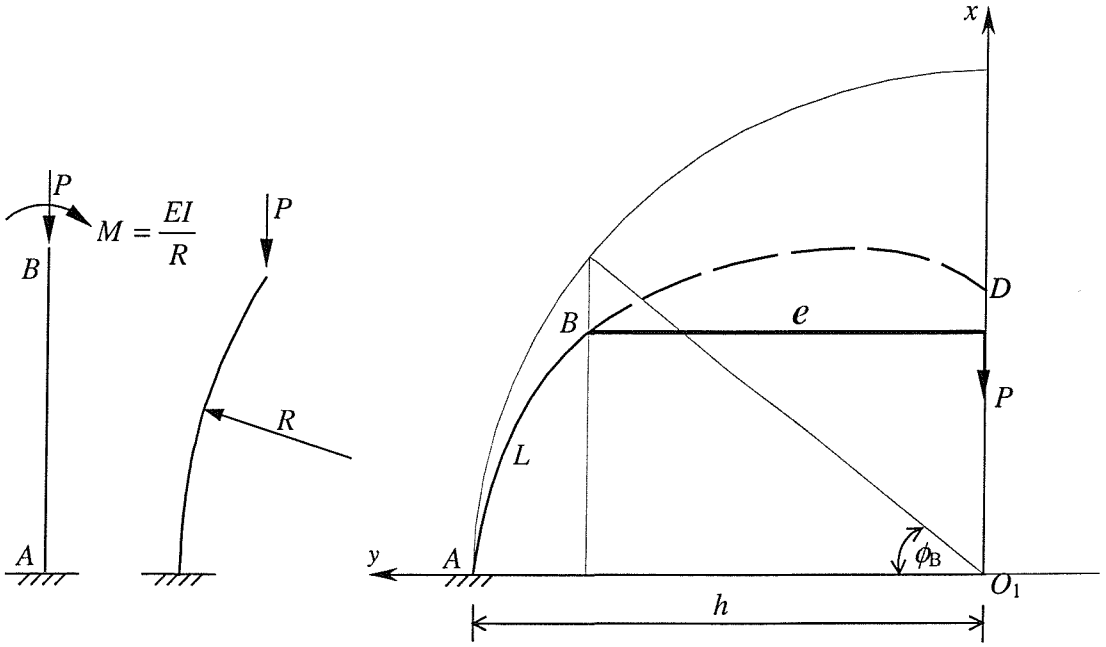

Figure 10.9 Model sketch for the basic problem

Because it is more difficult to directly begin with the basic equations of curved bar under point loads to analyse its nonlinear deflection, the method of similarity is used here. At first consider a straight, vertical strut *AB* subjected to a load *P* on the top and a clockwise couple *M=EI/R* acting at the same point, as shown in Figure 10.9a. The action of the

couple M will bend the strut into a circular arc of radius R, while the load P is still acting on the free end, as shown in Figure 10.9b. This latter bar–the circular bar–will therefore be analysed in our approach to the present problem.

The couple M and the load P will now be replaced by a force P acting on a rigid lever of length $e=M/P$. Expressing e as

$$e = \frac{M}{P} = \frac{EI}{RP} = \frac{1}{k^2 R} \tag{10-34}$$

where $k = \left(\frac{P}{EI}\right)^{1/2}$, EI is the flexural rigidity of the curved beam.

Using the principle of elastic similarity, extend the bar past B until it intersects the line of action of P which is exerted on the lever. Let this point be D, as shown in Figure 10.9c. And so far as the shape AB is concerned, it does not matter whether the load acts on the bar ABD or through the lever e. The total length of the new strut AD is then:

$$L = L_1 + L_2 \tag{10-35}$$

L_1 is the length of original strut which is known, L_2 is the length of extension BD.

Using the knowledge of nonlinear deflection of flexible bar (Appendix C), introducing the modulus p and parameter ϕ --equation (C-6) (Appendix C), from Figure 10.9c and noting equation (C-5) (Appendix C)

$$\cos\phi_B = \frac{e}{h} = \frac{ek}{2p} \tag{10-36}$$

Substituting equation (10-34) into equation (10-36), the following is true

$$\cos\phi_B = \frac{1}{2pkR} \tag{10-37}$$

From equation (C-8), the modulus p can be solved out by

$$L_1 = \frac{1}{k} F(p, \phi_B) \tag{10-38}$$

and then the slope, arc length and coordinates at any point of bar AB can be calculated by the related formulae in Appendix C.

Let us now go back to the beginning of this section and look into the original question. If a curved composite beam is subjected to closing bending, its inner ply is likely to be subjected to snap buckling as shown in Figure 10.10a. It is assumed here that the new equilibrium state of outer ply (still named as beam 2 in Figure 10.10a, similarly to in last section) is still close to its initial state. So the linear theory is still used to analyse this ply. However when the inner ply (still named as beam 3 in Figure 10.10a), where the snap buckling occurs, is investigated, the nonlinear analyses mentioned above and in Appendix C must be used.

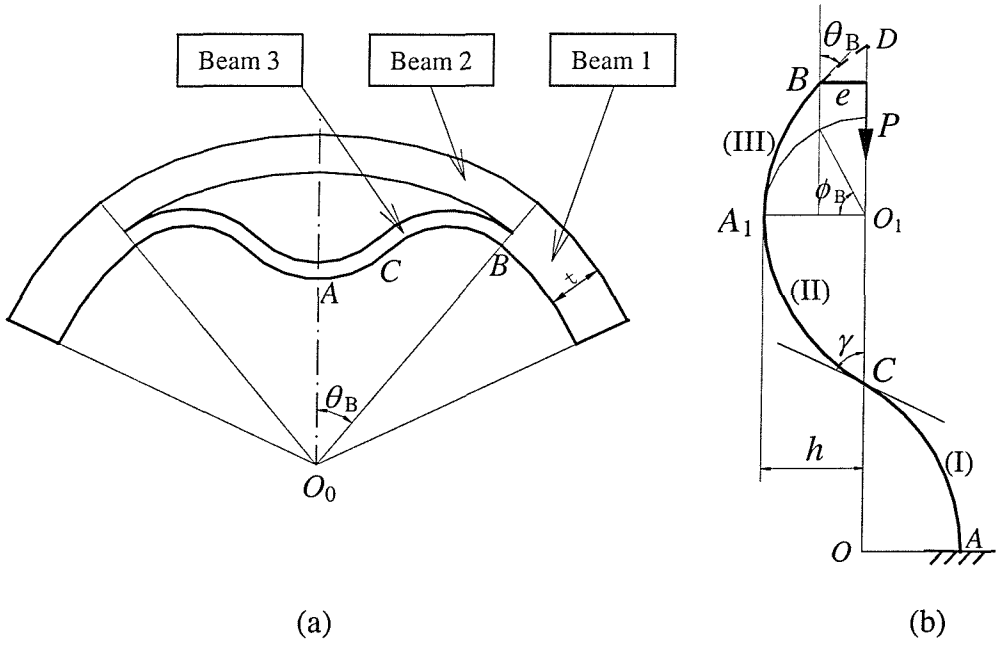

Figure 10.10 Model sketch for the problem

We still consider half of the global curved beam due to symmetry. As far as the buckled inner ply (beam 3) is concerned, from Figure 10.10b, the deformed shape of beam 3 has a

point of inflection –C. So in the following analyses, this beam must be divided into three parts for consideration – Part I, II and III are the parts between pointa A to C, C to A_1, and A_1 to B respectively.

Parts I and II are obviously antisymmetric with respect to point C. Their lengths can both be expressed from equation (10-38) in which the value of ϕ_B needs to be $\pi/2$

$$L^{(I)} = L^{(II)} = \frac{K(p)}{k} \tag{10-39}$$

The length of Part III can also be obtained from equation (10-38)

$$L^{(III)} = \frac{F(p,\phi_B)}{k} \tag{10-40}$$

where in equations (10-39) and (10-40), $F(p,\phi)$ and $K(p)$ are first kind Legendre's elliptic integral and complete elliptic integral of the first kind respectively, $K(p) = F\left(p,\frac{\pi}{2}\right)$.

So the total length of beam 3 can be expressed as

$$L = L^{(I)} + L^{(II)} + L^{(III)} = \left[2K(p) + F(p,\phi_B)\right]\frac{1}{k} \tag{10-41}$$

From equation (10-37)

$$\cos\phi_B = \frac{1}{2kpR_3'} \tag{10-42}$$

where R_3' is the radius of curvature of beam 3 under the action of the same load before snap buckling.

Combining equation (10-42) with equation (C-6) (Appendix C):

$$\cos\theta_B = 1 - 2\sin^2\frac{\theta_B}{2} = 1 + \frac{1}{2k^2R_3'^2} - 2p^2 \tag{10-43}$$

So

$$\frac{1}{k} = \sqrt{2}R_3'\sqrt{\cos\theta_B + 2p^2 - 1} \tag{10-44}$$

and noting equation (10-42), then

$$\phi_B = \cos^{-1}\frac{\sqrt{\cos\theta_B + 2p^2 - 1}}{\sqrt{2}p} \tag{10-45}$$

Again from equation (10-44) and noting that for beam 3 $k = \left(\frac{P}{D_3}\right)^{1/2}$, then

$$\frac{1}{R_3'} = \sqrt{\frac{2P}{D_3}\left(\cos\theta_B + 2p^2 - 1\right)} \tag{10-46}$$

Meanwhile according to the assumption that the length of the beam does not change during buckling

$$L = R_3\beta \tag{10-47}$$

where, as in the preceding section, R_3 and β are respectively the original curvature radius and half original arc angle of inner delaminated layer (layer ACB in Figure 10.10a). Substituting it together with equations (10-44) and (10-45) into equation (10-41), then the following equation can be obtained finally:

$$R_3\beta = \sqrt{2}R_3'\left[2K(p) + F\left(p, \cos^{-1}\frac{\sqrt{\cos\theta_B + 2p^2 - 1}}{\sqrt{2}p}\right)\right]\sqrt{\cos\theta_B + 2p^2 - 1} \tag{10-48}$$

According to the bending equation for beam 3, at point B, the following is true

$$\frac{M_3(\beta)}{EI_3} = \frac{1}{R_3'} - \frac{1}{R_3} \tag{10-49a}$$

Substituting equation (10-46) into it, the following equation can then be obtained

$$\frac{M_3(\beta)}{EI_3} = \sqrt{\frac{2P}{D_3}\left(\cos\theta_B + 2p^2 - 1\right)} - \frac{1}{R_3} \tag{10-49b}$$

The third equation can be acquired from equilibrium of the global beam—equation (10-9)

$$M_2(\beta) + M_3(\beta) + \frac{Pt}{2}\cos\theta_B = M_0 \tag{10-50}$$

where for the reason of clarification the positive direction of every term is actually adverse to the ones in equation (10-9) because in present question the curved beam is subjected to closing bending moment, and hence $P = -P_2 = P_3$.

According to the assumption in the section of Problem Statements, linear theory will still be used to analyse the outer ply—beam 2 in Figure 10.10a. Then by Castigliano's second theorem

$$\Delta\theta_B = \theta_B - \beta = \frac{\partial U_2}{\partial M_2(\beta)} \tag{10-51}$$

$$\Delta x_2 = \frac{\partial U_2}{\partial P_2} \tag{10-52}$$

where $\Delta\theta_B$ and Δx_2 are respectively the rotation and displacement in x direction of outer layer (beam 2) at the section B owing to the action of corresponding loads. U_2 is the strain energy of beam 2 whose description is shown by substituting equation (10-14) into (10-15).

Another displacement compatibility condition for the global beam at section B in x direction (horizontal direction in Figure 10a) can be expressed as

$$R_2 \cos\beta + \Delta x_2 = x_3 + \frac{t}{2}\sin\theta_B \tag{10-53}$$

where x_3 is the vertical deflection of beam 3, which can be calculated from the nonlinear analyses for beam 3, as shown in the following.

The vertical deflections of Parts I and II of beam 3 are equal due to antisymmetry, which, according to equation (C-14) (Appendix C), is

$$x_3^{(\mathrm{I})} = x_3^{(\mathrm{II})} = \frac{2E(p) - K(p)}{k} \tag{10-54}$$

and the vertical deflection of Part III from equation (C-12) (Appendix C) is

$$x_3^{(\mathrm{III})} = \frac{2E(p,\phi_B) - F(p,\phi_B)}{k} \tag{10-55}$$

where $F(p,\phi)$ and $E(p,\phi)$ are respectively first and second kind Legendre's elliptic integral and complete elliptic integral of the first kind. $K(p)$ and $E(p)$ are respectively complete elliptic integral of the first and second kind, $K(p) = F\left(p,\frac{\pi}{2}\right)$ and $E(p) = E\left(p,\frac{\pi}{2}\right)$.

So

$$x_3 = x_3^{(\mathrm{I})} + x_3^{(\mathrm{II})} + x_3^{(\mathrm{III})} = \frac{2}{k}\left[2E(p) - K(p)\right] + \frac{1}{k}\left[2E(p,\phi_B) - F(p,\phi_B)\right] \tag{10-56}$$

Substituting equation (10-56) together with (10-52) into equation (10-53) and noting $k = (P/D_3)^{1/2}$, then combined with equations (10-48), (10-49b), (10-50) and (10-51) there forms a group of 5 equations which contain θ_B, p, $M_2(\beta)$, $M_3(\beta)$ and P. These five variables can be totally determined by the above 5 equations, consequently achieving the solution of the initial problem.

However, as can be seen, the general solution actually cannot directly be solved out in explicit description, and generally it is not very easy to solve the above 5 equations either, even by ordinary numerical techniques such as the iteration method. Therefore further assumptions are needed when this analytical approach is applied to study some special cases.

10.4.2 Delamination very close to inner surface

Consider the case that the layer next to the inner surface, which is potentially to be subjected simultaneously to delaminations and snap buckling, is very thin. The stress in this thin film is then considered approximately as uniform distribution. It is further assumed that the snap buckling of this thin film has little effect on the global deformation of the other parts. So before and after snap buckling of the inner thin film, the shape of the outer base layer and undelaminated part of the global curved beam stays constant. This is shown schematically in Figure 10.11. t and t' are the thicknesses of the global beam and inner delaminated layer respectively and here $t' << t$.

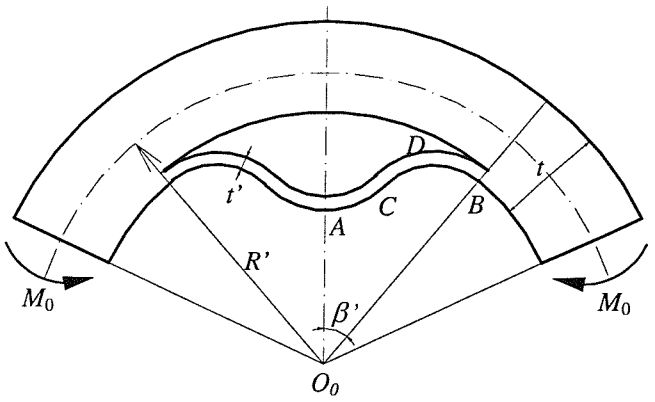

Figure 10.11 Delamination occurs very close to inner face

The compressed stress σ' in this thin film with unit width before buckling approximates to:

$$\sigma' \approx \frac{Mt}{2I} \tag{10-57}$$

where t and I are thickness and moment inertia of the global curved beam with unit width. The strain energy of the thin film before buckling can be expressed as

$$U^{(1)} = \frac{\sigma'^2}{2E'} R'\beta' t' \tag{10-58}$$

where $E' = \frac{E_1}{1-\nu^2}$, E_1 is the effective Young's modulus in the circumferential direction, t' is the thickness of thin film, R' and β' are respectively radius of curvature and assumed half arc angle of the delamination crack before thin film's snap buckling.
Here again for the reasons of simplification, the approximation: $R_2' = R_3' = R'$ is taken based on the assumption of $\delta << 1$. The bending energy of thin film after buckling is:

$$U^{(2)} = \frac{D'}{2} \int_0^{R'\beta'} \left(\frac{d\theta}{ds} + \frac{1}{R'} \right)^2 ds \tag{10-59}$$

where D' is effective flexural rigidity of thin film.

From the above subsection, the deformed shape of buckled film is divided into three parts due to the existence of the inflection point C. Part I, II and III are the parts between points A to C, C to D, and D to B respectively. The upper-limits of integration for both Parts I and II is then $R'\gamma$, while that for Part III is $R'\beta'$. γ is the slope angle at inflection point C, as shown in Figure 10b.

From equation (C-6) and (C-7) (Appendix C), we can get the relation

$$\frac{d\theta}{ds} = \frac{d\theta}{d\phi}\cdot\frac{d\phi}{ds} = \frac{2p\cos\phi}{\sqrt{1-p^2\sin^2\phi}}\cdot k\sqrt{1-p^2\sin^2\phi} \\ = 2kp\cos\phi \tag{10-60}$$

Using the elliptic integrals description (Appendix C), and also noting that in the Part II, $\frac{d\theta}{ds}$ is negative, the above equation for each part can be finally expressed as:

$$U_I^{(2)} = \frac{D'}{2}\left\{4k\left[E(p)-(1-p^2)K(p)\right]+\frac{3\gamma}{R'}\right\} \\ U_{II}^{(2)} = \frac{D'}{2}\left\{4k\left[E(p)-(1-p^2)K(p)\right]-\frac{\gamma}{R'}\right\} \\ U_{III}^{(2)} = \frac{D'}{2}\left\{4k\left[E(p,\phi_B)-(1-p^2)F(p,\phi_B)\right]+\frac{3\beta'}{R'}\right\} \tag{10-61}$$

where $\gamma = 2\sin^{-1}(p)$ as found from equation (C-6) (Appendix C), which is the slope angle at inflection point C.

So:

$$U^{(2)} = U_1^{(2)} + U_2^{(2)} + U_3^{(2)} \\ = D'\left\{4k\left[E(p)-(1-p^2)K(p)\right]+2k\left[E(p,\phi_B)-(1-p^2)F(p,\phi_B)\right]+\frac{\gamma}{R'}+\frac{3\beta'}{2R'}\right\} \tag{10-62}$$

Noting that modulus p can be determined only from equation (10-48) in which θ_B is replaced by β' which is known in the present problem. Then from equation (10-44), k can be also determined

$$k = \frac{1}{R'\sqrt{2(\cos\beta' + 2p^2 - 1)}} \tag{10-63}$$

By using the energy criterion:

$$U^{(1)} = W + U^{(2)} \tag{10-64}$$

where $W = 2R'\beta'\Gamma$, which is the fracture work.

The final equation can then be obtained after substitutions and reductions as:

$$\frac{\left(\frac{Mt}{I}\right)^2}{8E'} = \frac{2\Gamma}{t'} + \frac{E'F(\beta')}{12R'^2}t'^2 \tag{10-65}$$

where

$$F(\beta') = \frac{1}{\beta'}\left\{\frac{1}{\sqrt{2(\cos\beta' + 2p^2 - 1)}}\left[4\left(E(p) - (1-p^2)K(p)\right)\right.\right.$$
$$\left.\left. +2\left(E(p,\phi_B) - (1-p^2)F(p,\phi_B)\right)\right] + \gamma + \frac{3\beta'}{2}\right\} \tag{10-66}$$

The trend of function $F(\beta')$ is shown in Figure 10.12

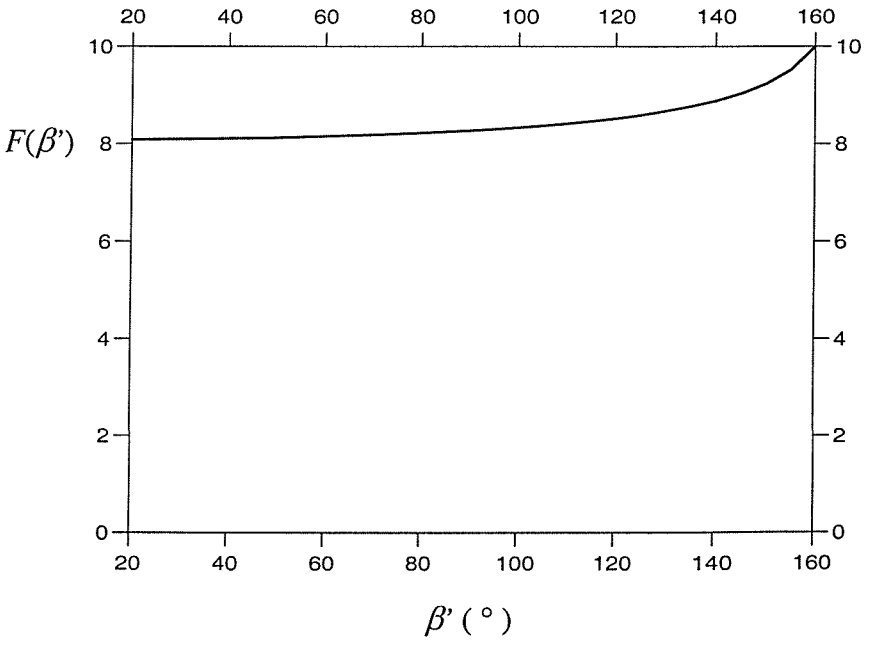

Figure 10.12 The trend of function $F(\beta')$ with respect to β'

It can be seen that although $F(\beta')$ increases with respect to β', it changes very little in a large range of β' (as shown in Figure 10.12, from 20° to 120°). The critical bending load corresponding to this large range of β', from equation (10-66), therefore increases very little. Hence it can be concluded that the delamination coupled with snap buckling is very easy to progress.

If there already exists delamination whose half arc angle before snap buckling is β', then the critical bending moment for this delaminated thin film next to inner face can also be obtained from equation (10-65) by letting the first term in right side be zero.

In order to estimate the effect of original curvature radius of beam R on the value of critical load, according to bending equation for curved beam, there is

$$\frac{1}{R'} = \frac{M}{E'I} + \frac{1}{R} \tag{10-67}$$

Substituting this into equation (10-65) and noting that $F(\beta')$ is approximately a constant in a large range of β', assumed as F_0, equation (10-65) can then be re-written as

$$\left(\frac{t^2}{8E'} - \frac{F_0 t'^2}{12E'}\right)\cdot\left(\frac{M}{I}\right)^2 - \frac{F_0 t'^2}{6R}\cdot\left(\frac{M}{I}\right) - \left(\frac{2\Gamma}{t'} + \frac{E'F_0 t'^2}{12}\frac{1}{R^2}\right) = 0 \tag{10-68}$$

M can then be solved out from the above equation as

$$M = \frac{I}{\dfrac{t^2}{4E'} - \dfrac{F_0 t'^2}{6E'}}\left[\frac{F_0 t'^2}{6R} + \sqrt{\left(\frac{t^2}{2E'} - \frac{F_0 t'^2}{3E'}\right)\left(\frac{2\Gamma}{t'} + \frac{E'F_0 t'^2}{12}\cdot\frac{1}{R^2}\right)}\right] \tag{10-69}$$

It can be seen that the original radius of curvature of the beam, R, definitely has an effect on the value of critical load M. Larger R will lead to small M, which means that the snap

buckling of inner surface layer is more likely to happen in the curved beam with larger curvature radius.

Assuming the condition that surface energy Γ is very small or a delamination crack has already existed before the occurrence of snap buckling of this delaminated thin film, then equation (10-69) can be simplified as

$$M = \frac{G_0}{R} \tag{10-70}$$

where G_0 is approximately a constant:

$$G_0 = \frac{I}{\frac{t^2}{2E'} - \frac{F_0 t'^2}{3E'}}\left[\frac{F_0 t'^2}{3} + \sqrt{\frac{E' F_0 t'^2}{3}\left(\frac{t^2}{2E'} - \frac{F_0 t'^2}{3E'}\right)}\right] \tag{10-71}$$

Therefore under this condition, equation (10-70) shows that the value of critical bending moment M is approximately inversely proportional to the original radius of curvature of the beam, R.

Now note that the value of right side of equation (10-65) is also dependent on the thickness of delaminated film, t'. It can be seen in the following that in theory, the value of critical bending moment M can achieve minimum when t' is a designated value.

As in the front sections, let $\eta = t'/t$ and then equation (10-69) can be re-written as

$$M = \frac{E'I}{\frac{1}{4} - \frac{F_0}{6}\eta^2}\left[\frac{F_0}{6R}\eta^2 + \frac{1}{t}\sqrt{\frac{1}{E'}\left(\frac{1}{2} - \frac{F_0}{3}\eta^2\right)H}\right] \tag{10-72}$$

where

$$H = \frac{2\Gamma}{t'} + \frac{E' F_0 t'^2}{12} \cdot \frac{1}{R^2} \tag{10-73}$$

Because $t' << t$, $\eta << 1$. Hence M in equation (10-72) approximates to

$$M \approx \frac{2\sqrt{2E'I}}{t}\sqrt{H} \tag{10-74}$$

Note that M will achieves minimum when H reaches minimum.

By rewriting Equation (10-73) and using the fact that

$$\frac{1}{n}\sum_{i=1}^{n} a_i \geq \sqrt[n]{\prod_{i=1}^{n} a_i} \qquad \left(a_i > 0, \text{ and the equality stands only if } a_1 = \cdots = a_i = \cdots = a_n\right) \tag{10-75}$$

the following relation can be deduced:

$$\begin{aligned} H &= \frac{\Gamma}{t'} + \frac{\Gamma}{t'} + \frac{E'F_0}{12R^2}t'^2 \\ &\geq 3\sqrt[3]{\frac{\Gamma}{t'}\cdot\frac{\Gamma}{t'}\cdot\frac{E'F_0}{12R^2}t'^2} = 3\sqrt[3]{\frac{E'\Gamma^2F_0}{12R^2}} \end{aligned} \tag{10-76}$$

Therefore, if and only if:

$$\frac{\Gamma}{t'} = \frac{E'F_0}{12R^2}t'^2 \tag{10-77}$$

the minimum of M can then be achieved by substituting relation (10-76) into equation (10-74)

$$M^*_{\min} \approx \frac{2I}{t}\sqrt[6]{\frac{18E'^4\Gamma^2F_0}{R^2}} \tag{10-78}$$

Equation (10-77) leads to:

$$t'^{*} = \sqrt[3]{\frac{12\Gamma R^2}{E'F_0}} \tag{10-79}$$

Hence, in the problem being considered here, there exists a "weak layer" which is most prone to be de-laminated. This phenomenon was also mentioned in Kachanov's (1988) and Bugakov's (1977) analytical and experimental work on circular fibre/glass ring under uniform external pressure. Also from the above, $F(\beta')$ is approximately a constant, F_0, in a large range of β'. So the thickness of this weak layer can actually be directly calculated from equation (10-79). Then the approximate minimum value of the critical bending moment can be estimated consequently.

However it should also be pointed out that the use of equations (10-78) and (10-79) has limits. As mentioned in the beginning of this subsection, the results obtained above are based on the assumption of thin film snap buckling. The result from equation (10-79) should be compared with the thickness of global beam *t*. If $t'^{*} << t$, then the minimum of critical bending moment can be obtained by equation (10-78), otherwise the value calculated from equation (10-78) is meaningless.

10.5 Summary

Theoretical approaches are developed for linear and nonlinear problems of delamination buckling in curved composite beam which corresponds to the cases of curved composite laminate subjected to opening and closing bending moments respectively. The general solutions are applied to analyse some special cases such as delamination occurring either at midplane or very close to surface of the beam. The effect of the arc angle of delamination crack on the critical load in each case is also studied.

The results show that both the radius of curvature of the beam and the arc angle of delamination have a big effect on the delamination buckling of curved composite beam

when it is subjected to opening bending load. Increasing radius of curvature of the beam generally leads to larger value of critical bending load. The curvature radius of beam also has a significant effect on the snap buckling of inner thin layer of curved composite beam when it is subjected to closing bending load. However contrary to the case of the opening load, the inner layer is more likely to be induced into snap buckling with increased radius of curvature of the beam. In the condition of low surface energy Γ of the material, the value of critical load is even nearly inversely proportional to the original radius of curvature of the beam.

Chapter 11 Concluding Remarks

11.1 Main achievements

The aim of this work has been to investigate the flexural behaviour of curved laminates and sandwich beams, and predict their strengths by theoretical approaches. The major achievements of this work are given below

11.1.1 Flexural response of a curved composite beam on an elastic foundation

A model is developed for characterising the mechanical behaviour of curved composite structure element such as overlaminate in tee joint or skin of curved sandwich beam. The governing differential equation for general curved composite beam on an elastic foundation is derived from force-moment equilibrium considerations and classical laminate theory. The flexural response of a circular composite beam on an elastic foundation is investigated in detail. The results show that the existence of tension-bending coupling in the constitutive relations of general laminate results in larger oscillation in the distributions of mechanical variables such as bending moment, shear force etc. along the span of curved beam on an elastic foundation. The solution for mid-plane symmetric laminate case is similar to that for curved isotropic beam on an elastic foundation.

11.1.2 Estimation of response using a stress function approach

An elasticity based approach for treating curved orthotropic beams resting on an elastic foundation and subjected to flexural loading has been presented using the Airy stress

function approach. The resulting equations have been applied to investigate the effects of key parameters defining beam structure on performance. The radius of curvature of the beam has a large effect on the through-thickness stress; decreasing the radius of curvature resulting in the increased maximum through-thickness tensile stress in a curved beam. The results show that, at least in theory, it is possible to design for a "good thickness" or "good radius" of the anisotropic material curved beam on elastic foundation according to related parameters. The approach has been also used to analyse four tee joint samples. The analytical results show close qualitative agreement with the results of FEM in all cases. The trend is consistent with the conclusions of numerical analyses or experiments.

11.1.3 Through-thickness stresses in curved composite laminates and sandwich beams

Based on this solution for curved orthotropic beam on an elastic foundation, an approach to define the elasticity solutions for general curved layered composite beam consisting of arbitrary numbers of orthotropic or isotropic layers in a no-circumferential-dependence case is also presented. Since the approach ensures an accurate description of stresses in curved laminated beams, within the assumptions of linear elasticity, there needs to be no strict distinction between thick and thin curved beams. Further there is no limitation on whether the skin of sandwich panel is thin or thick.

The effect of stacking sequence and radius of curvature of a curved layered composite beam on the distribution and value of through-thickness stress is chiefly investigated. Curved sandwich beams with thin and thick skin are studied. The results show that the stacking sequences have a significant effect on the delamination and in-plane tensile failure to some extent. The radius of curvature of the beam also has a large effect on the through-thickness stress, which is consistent with the results for a single layer curved orthotropic beam. The biggest through-thickness stress in a curved sandwich beam always occurs at the interface between inner skin and core or in the core but very close to that interface. Due to the geometry curvature, even in mid-plane symmetric layered

beams or same-skin sandwich beams, the distributions of through-thickness and in-plane stresses are not strictly symmetric with respect to the mid-plane.

11.1.4 Local instability of the skin of curved sandwich beam

The critical bending moment for curved sandwich beam in terms of the local instability of the compressed skin is presented. The solution is based on consideration for buckling /wrinkling of curved beam on an elastic foundation by beam theory and virtual displacement principle. The effects of key parameters such as the flexural rigidity of the beam and the stiffness of the elastic foundation (i.e. core material of sandwich beam) are evaluated. The results show that if the elastic foundation is hard enough to make wrinkling rather than buckling occur, the curved beam has nearly the same possibility to lose its stability as the flat one. But if foundation is soft or beam is stiff, then buckling occurs, and the critical values for curved beam and straight beam respectively are quite different. The solution developed in this part of thesis yields results which are very close to experimental values.

11.1.5 Delamination buckling of curved composite beam subjected to opening bending

The problem of delamination buckling of a curved beam with pre-induced delamination and under the action of opening bending moment is considered. The general solution for this problem is derived from curved beam theory and a displacement compatibility condition coupled with fracture concepts. Two usual important cases that delamination occurs at the mid-plane or very close to the surface of curved beam are investigated in detail, and an approximate formula for a general case is provided based on the interpolation of these two cases. The results show that both the radius of curvature of the beam and the arc angle of delamination have a big effect on the delamination buckling of curved beam when it is subjected to opening bending load. Increasing radius of curvature of the beam generally leads to larger value of critical bending load, which also means that

a curved beam with smaller radius of curvature is more likely to induce delamination buckling.

11.1.6 Snap buckling of the inner layer of a curved composite beam subjected to closing bending

The problem of snap buckling of inner layer when a curved beam is under the action of opening bending moment is also considered. The general solution for this problem is acquired based on non-linear beam theory, the principle of similarity and fracture concepts. The case of thin film delamination is investigated further. The results show that in a large range of arc angle of delamination, the delamination coupled with snap buckling is very easy to progress. The radius of curvature of the beam has a significant effect on the snap buckling of inner thin layer of curved composite beam. However contrary to the case of the opening load, the inner layer is more likely to be induced into snap buckling with increased radius of curvature of the beam. In the condition of low surface energy of the material, the value of critical load is even nearly inversely proportional to the original radius of curvature of the beam.

11.2 Further work

Three proposals aimed at improving the accuracy of approaches and scope of their applications are outlined below.

11.2.1 Elastic foundation

In this thesis, the Winkler hypothesis is assumed for the behaviour of elastic foundation. It is the simplest model for the foundation material. The accuracy of the solution can be improved by using more complex models for foundation, for example Pasternak type which considers the reaction of foundation including not only the normal supporting

force but also the shear force. However, it is obvious that it becomes then more difficult to obtain the final governing differential equation and the corresponding solution, because the distribution of bending moment is also dependent on the circumferential displacement.

11.2.2 Non-linear analysis

As is known, under the same load condition, a curved composite beam generally has more apparent or larger deformation compared to a flat one. This is due to the original geometry curvature. Therefore, in order to improve the accuracy of solution or the range of its application further, non-linear beam theory should be also used to analyse the flexural behaviour of curved composite beam.

11.2.3 Experimental modelling

Validation of the practical aspects of the theory presented in this thesis would be a further avenue for future work. Since there are no standard ASTM/BS/ISO procedures, specific tests involving curved sandwich beams or curved thick/thin laminates with and without delaminations would need to be devised.

List of References:

Allen, H.G., (1969), *Analysis and Design of Structural Sandwich Panels*, Pergamon Press, Oxford

Berger, H.M., (1955), A New Approach to The Analysis of Large Deflections of Plates, *Journal of Applied Mechanics*, ASME, Vol.22, p465-472.

Bhate, S.R., Nayak, U.N. and **Patki, A.V.,** (1995), Deformation of Composite Beam Using Refined Theory, *Computers & Structure*, Vol.54, No.3, p541-546

Bugakov, I.I., (1977), Delamination of Fibre-Glass Tubes under External Pressure, *Vestnik of Leningrad University*, No.13, p126-131

Chai, H., Babcock, C.D. and **Knauss, W.G.,** (1981), One Dimensional Modeling of Failure in Laminated Plates by Delamination Buckling, *International Journal of Solids Structures*, Vol.17, No.11, p1069-1083

Chandler, H.W., Longmuir, A.J., McRobbie, S., Wu, Y.S. and **Gibson, A.G.,** (1993), Tensile Delamination Failure of Curved Laminates of Single and Double-Skinned Construction, *Proceedings of 2nd International Conference on Deformation and Fracture of Composites*, UMIST, Manchester, UK, p29-31

Chang, Fu-Kuo, (1986), The Strength Analysis of Wooden Bends, *Journal of Reinforced Plastics and Composites*, Vol.5, p239-252

Charalambidi, M.N., Kinloch, A.J., Matthews, F.L., (1998), Adhesively Bonded Repairs to Fibre-Composite Materials II: Finite Element Modeling, *Composites Part A—Applied Science and Manufacturing*, Vol.29, No.11, p1383-1396

Chattopadhyay, A. and **Gu, H.,** (1996), Exact Elasticity Solution for Buckling of Composite Laminates, *Composite Structures*, Vol.34, p291-299

Chia, C.Y., (1980), *Nonlinear Analysis of Plates*", McGraw Hill, New York

Clark, S.D., Shenoi, R.A. and **Allen, H.G.,** (1999), Modelling the Fatigue Behaviour of Sandwich Beams under Monotonic, 2-step and Block-loading Regimes, *Composites Science and Technology*, Vol.59, p471-486.

Cui, W.C., Wisnom, M.R. and **Jones.M,** (1994), An experimental and Analytical Study of Delamination of Unidirectional Specimens with Cut Central Plies, *Journal of Reinforced Plastics and Composites*, Vol.13, No.8, p722-739

Dodkins, A.R., Shenoi, R.A. & Hawkins, G.L., (1994), Design of Joints and Attachments in FRP Ships' Structures, *Marine Structures*, Vol.7, p365-398.

Flanagan, G., (1993), A Sublaminate Analysis Method for Predicting Disbond and Delamination Loads in Composite Structures, *Journal of Reinforced Plastics and Composites*, Vol.12, p876-887

Frish-Fay, R., (1962), *Flexible Bars*, Butterworths & Co. (Publishers) Ltd., London

Ghosh, P.K., (1977), Large Deflection of a Rectangular Plate Resting on a Pasternak-type Elastic Foundation, *Journal of Applied Mechanics*, ASME, Vol.44, p509-511

Gu., H. and **Chattopadhyay, A.,** (1998), Elasticity Approach for Delamination Buckling of Composite Beam Plates, *AIAA Journal*, Vol.36, No.8, p1529-1534

Gibson, A.G., Chandler, H.W., Longmuir, A.J. and **Wilcox, J.A.D.,** (1994), Delamination and Failure of Curved Composite Laminates, *Proceedings of Structural Materials In Marine Environment*, The Royal Society, London, UK, p88-98

Hawkins, G.L., Holness, J.W., Dodkins, A.R. & **Shenoi, R.A.,** (1993), The Strength of Bonded Tee-Joints in FRP Ships, *Plastics Rubber and Composites Processing and Applications*, Vol.19, p279-284

Hetenyi, M., (1946), *Beams On Elastic Foundation—Theory with Applications in the Fields of Civil and Mechanical Engineering*, The University of Michigan Press

Hill, G.F.J., (2000), The Development and Application of a Delamination Prediction Method to Composite Structures, *Ph.D Thesis*, Department of Aerospace Engineering, University of Bristol, Bristol, UK

Hoff, N.J. and **Mautner, S.E.,** (1945), Buckling of Sandwich Type Panels, *Journal of the Aeronautical Sciences*, Vol.12, No.3, p285-297

Jiang Yongqiu, Lu Fengsheng and **Gu Zhijian,** (1990), *Composites Mechanics* (in Chinese), Xi'an Jiao Tong University Press, Xi'an, China

Kachanov, L.M., (1988), *Delamination Buckling of Composite Materials*, Kluwer Academic Publishers, The Netherlands

Kaczmarek, K., Wisnom, M.R., Jones, M.I., (1998), Edge Delamination in Curved $(0_4/45_6)_s$ glass-fibre/epoxy beams loaded in bending. *Composites Science and Technology* Vol.58, p155-161

Kinloch, A.J., (1997), Adhesives in Engineering, *Proceedings of The Institution of Mechanical Engineers Part G—Journal of Aerospace Engineering*, Vol.61, No.1-4, p71-95

Lekhnitskii, (1981), *Theory of Elasticity of an Anisotropic Body*, Moscow, Mir

Lu, T.J., Xia, Z.C., and **Hutchinson, J.W.,** (1994), Delamination of Beams under Transverse Shear and Bending, *Materials Science and Engineering*, A188, p103-112

Meunier, M., (2001), Dynamic Analysis of FRP Laminated and Sandwich Plates, *Ph.D Thesis*, School of Engineering Sciences, Ship Science, University of Southampton, Southampton, UK

Moshaiov, A. and **Marshall, J.,** (1991), Analytical Determination of the Critical Load of Delaminated Plates, *Journal of Ship Research*, Vol.35, No.1, p87-90

Narayanan, R., eds. (1985), *Shell Structures: Stability and Strength*, Elsevier Applied Science Publishers, London and New York

Padhi, G.S., Shenoi, R.A., Moy, S.S.J., and **Hawkins, G.L.,** (1998), Progressive Failure and Ultimate Collapse of Laminated Composite Plates in Bending, *Composite Structures*, Vol.40, Nos. 3-4, p277-291

Pagano, N.J., (1969), Exact solution for composite laminates in cylindrical bending. Journal of Composite Materials,Vol.3, No.3, p398-411

Pagano, N.J., (1967), Analysis of the flexure test of bidirectional composites. *Journal of Composite Materials*, Vol.1, No.4, p336-442

Pei, J. and **Shenoi R.A.**, (1996), Examination Of Key Aspects Defining The Performance Characteristics Of Out-Of-Plane Joints In FRP Marine Structures. *Composites*, Vol.**27A, No.2**, p89-103

Press, W.H., Teukolsky, S.A., Vetterling, W.T. and **Flannery, B.P** (1999), *Numerical Recipes in FORTEAN, The Art of Scientific Computing*, Second edition, Cambridge University Press, UK

Read, P.J.C.L. & **Shenoi, R.A.,** (1999), Fatigue Behaviour of Single Skin FRP Tee Joints, *International Journal of Fatigue*, Vol.21, p281-296

Reddy, J.N., (1984), A Simple Higher Order Theory for Laminated Composite Plates, *Journal of Applied Mechanics*, Vol.51, p745-752

Reissner, E. and **Stavsky, Y.S.,** (1961), Bending and stretching of certain types of heterogeneous aeolotropic elastic plates, *Journal of Applied Mechanics*, Vol.28, p402-408

Selvadurai, A.P.S., (1979), *Elastic Analysis of Soil-foundation interaction*, Elsevier Scientific Publishing Company, Amsterdam-Oxford-New York

Shen, H.S., (2000), Non-linear Bending of Shear Deformable Laminated Plates under Lateral Pressure and Thermal Loading and Resting on Elastic Foundation, *Journal of Strain Analysis*, Vol.35, No.2, p93-108

Shenoi, R.A. & **Hawkins, G.L.,** (1992), "Influence of Material and Geometry Variations on the Behaviour of Bonded Tee Connections in FRP Ships", *Composites*, Vol.23, No.5, p335-345

Shenoi, R.A. and **Hawkins, G.L.,** (1994), The Formulation of A Curved Composite Brick Finite Element Using A Layer-Wise Theory, *Proc. ICCM-12*, Whistler,Canada, Vol. v, p149-156

Shenoi, R.A. & **Hawkins, G.L.,** (1995), An Investigation into the Performance Characteristics of Top-hat Stiffener to Shell Plating Joints, *Composite Structures*, Vol.30

Shenoi, R.A., Read, P.J.C.L. and **Hawkins, G.L.,** (1995), Fatigue Failure Mechanisms in Fibre-reinforced Plastic Laminated Tee Joints, *International Journal of Fatigue*, Vol.17, No.6, p415-426

Shenoi, R.A., Read, P.J.C.L. and **Jackson, C.L.,** (1998), Influence of Joint Geometry and Load Regimes on Sandwich Tee Joint Behaviour, *Journal of Reinforced Plastics and Composites*, Vol.17, No.8, p725-740.

Shenoi, R.A. & **Wellicome, J.F. eds.,** (1993) *Composite Materials in Maritime Structures*, Ocean Technology Series, Cambridge University Press

Shenoi, R.A. and **Wang, W.,** (2001), Flexural Behaviour of a Curved Orthotropic Beam on an Elastic Foundation, *Journal of Strain Analysis for Engineering Design*, Vol.36, No.1, p1-16

Shenoi, R.A., and **Wang, W.,** (2001), Through-Thickness Stress in Curved Composite Laminates and Sandwich beams, *Composites Science and Technology*, Vol.61, No.11, p1501-1512

Shenoi, R.A. and **Wang, W.,** (2001), Design of Connections in FRP Ships Using an Analytical Approach, *Proceedings of the 8th International Symposium on Practical Design of Ships and Other Floating Structures*, Shanghai, China, Vol.2, p1339-1344

Sinha, S.N., (1963), Large Deflections of Plates on Elastic Foundations, *Journal of Engineering Mechanics*, ASCE, Vol.89, p1-24

Smidt, S., Curved Sandwich Beams and Panels: Theoretical and Experimental Studies, Report No.93-10, Royal Institute of Technology, Stockholm, Sweden

Smidt, S., (1996), Bending of Curved Sandwich Beams: a Numerical Approach, *Composite Structures*, Vol.34, p279-290

Simitses, G.J., (1996), Buckling of Pressure-loaded, Delaminated, Cylindrical Shells and Panels, *Key Engineering Materials*, Vols.121-122, p407-426

Thomas, R., Garcia, I., Guild, F.J., Adams, R.D., (1998), Adhesive Joining of Composite Laminates, *Plastics Rubber and Composites Processing and Applications*, Vol.27, No.4, p.200-205

Timoshenko, S., (1934), *Theory of Elasticity*, New York and London: McGraw-Hill book Company, Inc.

Timoshenko, S. (1936), *Theory of Elastic Stability*, McGraw-Hill Book Company, Inc., New York and London

Tolf, G., (1983), Stress in a Curved Laminated Beam, *Fibre Science and Technology*, Vol.19, pp243-267

Towse, A., et al, (1998), Specimen Size Effects in the Tensile Failure Strain of an Epoxy Adhesive, *Journal of Materials Science*, Vol.33, No.17, p4307-4314

Vieira Carneiro, C.A. and **Savi, M.A.**, (2000), Modelling and Simulation of the Delamination in Composite Materials, *Journal of Strain Analysis*, Vol.35, No.6, p479-492

Wang, W., and Shenoi, R.A., Analytical Solutions to Predict Flexural Behaviour of Curved Sandwich Beams, *Journal of Sandwich Structures & Materials*, (submitted for publication)

Wang, W., and Shenoi, R.A., (2001), Estimation of Delamination and Local Instability Damage in Curved Sandwich Beams, *Proceedings of 6th International Conference on Deformation and Fracture of Composites*, UMIST, Manchester, UK, p67-75

Wang, W., and **Shenoi, R.A.,** Delamination Buckling in Curved Composite Beam subjected to pure bending, (accepted by FRC2002, *Ninth International Conference on Fibre Reinforced Composites*, 26-28 March 2002, Newcastle, UK)

Wang, S.S., Zahlan, N.M. and **Suemasu, H.,** (1985), Compressive Stability of Delaminated Random Short-Fibre Composites, Part I – Modelling and Methods of Analysis, *Journal of Composite Materials*, Vol.19, p296-316

Wang, S.S., Zahlan, N.M. and **Suemasu, H.,** (1985), Compressive Stability of Delaminated Random Short-Fibre Composites, Part II – Experimental and Analytical Results, *Journal of Composite Materials*, Vol.19, p317-333

Whitney, J.M., (1969), Effect of Transverse Shear Deformation on the Bending of Laminated Plates. *Journal of Composite Materials*, Vol. 3, p534-547

Wisnom, M.R., (1996), Modelling the effect of Cracks on Interlaminar Shear Strength, *Composites Part A: Applied Science and Manufacturing*, Vol.27, No.1, p17-24

Wisnom, M.R., (1996), 3-D Finite Element Analysis of Curved Beam in Bending. *Journal of Composite Materials*, Vol.30, No.11, p1178-1190

Wisnom, M.R., Jones, M.I., (1995), Delamination Due to Interaction between Curvature Induced Interlaminar Tension and Stresses at Terminating Plies, *Composites Structure*, Vol.32, No.32, p615-620

Whitcomb, J.D., (1982), Approximate Analysis of Post-buckled Through-width Delaminations, *Composites Technology Review*, Vol.4 No.3, p71-77

Wu, Y.S., Longmuir, A.J., Chandler, H.W. and **Gibson, A.G.,** (1993), Delamination of Curved Composite Shells due to Through-Thickness Tensile Stress, *Plastics Rubber and Composites Processing and Applications.* Vol.19, No.1, p39-46

Yang, H.T., (1970), "Flexible Plate Finite Element on Elastic Foundation", *Journal of Structural Division*, ASE, Vol.96, p2033-2101

Appendix A: Preliminaries Related to Layered Anisotropic Materials

A.1 Elasticity of homogeneous anisotropic materials

A.1.1 Generalized Hooke's law

Generalized Hooke's law can be expressed by the following tensor equation:

$$\sigma_{ij} = E_{ijkl}\varepsilon_{kl} \tag{A-1}$$

where E_{ijkl} is elasticity tensor, σ_{ij} and ε_{kl} stand for stress and strain tensor. i, j, k, l can independently be 1,2 or 3 in a 3-dimensional case.

Four order tensor E_{ijkl} in 3-dimensional case has 81 components. However, because of the symmetry of stress and strain components, and also because of the existing of strain energy density function, E_{ijkl} actually has only 21 independently constants for general anisotropic materials. Equation (A-1) can then be expressed in matrix form as:

$$\begin{Bmatrix} \sigma_1 \\ \sigma_2 \\ \sigma_3 \\ \sigma_4 \\ \sigma_5 \\ \sigma_6 \end{Bmatrix} = \begin{bmatrix} C_{11} & C_{12} & C_{13} & C_{14} & C_{15} & C_{16} \\ & C_{22} & C_{23} & C_{24} & C_{25} & C_{26} \\ & & C_{33} & C_{34} & C_{35} & C_{36} \\ & & & C_{44} & C_{45} & C_{46} \\ & & & & C_{55} & C_{56} \\ & & & & & C_{66} \end{bmatrix} \cdot \begin{Bmatrix} \varepsilon_1 \\ \varepsilon_2 \\ \varepsilon_3 \\ \varepsilon_4 \\ \varepsilon_5 \\ \varepsilon_6 \end{Bmatrix} \tag{A-2}$$

A.1.2 Orthotropic materials

Orthotropic material system has three mutually perpendicular planes of elastic symmetry. Then the number of independent elastic constants can be reduced to nine. The stress-strain relations for an orthotropic material are given by:

$$\begin{Bmatrix}\sigma_1\\ \sigma_2\\ \sigma_3\\ \sigma_4\\ \sigma_5\\ \sigma_6\end{Bmatrix} = \begin{bmatrix} C_{11} & C_{12} & C_{13} & 0 & 0 & 0 \\ & C_{22} & C_{23} & 0 & 0 & 0 \\ & & C_{33} & 0 & 0 & 0 \\ & & & C_{44} & 0 & 0 \\ & & & & C_{55} & 0 \\ & & & & & C_{66} \end{bmatrix} \cdot \begin{Bmatrix}\varepsilon_1\\ \varepsilon_2\\ \varepsilon_3\\ \varepsilon_4\\ \varepsilon_5\\ \varepsilon_6\end{Bmatrix} \tag{A-3}$$

The stiffness coefficients C_{ij} for an orthotropic material may be expressed in terms of the engineering constants:

$$C_{11} = \frac{1-\nu_{23}\nu_{32}}{\Delta} E_1 \;,\; C_{12} = \frac{\nu_{21}+\nu_{31}\nu_{23}}{\Delta} E_1 = \frac{\nu_{12}+\nu_{32}\nu_{13}}{\Delta} E_2 = C_{21}$$

$$C_{22} = \frac{1-\nu_{13}\nu_{31}}{\Delta} E_2 \;,\; C_{13} = \frac{\nu_{31}+\nu_{21}\nu_{32}}{\Delta} E_1 = \frac{\nu_{13}+\nu_{12}\nu_{23}}{\Delta} E_3 = C_{31}$$

$$C_{33} = \frac{1-\nu_{12}\nu_{21}}{\Delta} E_3 \;,\; C_{23} = \frac{\nu_{32}+\nu_{12}\nu_{12}}{\Delta} E_2 = \frac{\nu_{23}+\nu_{21}\nu_{13}}{\Delta} E_3 = C_{32} \tag{A-4}$$

$$C_{44} = \mu_{23} \;,\; C_{55} = \mu_{13} \;,\; C_{66} = \mu_{12}$$

$$\nu_{ij} = -\frac{\varepsilon_j}{\varepsilon_i} \;,\; \Delta = 1-\nu_{12}\nu_{21}-\nu_{23}\nu_{32}-\nu_{31}\nu_{13}-\nu_{21}\nu_{32}\nu_{13}-\nu_{12}\nu_{23}\nu_{31}$$

A.1.3 Transverse isotropic materials

If the material is isotropic in one plane of elastic symmetry of an orthotropic material system, it is referred to as a transverse isotropic material system. Only five coefficients

are independent. In the expressions of stiffness matrix components of orthotropic material (A-4):

$$C_{33} = C_{22}\ ,\ C_{13} = C_{12}\ ,\ C_{44} = \frac{1}{2}(C_{22} - C_{23})\ ,\ C_{55} = C_{66} \tag{A-5}$$

Most of fibre cross-sections in the transverse plane of a unidirectional FRP are randomly distributed. In the transverse plane, the properties of the material are independent of direction, so that the material is transversely isotropic.

A.2 Two dimensional problem of orthotropic materials

A.2.1 Orthotropic laminae—plane stress problem

In orthotropic analyses, assuming plane stress condition $(\sigma_{33} = 0, \tau_{13} = 0, \tau_{23} = 0)$, the stress-strain relations can be written in axes aligned with the local axes of orthotropy:

$$\begin{cases} \varepsilon_{11} = \dfrac{1}{E_1}\sigma_{11} - \dfrac{\nu_{21}}{E_2}\sigma_{22} \\ \varepsilon_{22} = -\dfrac{\nu_{12}}{E_1}\sigma_{11} + \dfrac{1}{E_2}\sigma_{22} \\ \varepsilon_{33} = -\dfrac{\nu_{13}}{E_1}\sigma_{11} - \dfrac{\nu_{23}}{E_2}\sigma_{22} \\ \varepsilon_{12} = \dfrac{1}{2\mu_{12}}\sigma_{12} \end{cases} \tag{A-6}$$

which induce to orthotropic laminae. The above equation can be rewritten as the following style, which is familiar to researchers:

$$\begin{Bmatrix} \sigma_1 \\ \sigma_2 \\ \sigma_3 \end{Bmatrix} = \begin{bmatrix} \overline{Q}_{11} & \overline{Q}_{12} & 0 \\ & \overline{Q}_{22} & 0 \\ & & \overline{Q}_{66} \end{bmatrix} \begin{Bmatrix} \varepsilon_1 \\ \varepsilon_2 \\ \varepsilon_6 \end{Bmatrix} \tag{A-7}$$

Where:

$$\overline{Q}_{11} = \frac{E_1}{1-\nu_{12}\nu_{21}},\quad \overline{Q}_{22} = \frac{E_2}{1-\nu_{12}\nu_{21}},$$

$$\overline{Q}_{12} = \frac{\nu_{12}E_1}{1-\nu_{12}\nu_{21}},\quad \overline{Q}_{66} = \mu_{12} \tag{A-8}$$

Considering the lamina with arbitrary orientation, here should introduces coordinate transformation matrix $\{T\}$ and let:

$$[Q] = [T]^{-1}[\overline{Q}][T] \tag{A-9}$$

Then the similar stress-strain relation is achieved:

$$\{\sigma\} = [Q]\{\varepsilon\} \tag{A-10}$$

However it should be noticed that $[Q]$ is a full matrix here.

A.2.2 Plane strain problem

For Plane strain problem, the expression of stress-strain relation (A.6) can still be used; however, the elastic constants need to be respectively by the following quantities:

$$E_1' = \frac{E_1}{1-\nu_{13}\nu_{31}} \qquad E_2' = \frac{E_2}{1-\nu_{23}\nu_{32}}$$

$$\nu_{12}' = \frac{\nu_{12}+\nu_{13}\nu_{32}}{1-\nu_{13}\nu_{31}} \qquad \nu_{21}' = \frac{\nu_{21}+\nu_{23}\nu_{31}}{1-\nu_{23}\nu_{32}} \tag{A-11}$$

Obviously, the Plane strain problem is a little more complicated than the Plane stress problem, because the elastic constants related to the third direction appear in the expression of stress-strain relation.

A.3 Classical laminate theory (CLT)

The Kirchhof-Love hypothesis is used in the derivation of the classical laminate theory. The Kirchhof-Love hypothesis chiefly involves following assumptions: Straight lines perpendicular to the midplane before deformation remain (1) straight; (2) inextensible; (3) normal to the midplane after deformation. Based on Kirchhof-Love hypothesis, the functional form of the displacement for the plate are:

$$\begin{cases} u(x,y,z) = u_0(x,y) - z\dfrac{\partial w_0}{\partial x} \\ v(x,y,z) = v_0(x,y) - z\dfrac{\partial w_0}{\partial y} \\ w(x,y,z) = w_0(x,y) \end{cases} \tag{A-12}$$

Substituting it into geometry equations, the following can then be obtained:

$$\begin{Bmatrix} \varepsilon_x \\ \varepsilon_y \\ \gamma_{xy} \end{Bmatrix} = \begin{Bmatrix} \varepsilon_x^0 \\ \varepsilon_y^0 \\ \gamma_{xy}^0 \end{Bmatrix} + z\begin{Bmatrix} \kappa_x \\ \kappa_y \\ \kappa_{xy} \end{Bmatrix} \tag{A-13}$$

where $\{\kappa\}$ is the curvature of midplane:

$$\kappa_x = -\frac{\partial^2 w}{\partial x^2}\ ,\quad \kappa_y = -\frac{\partial^2 w}{\partial y^2}\ ,\quad \kappa_{xy} = -2\frac{\partial^2 w}{\partial x \partial y} \tag{A-14}$$

Assuming there are N-plies in laminate, substituting equation (A.13) into equation (A.10), and integrate it, and also using external force components instead of stress components in the expression:

$$\begin{Bmatrix} N_x \\ N_y \\ N_{xy} \\ M_x \\ M_y \\ M_{xy} \end{Bmatrix} = \begin{bmatrix} A_{11} & A_{12} & A_{16} & B_{11} & B_{12} & B_{16} \\ A_{12} & A_{22} & A_{26} & B_{12} & B_{22} & B_{26} \\ A_{16} & A_{26} & A_{66} & B_{16} & B_{26} & B_{66} \\ B_{11} & B_{12} & B_{16} & C_{11} & C_{12} & C_{16} \\ B_{12} & B_{22} & B_{26} & C_{12} & C_{22} & C_{26} \\ B_{16} & B_{26} & B_{66} & C_{16} & C_{26} & C_{66} \end{bmatrix} \cdot \begin{Bmatrix} \varepsilon_x^0 \\ \varepsilon_y^0 \\ \gamma_{xy}^0 \\ \kappa_x \\ \kappa_y \\ \kappa_{xy} \end{Bmatrix} \tag{A-15}$$

where A_{ij}, B_{ij}, C_{ij} are tension stiffness, coupling stiffness, flexible stiffness respectively, they can be expressed as:

$$\begin{aligned} A_{ij} &= \sum_{k=1}^{N} Q_{ij}^{(k)} (z_k - z_{k-1}) = \sum_{k=1}^{N} Q_{ij}^{(k)} t_k \\ B_{ij} &= \frac{1}{2} \sum_{k=1}^{N} Q_{ij}^{(k)} \left(z_k^{\,2} - z_{k-1}^{\,2} \right) = \sum_{k=1}^{N} Q_{ij}^{(k)} t_k \bar{z}_k \\ D_{ij} &= \frac{1}{3} \sum_{k=1}^{N} Q_{ij}^{(k)} \left(z_k^{\,3} - z_{k-1}^{\,3} \right) = \sum_{k=1}^{N} Q_{ij}^{(k)} (t_k \bar{z}_k^{\,2} + \frac{t_k^{\,3}}{12}) \end{aligned} \tag{A.16}$$

$t_k = z_k - z_{k-1}$ is the thickness of the ith ply, $\bar{z}_k = \frac{1}{2}(z_k + z_{k-1})$ is the location of midplane of ith ply.

Obviously, for the laminate symmetric with respect to the midplane, $B_{ij} = 0$, which means there does not exit the tension-bending coupling. This will simplify the analyses of midplane symmetric laminate.

References for Appendix A

1. R.A.Shenoi & J.F.Wellicome, "Composite Materials in Maritime Structures", Britain: Cambridge University Press, 1993.
2. Jiang Yongqiu, Lu Fengsheng and Gu Zhijian, "composites Mechanics", China: Xi'an Jiao Tong University Press, 1990.

3. J.M.Whitney, "Structural Analysis Of Laminated Anisotropic Plates", America: Technomic Publishing Co.,Inc, 1987
4. G.S.Padhi, "Critical Assessment of Shear Deformation Theories For Multilayered Composite Plates", Ph.D student Report, University of Southampton, 1997
5. Han-koo Jeong, "Mechanical Behavior of A Laminate", Ph.D student Report, University of Southampton, 1997

Appendix B: The Curvature Change of Shell

B.1 Curved surface and local co-ordinate system

Consider a general curved surface: $z = f(x, y)$, the location of any point on this curved surface can be described by the vector

$$\vec{r} = x\vec{\mathrm{i}} + y\vec{\mathrm{j}} + z\vec{\mathrm{k}} \tag{B-1}$$

Assuming that (α, β) is one kind of local co-ordinate system on this curved surface, $\vec{r}$ can be alternatively described as

$$\vec{r} = \vec{r}(\alpha, \beta) \tag{B-2}$$

and here is $x = x(\alpha, \beta)$, $y = y(\alpha, \beta)$, $z = z(\alpha, \beta)$. Then let

$$\begin{aligned} \vec{r}_\alpha &= \frac{\partial \vec{r}}{\partial \alpha} = x_\alpha \vec{\mathrm{i}} + y_\alpha \vec{\mathrm{j}} + z_\alpha \vec{\mathrm{k}} \\ \vec{r}_\beta &= \frac{\partial \vec{r}}{\partial \beta} = x_\beta \vec{\mathrm{i}} + y_\beta \vec{\mathrm{j}} + z_\beta \vec{\mathrm{k}} \end{aligned} \tag{B-3}$$

The Lame coefficients can then be defined as

$$\begin{aligned} A &= |\vec{r}_\alpha| = \sqrt{x_\alpha{}^2 + y_\alpha{}^2 + z_\alpha{}^2} \\ B &= |\vec{r}_\beta| = \sqrt{x_\beta{}^2 + y_\beta{}^2 + z_\beta{}^2} \end{aligned} \tag{B-4}$$

B.2 Curvature change of shell

B.2.1 Curvature change of general shell

According to the theory of shell and theory of curved surface, the final expression about the curvature changes of mid-surface of the general shell along α and β directions respectively and the twist curvature after deformation can be derived as below.

$$\begin{cases} \kappa_1 = \frac{1}{A}\cdot\frac{\partial}{\partial\alpha}\left(\frac{u}{R_1}\right)+\frac{1}{AB}\cdot\frac{\partial A}{\partial\beta}\cdot\frac{v}{R_2}-\frac{1}{A}\cdot\frac{\partial}{\partial\alpha}\left(\frac{1}{A}\cdot\frac{\partial w}{\partial\alpha}\right)-\frac{1}{AB^2}\cdot\frac{\partial A}{\partial\beta}\cdot\frac{\partial w}{\partial\beta}-\frac{\varepsilon_\alpha}{R_1} \\ \kappa_2 = \frac{1}{B}\cdot\frac{\partial}{\partial\beta}\left(\frac{v}{R_2}\right)+\frac{1}{AB}\cdot\frac{\partial B}{\partial\alpha}\cdot\frac{u}{R_1}-\frac{1}{B}\cdot\frac{\partial}{\partial\beta}\left(\frac{1}{B}\cdot\frac{\partial w}{\partial\beta}\right)-\frac{1}{A^2B}\cdot\frac{\partial B}{\partial\alpha}\cdot\frac{\partial w}{\partial\alpha}-\frac{\varepsilon_\beta}{R_2} \\ \chi = \frac{1}{R_1}\cdot\frac{A}{B}\cdot\frac{\partial}{\partial\beta}\left(\frac{u}{A}\right)+\frac{1}{R_2}\cdot\frac{B}{A}\cdot\frac{\partial}{\partial\alpha}\left(\frac{v}{B}\right)-\frac{1}{AB}\left(\frac{\partial^2 w}{\partial\alpha\partial\beta}-\frac{1}{A}\cdot\frac{\partial A}{\partial\beta}\cdot\frac{\partial w}{\partial\alpha}\right. \\ \quad \left.-\frac{1}{B}\cdot\frac{\partial B}{\partial\alpha}\cdot\frac{\partial w}{\partial\beta}\right)-\frac{1}{2}\left(\frac{1}{R_1}+\frac{1}{R_2}\right)\cdot\gamma_{\alpha\beta} \end{cases} \tag{B-5}$$

where u, v, w are respectively displacement components in direction of $\vec{r}_\alpha$, $\vec{r}_\beta$ and $\vec{r}_\alpha\times\vec{r}_\beta$, R_1 and R_2 are curvature radiuses in directions of $\vec{r}_\alpha$, $\vec{r}_\beta$. ε_α, ε_β and $\gamma_{\alpha\beta}$ are strain components of mid-surface

$$\begin{aligned} \varepsilon_\alpha &= \frac{1}{A}\frac{\partial u}{\partial\alpha}+\frac{v}{AB}\frac{\partial A}{\partial\beta}+\frac{w}{R_1} \\ \varepsilon_\beta &= \frac{1}{B}\frac{\partial v}{\partial\beta}+\frac{u}{AB}\frac{\partial B}{\partial\alpha}+\frac{w}{R_2} \\ \gamma_{\alpha\beta} &= \frac{B}{A}\frac{\partial}{\partial\alpha}\left(\frac{v}{B}\right)+\frac{A}{B}\frac{\partial}{\partial\beta}\left(\frac{u}{A}\right) \end{aligned} \tag{B-6}$$

As can be seen, in any of the above equations (B-5), the last term shows that in-plane strain $\varepsilon_\alpha,\varepsilon_\beta,\gamma_{\alpha\beta}$ have effects on the curvature and the twist curvature κ_1,κ_2,χ.

B.2.2 Shell curved about one axis

In the case that shell is curved about only one axis like a cylindrical shell however its cross section is not conformed to circle or arc but a general smooth curve, the generator x and the tangent of cross section line s are taken as local co-ordinate, corresponding to α and β respectively, which means

$$\begin{cases} x = \alpha, ds_1 = Ad\alpha = dx \\ s = \beta, ds_2 = Bd\beta = ds \end{cases} \tag{B-7}$$

Therefore: $A = B = 1$ and $R_1 = \infty$

Then substituting equation (B-6) into equation (B-5), equation (B-5) ban be reduced as following

$$\begin{aligned} \kappa_1 &= -\frac{\partial^2 w}{\partial x^2} \\ \kappa_2 &= v\frac{\partial}{\partial s}\left(\frac{1}{R_2}\right) - \frac{\partial^2 w}{\partial \beta^2} - \frac{w}{R_2^2} \\ \chi &= \frac{1}{R_2}\frac{\partial v}{\partial x} - \frac{\partial^2 w}{\partial x \partial s} - \frac{1}{2R_2}\left(\frac{\partial v}{\partial x} + \frac{\partial u}{\partial s}\right) \end{aligned} \tag{B-8}$$

If the intrinsic equation of cross section line of this shell is expressed as: $\theta = s(s)$, where θ is the slope angle at any point on the line, then the original curvature radius $R_2 = \frac{ds}{d\theta}$.

The above equation can be rewritten as

$$\begin{aligned} \kappa_1 &= -\frac{\partial^2 w}{\partial x^2} \\ \kappa_2 &= v\frac{d^2\theta}{ds^2} - \frac{\partial^2 w}{\partial s^2} - w\left(\frac{d\theta}{ds}\right)^2 \\ \chi &= \frac{1}{R_2}\frac{\partial v}{\partial x} - \frac{\partial^2 w}{\partial x \partial s} - \frac{1}{2R_2}\left(\frac{\partial v}{\partial x} + \frac{\partial u}{\partial s}\right) \end{aligned} \tag{B-9}$$

Obviously, the circumferential displacement v has effect on curvature change as well as the normal displacement w.

B.2.3 Cylindrical shell

In cylindrical shell cases, the second curvature radius R_2 is a constant R . Equation (B-9) can be further reduced. And noting: $ds = Rd\theta$, the final expression of κ_1, κ_2, χ in cylindrical shell deformation can be obtained as:

$$\begin{cases} \kappa_1 = -\dfrac{\partial^2 w}{\partial x^2} \\ \kappa_2 = -\dfrac{1}{R^2}\cdot\dfrac{\partial^2 w}{\partial \theta^2} - \dfrac{w}{R^2} \\ \chi = \dfrac{1}{2R}\left(\dfrac{\partial v}{\partial x} - \dfrac{1}{R}\cdot\dfrac{\partial u}{\partial \theta} - 2\dfrac{\partial^2 w}{\partial x \partial \theta}\right) \end{cases} \tag{B-10}$$

If A very long cylindrical shell is considered here, and also the applied forces and boundary conditions are both assumed uniform in cylinder axial direction (x-direction), the deformation is then independent of x. Thus this cylindrical can be considered as a curved beam with unit width in x-direction. During its happening deformation, the change of curvature in x-direction is then κ_2 in equation (B-10), i.e.:

$$\kappa_\theta = -\frac{1}{R^2}\cdot\frac{\partial^2 w}{\partial \theta^2} - \frac{w}{R^2} \tag{B-10}$$

Reference for Appendix B:

1. **Liu Hongwen, Lin Jianxing** and **Cao Manling,** "Theory of Plates and Shells"(in Chinese), Zhe Jiang University Press, 1987

Appendix C: Non-linear Deflection of Flexible Bar

C.1 The concept of linear and non-linear deflections

When the deflections of a loaded bar is investigated, analysis usually begins with the Bernoulli-Euler law. At any point of the bar, the following formula holds:

$$\frac{1}{r} = \frac{d\theta}{ds} = \frac{M(s)}{EI} \tag{C-1}$$

where s is measured along the length of the arc and θ is the slope at s . In rectangular coordinates the curvature is expressed as:

$$\frac{1}{r} = \frac{d^2y/dx^2}{\left[1+(dy/dx)^2\right]^{3/2}} \tag{C-2}$$

because the bending moment M is a function of x, substituting the above equation into the Bernoulli-Euler formula, a second order nonlinear differential equation arise. In linear approach, the square of the slope $(dy/dx)^2$ is neglected in comparison with unity, as is known well in conventional engineering applications. This approach is justified provided the deflections are very small compared with the length of the bar; on the other hand, this approximation is not permissible for slander bars where the deflections are appreciable compared to the length or the new equilibrium state after deflection is far away from the original shape of the bar. The well-known elementary theory, therefore, is not applicable for the calculation of "large deflections". It should also be noted, in nonlinear cases, the deflections are no longer a linear function of the bending moment or of the load, hence the principle of superposition is not applicable.

C.2 Elliptic functions and integrals

There is no general method for the solution of second order nonlinear differential equations, a certain type, called Newton's equation, may be solved by a simple procedure and will involve elliptic integrals. Newton's equation contains the second derivative of the dependent variable and a nonlinear function of the same variable. It is of the form

$$\frac{d^2y}{dx^2} + a\Phi(y) = 0 \tag{C-3}$$

The name 'elliptic integral' was used by Lengendre to designate integrals of the types

$$\int \frac{dx}{\sqrt{X}}, \quad \int \frac{x^2 dx}{\sqrt{X}} \text{ and } \int \frac{dx}{(x-b)\sqrt{X}}$$

where X is either of the third or fourth degree in x. These are called 'elliptic integral' of the first, second and third kind respectively.

For the analyses in this thesis, only the first and second kind elliptic integrals are involved. Suitable transformation turns these into

$$\int_0^x \frac{dx}{\left[(1-x^2)(1-p^2x^2)\right]^{1/2}} \text{ and } \int_0^x \frac{(1-p^2x^2)^{1/2}\,dx}{(1-x^2)^{1/2}}$$

writing $x = \sin\phi$, Legendre's standard form of the first kind:

$$F(p,\phi) = \int_0^{\phi} \frac{d\phi}{(1-p^2\sin^2\phi)^{1/2}} \tag{C-4}$$

and of the second:

$$E(p,\phi)=\int_0^{\phi}\left(1-p^2\sin^2\phi\right)^{1/2}d\phi \tag{C-5}$$

It is obvious that $F(p,\phi)$ and $E(p,\phi)$ both are functions of p, which is called the modulus, and of the limit ϕ. $K(p)$ and $E(p)$ are then designated as:

$$\begin{aligned}K(p)&=F\left(p,\frac{\pi}{2}\right)\\E(p)&=E\left(p,\frac{\pi}{2}\right)\end{aligned} \tag{C-6}$$

which are called 'complete elliptic integral' of the first kind and second kind respectively, and their values both depend on p only.

C.3 The basic problem: vertical strut under vertical load

Consider a vertical strut AB, fixed at the bottom and subject to a vertical load P at the top as shown in Figure C.1a. If the bar is sufficiently flexible it will take the shape in Figure C.1b. The related coordinate is also shown in Figure C.1. The bending moment in any section of the strut (its location after deformation assumed to be $Z(x,y)$) due to P is

$$M=-Py=\frac{EI}{r} \tag{C-7}$$

so: $$y=-\frac{EI}{rP}=-\frac{1}{k^2r} \tag{C-8}$$

where $k=\left(\frac{P}{EI}\right)^{1/2}$ and r is the radius of curvature. Substituting equation (C-2) into the above, and then integrating with respect to x, the following result is obtained

$$y^2 = \frac{2}{k^2\left[1+\left(dy/dx\right)^2\right]^{1/2}} + C \qquad \text{(C-9)}$$

Noting that $\frac{dx}{ds} = \cos\theta$, hence $\left[1+\left(dy/dx\right)^2\right]^{1/2} = \frac{1}{\cos\theta}$, equation (C-9) reduces to

$$y^2 = \frac{2}{k^2}\cos\theta + C = \frac{2}{k^2}\left[1-2\sin^2\frac{\theta}{2}\right] + C \qquad \text{(C-10)}$$

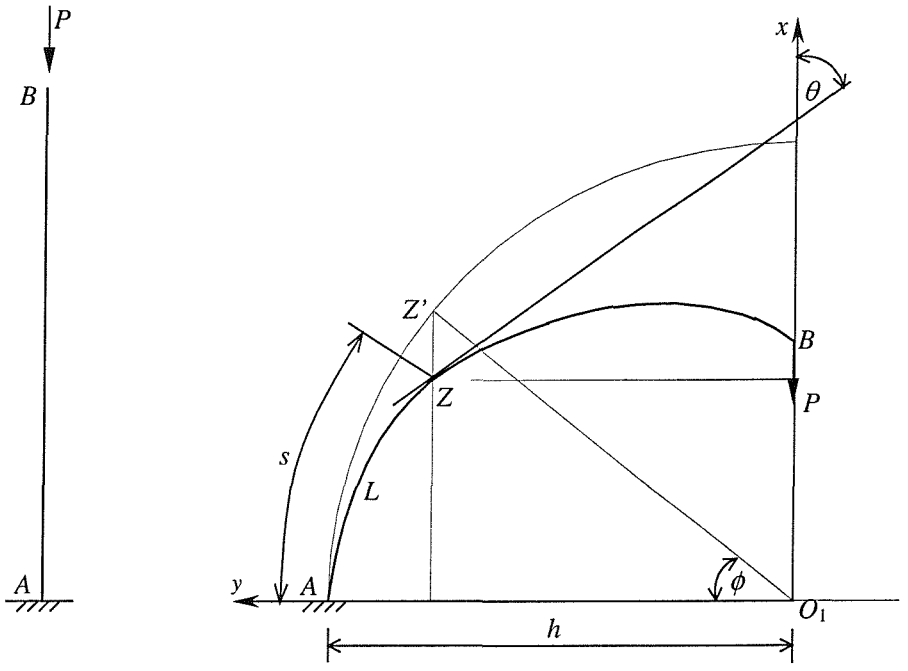

C.1(a) C.1(b)

Figure C.1 Vertical Strut under Vertical Load

Introducing h as the total horizontal deflection of the bar, as shown in Figure C.1, which means $h = y|_{\theta=0}$, leading to $h^2 = \frac{2}{k^2} + C$. So

$$y^2 = h^2 - \frac{4}{k^2}\sin^2\frac{\theta}{2} \tag{C-11}$$

since y^2 is positive, and assuming $h^2 < \frac{4}{k^2}$, let

$$h = \frac{2p}{k} \tag{C-12}$$

where $p < 1$ and select ϕ such that

$$\sin\frac{\theta}{2} = p\sin\phi \tag{C-13}$$

Using equation (C-13) and noting $y = h\cos\phi$ and $\frac{dy}{ds} = \sin\theta$, after some reductions, the following result can be obtained

$$ds = -\frac{d\phi}{k\left(1 - p^2\sin^2\phi\right)^{1/2}} \tag{C-14}$$

θ is negative as shown in Figure C.1, hence ϕ is also negative. The negative sign in equation (C-14) means that ϕ is decreasing while s increase. Integrating ds from 0 to s and disregarding the negative sign

$$s = \frac{1}{k}\int_0^{\phi}\frac{d\phi}{\left(1 - p^2\sin^2\phi\right)^{1/2}} = \frac{1}{k}F(p,\phi) \tag{C-15}$$

Assuming that the length of strut does not change during bending

$$L = \frac{1}{k}\int_0^{\frac{\pi}{2}}\frac{d\phi}{\left(1 - p^2\sin^2\phi\right)^{1/2}} = \frac{1}{k}K(p) \tag{C-16}$$

From this equation, the modulus can then be solved out. Hence then by equations (C-15) and (C-13) the function for curve *AZB* $s=f(\theta)$ is determined. Thus the present problem considered here is solved.

Because the value of ϕ at top point of strut *B* is $\frac{\pi}{2}$, then from equation (C-13), the slope at *B* can be found by

$$\sin\frac{\theta_C}{2} = p \tag{C-17}$$

From the above the total horizontal deflection of the bar has been designated as *h*, from Figure C.1b, the horizontal deflection at any point of bar is

$$y = h\cos\phi = \frac{2p}{k}\cos\phi \tag{C-18}$$

From equation (C-14) and noting $dx = ds\cos\theta = ds\left(1-2p^2\sin^2\phi\right)$, the vertical deflection at any point of bar can be obtained by integrating

$$\begin{aligned} x &= \frac{1}{k}\int_0^{\phi}\frac{d\phi}{\left(1-p^2\sin^2\phi\right)^{1/2}} - \frac{2p^2}{k}\int_0^{\phi}\frac{\sin^2\phi d\phi}{\left(1-p^2\sin^2\phi\right)^{1/2}} \\ &= \frac{1}{k}\left[2E(p,\phi)-F(p,\phi)\right] \end{aligned} \tag{C-19}$$

so the total vertical deflection of the bar is

$$v = \frac{1}{k}\left[2E(p)-K(p)\right] \tag{C-20}$$

C.4 Vertical strut with a load and a couple at end – principle of elastic similarity

Consider a vertical strut the same as in the above but with a load P and a clockwise couple M applied at end B, as shown in Figure C.2a. They can be replaced by a force acting on a rigid lever-- Figure C.2b. The length of this lever is $e = \frac{M}{P}$. From the principle of similarity, this problem can be converted into the basic problem by extending the bar past B until it intersects the line of action of P which is exerted on the lever. Let this point be D.

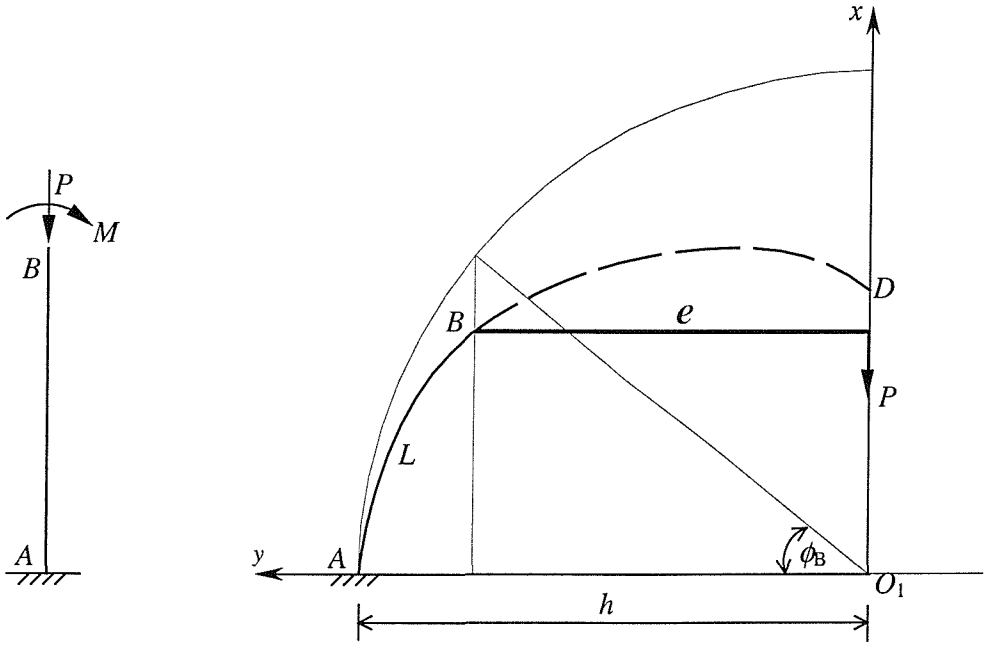

C.2(a) C.2(b)

Figure C.2 Vertical Strut with a Load and a Couple at End

The total length of the new strut AD is then

$$L = L_1 + L_2 \tag{C-21}$$

L_1 is the length of original strut which is known, L_2 is unknown.

From figure C.2b and noting equation (C-12)

$$\cos\phi_B = \frac{e}{h} = \frac{ek}{2p} \tag{C-22}$$

by which parameter ϕ_B can be determined. Then from equation (C-15)

$$L_1 = \frac{1}{k} F(p, \phi_B) \tag{C-23}$$

by which the modulus p can be solved out, and all other dimensions of the loaded bar can be obtained consequently. The function of the curve ABC can also be expressed as equation (C-15), where $\phi = \arcsin\dfrac{\sin(\theta/2)}{p}$, but here $\dfrac{\pi}{2} < \theta < \theta_B$. θ_B can be obtained from $\sin\dfrac{\theta_B}{2} = p\sin\phi_B$.

It should be pointed out that it is not certain that in any cases the imaginary extension of bar can intersect with the line of action of P . Under some conditions, e.g. small force P and large couple M, it is possible the line of P will by pass the elastica. This corresponding the assumption $h^2 > \dfrac{4}{k^2}$ in equation (C-12). In this thesis, this case is not concerned and considered.

C.5 Curved bar under point loads

Consider a curved bar in Figure C.3. The line a represents the initial free shape of curved bar fixed at original point O and its intrinsic equation is

$$\eta = \eta(s)$$

Line b is the loaded shape which expressed as

$$\psi = \psi(s)$$

The bar is assumed to be inextensible, hence s is the same in both equations and let L be the length of the bar. And it is also assumed that the bar is subjected to an arbitrary load distribution which can be expressed as $v(s)$ vertically and $h(s)$ horizontally. The bending equation for an arbitrary plane curve under an arbitrary coplanar loading is then

$$\frac{d}{ds}\left[EI\left(\frac{d\psi}{ds}-\frac{d\eta}{ds}\right)\right]-V(s)\cos\psi-H(s)\sin\psi=0 \qquad \text{(C-24)}$$

where $V(s)=\int_s^L v(s)ds$

and $H(s)=\int_s^L h(s)ds$

For a bar of constant flexural rigidity, then

$$EI\frac{d^2\psi}{ds^2}-V(s)\cos\psi-H(s)\sin\psi=EI\frac{d^2\eta}{ds^2} \qquad \text{(C-25)}$$

Equation (C-25) generally has no closed form solution. For a circular bar there is $\frac{d^2\eta}{ds^2}=0$, and if the load is concentrated force e.g. downward load P shown in Figure C.3, then the equation can be simplified

$$\frac{d^2\theta}{ds^2}+k^2\sin\theta=0 \qquad \text{(C-26)}$$

where $k=\sqrt{\frac{P}{EI}}$

Above all the nonlinear analyses for curved beam is more difficult than straight beam, so based on the results for straight beam, the method of analogy and principle of similarity can often be used for many kinds of problems concerning curved beam, as shown in the thesis.

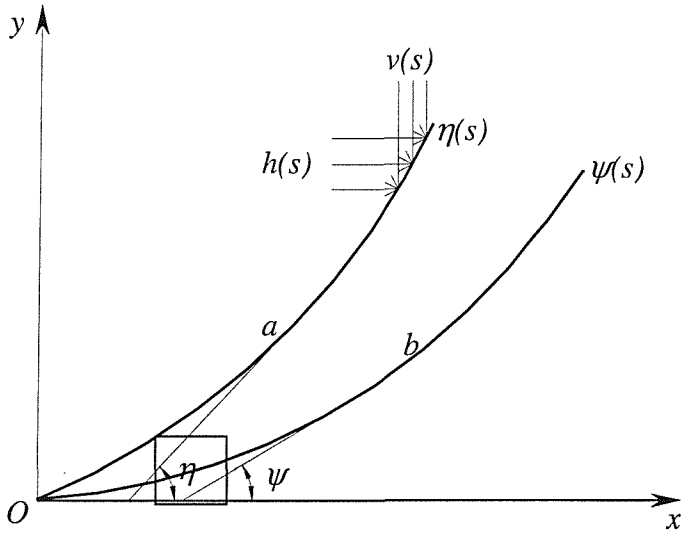

Figure C.3 Deflection of Initially Curved Bar under Loads

Reference for Appendix C

1. Frish-Fay, R., "Flexible Bars", Butterworths & Co. (Publishers) Ltd., London, 1962.